

Disruption of UHRF1 expression

in chicken DT40 cells



Huaping Sun, MSc

This thesis is submitted in fulfilment of the requirements
for the Degree of Doctor of Philosophy

Submitted September 2017

Medical School, Lancaster University

Abstract

Epigenetics regulate the gene expression while imposing no change in the underlying gene sequence constitution. The abnormal regulation of epigenetics is associated with the development and progression of cancer. Among the epigenetic regulators, UHRF1 (ubiquitin-like with PHD and ring finger domain containing protein 1) has attracted considerable attentions in cancer research in past years due to its universally increased expression in a wide range of different cancer cells, and its ability to facilitate the crosstalk between DNA methylation and histone modification, thereby driving the occurrence of cancer and ensuring the inheritance of accurate epigenomic information to descendent cells. Depletion of UHRF1 proteins in nuclear significantly blocked DNA replication in *Xenopus* egg extracts. However, the mechanism underlying the role of UHRF1 in DNA replication remains unclear. Considering the effects of UHRF1 depletion on DNA replication is independent of cell cycle checkpoints and transcription events in *Xenopus* egg extracts, it is important to extend the work into a higher eukaryote system. Therefore, we planned to generate *UHRF1* knockout cell line in the most effective gene targeting system of DT40 cells to observe the effect of *UHRF1* deletion on DNA replication and the cellular response to DNA damage. CRISPR/Cas9 technology and traditional gene targeting were applied to generate conditional *UHRF1* knockout cell lines. It was found that knocking out the expression of both alleles of *UHRF1* was lethal to cell viability and that there was a threshold of UHRF1 overexpression that can be tolerated by DT40 cells. Additionally, the ability of DT40 cells to tolerate DNA damage was positively related to the expression levels of UHRF1 proteins.

Acknowledgement

First and foremost, I would like to give all my thanks to my supervisors, Dr. Howard Lindsay and Dr. Elaine Taylor, for all they have done during my time in Lancaster University. Your support, feedback, and patience were invaluable and I am incredibly grateful you gave me the opportunity to embark on a Ph.D. project. My gratitude is also extended to the Faculty of Health and Medicine and Medical School for funding my Ph.D., as without the studentship, I definitely would not have been able to do my Ph.D. study in Lancaster University.

Secondly, I would like to extend a big thank to Dr. Nikki Copeland for your contributions to cell biological techniques during my Ph.D. Additional thanks also go to Dr. Helfrid Hochegger from the University of Sussex, for allowing me to spend the time in their laboratory to learn the skills of CRISPR and help me with the troubleshooting in the knockout of *UHRF1*.

I would like to thank Dr. Stephen Roberts, not only for providing me a job and the opportunity to develop my skills in yeast biology, but also for all your help in my final year as a Ph.D. student, and always being there to answer my seemingly obvious scientific questions. I have enjoyed the work with you and I cannot know what I have done with you in the past year.

I would like to thank Dr. Jane Andre and Dr. Elisabeth Shaw for teaching me so many microbiological technics, which have proved to be incredibly important and useful for my Ph.D. project. My sincere thanks also go to all the past and current members of BLS department and Medical School and all my office buddies. Thank you for your friendship and supports over the past years.

Finally, to my parents and brothers, there are not enough words to express my gratitude to you all. You have supported me so much in my pursuit of my dreams and I would not be writing this thesis now if it was not for you. I love you all.

Declaration

I confirm that the work presented in this thesis is my own and has not been submitted in substantially the same form for the award of a higher degree elsewhere. Where information has been derived from other sources, I confirm this has been indicated in the thesis.

Huaping Sun, MSc

Table of Contents

Chapter 1 Introduction	1
1.1 Epigenetic regulation.....	2
1.1.1 DNA methylation.....	2
1.1.2 Histone modifications	5
1.1.3 RNA interference.....	9
1.2 The structure of UHRF1.....	10
1.2.1 UBL	10
1.2.2 TTD	12
1.2.3 PHD.....	12
1.2.4 SRA domain	13
1.2.5 RING domain	14
1.2.6 Intramolecular interaction of UHRF1	15
1.2.7 Molecules interacting with UHRF1 in DNA methylation	18
1.3 The control of UHRF1 expression	21
1.3.1 cell cycle and checkpoint response.....	21
1.3.2 The involvement of UHRF1 in checkpoint response	23
1.3.3 The regulation of <i>UHRF1</i> promoter.....	26
1.3.4 The regulation of <i>UHRF1</i> mRNA by miRNA	30
1.3.5 The regulation of UHRF1 protein	32
1.3.6 UHRF1 mediated silencing of tumour suppressor genes.....	34
1.4 Role of UHRF1 in genomic stability.....	36
1.4.1 Involvement of UHRF1 in DNA repair.....	36
1.4.2 Involvement of UHRF1 in DNA replication	41

1.5 Clinical usage of UHRF1	44
1.5.1 Modulation of UHRF1 by natural polyphenols.....	44
1.5.2 UHRF1 as universal biomarker for cancer.....	47
1.6 Conclusion	51
1.7 Objectives	52
Chapter 2 Materials and methods.....	54
2.1 Materials	55
2.1.1 reagent supplier	55
2.1.2 Solutions and buffers	59
2.1.3 Stock solutions of antibiotics and selection drugs.....	61
2.1.4 List of antibodies	62
2.1.5 List of PCR primer	62
2.2 Molecular biology.....	65
2.2.1 Preparation of chemically competent <i>DH5α E. coli</i>	65
2.2.2 Purification of PCR product.....	65
2.2.3 DNA fragment purification	65
2.2.4 DNA agarose gel electrophoresis.....	66
2.2.5 DNA Ligation.....	66
2.2.6 Transformation into <i>DH5α E. coli</i>	67
2.2.7 Plasmid purification using DNA mini prep Kit	67
2.2.8 Plasmid purification using DNA midi prep Kit	67
2.2.9 DNA precipitation.....	68
2.2.10 Genomic DNA extraction.....	68
2.2.11 RNA extraction	69
2.2.12 cDNA synthesis.....	69
2.2.13 PCR	70

2.2.14 5' phosphate removal	71
2.2.15 <i>In vitro</i> translation of proteins	71
2.3 Eukaryotic cell culture	71
2.3.1 Cell culture	71
2.3.2 Cell freezing.....	72
2.3.3 Cell resurrection.....	72
2.3.4 Cell counting.....	72
2.3.5 Transient transfection.....	73
2.3.6 Enrichment of GeneArt CRISPR Nuclease Expressing Cells.....	73
2.3.7 Stable transfection	74
2.3.8 Cell proliferation assay.....	74
2.3.9 Clonogenic formation assay	75
2.4 Protein analysis	75
2.4.1 Sample preparation.....	75
2.4.2 SDS-PAGE.....	75
2.4.3 Semi-dry transfer.....	75
2.4.4 Immunoblotting and development.....	76
2.4.5 Immunoblotting stripping and re-probing	76
Chapter 3 Targeting of UHRF1 in DT40 cells using CRISPR/Cas9 system	77
3.1 Introduction of CRISPR technology.....	78
3.2 Strategy of CRISPR/Cas9 mediated <i>UHRF1</i> knockout.....	80
3.3 Identifying primary antibodies to chicken UHRF1 proteins.....	82
3.3.1 <i>Xenopus</i> UHRF1 antibody cross-reacted with chicken and human proteins	85
3.3.2 UHRF1 antibody cross reacted with DT40 UHRF1 proteins	87
3.4 Possibly essential role of UHRF1 for DT40 cell survival.....	91
3.4.1 The optimization of CRISPR/Cas9 mediated <i>UHRF1</i> disruption.....	91

3.4.2 <i>UHRF1</i> was possibly essential for cell survival	94
Chapter 4 A system for conditional expression of <i>UHRF1</i> in DT40 cells	96
4.1 Generation of DT40 cells with conditional expression of exogenous human <i>UHRF1</i> 99	
4.1.1 Generation of constructs with conditional human <i>UHRF1</i> expression	99
4.1.2 Generation of AID-GFP tagged human <i>UHRF1</i> in DT40 cells	101
4.1.3 The conditional expression of AID-GFP tagged human <i>UHRF1</i> in DT40 cell line .	105
4.2 Generation of conditional <i>UHRF1</i> knockout cell lines.....	107
4.3 Abolished proliferative capacity of <i>UHRF1</i> deleted cells.....	109
Chapter 5 Targeting <i>UHRF1</i> gene by Cre-Loxp combination system	112
5.1 Introduction of Cre-Loxp combination system	113
5.2 Strategy of targeting <i>UHRF1</i> gene by Cre-Loxp system	115
5.3 Generation of cell lines with conditionally expressed <i>UHRF1</i>	118
5.3.1 AID system controlled <i>UHRF1</i> deletion cell line.....	118
5.3.2 Cre-Loxp system controlled conditional <i>UHRF1</i> cell line	121
5.4 <i>UHRF1</i> level positively related to cell sensitivity to ICL reagents.....	124
Chapter 6 Discussion and future work.....	126
6.1 Proliferative block caused by abnormal <i>UHRF1</i> expression	127
6.1.1 The mechanisms underlying <i>UHRF1</i> -dependent proliferative block	131
6.1.2 The cell fates caused by <i>UHRF1</i> overexpression.....	136
6.2 AID/OSTIR2 system for conditional expression of <i>UHRF1</i>.....	138
6.3 Cell sensitivity to ICL damage positively correlates with <i>UHRF1</i> levels.....	139
Chapter 7 Conclusion.....	141
Reference.....	144
Appendices	160

List of figures

Figure 1.1 The schematic relationship between DNA methylation and cancer.	4
Figure 1.2 Schematic representation of histone post-translational modifications	6
Figure 1.3 Schematic representation of human UHRF1 domain structure.	11
Figure 1.4 Spacer region indication and UHRF1 dynamic conformation.	17
Figure 1.5 Working principle of UHRF1 with its interactive partners in DNA methylation and histone modification.	20
Figure 1.6 The schematic representation of cell cycle and checkpoints.	22
Figure 1.7 Schematic representation of G1/S and G2/M checkpoint response to DNA damage.	24
Figure 1.8 The regulation of UHRF1 expression.	27
Figure 1.9 Schematic signal pathway of ICL repair.	40
Figure 1.10 Schematic representation of DNA replication origin activation.	42
Figure 3.1 Working principle of CRISPR/Cas9 mediated gene disruption.	79
Figure 3.2 CRISPR/Cas9 mediated sgRNA loci and nucleotide sequence for disrupting <i>UHRF1</i> in DT40 cells.	81
Figure 3.3 <i>UHRF1</i> gene identity alignment.	84
Figure 3.4 Cross reactivity between <i>Xenopus</i> antibodies and eukaryotic cell extracted proteins.	86
Figure 3.5 The generation of defined UHRF1 expression vector.	89
Figure 3.6 Cross reaction of <i>Xenopus</i> UHRF1 antibody to DT40 UHRF1 proteins.	90
Figure 3.7 Screening of CRISPR/Cas9 mediated <i>UHRF1</i> gene deletion.	93
Figure 4.1 Schematic illustration of AID system.	98
Figure 4.2 Schematic representation of human <i>UHRF1</i> in AID-OSTIR2 vector and pCl-neo vector.	100
Figure 4.3 Screening of cell clones with cell clones with different tagged UHRF1.	103
Figure 4.4 Generation of cell lines with exogenous UHRF1 expression.	104
Figure 4.5 Conditional expression of AID-GFP tagged human UHRF1 protein.	106

Figure 4.6 Screening of CRISPR/Cas9 mediated <i>UHRF1</i> disruption in Ahg4 cell line.....	108
Figure 4.7 The proliferative block of <i>UHRF1</i> deleted cells.	110
Figure 4.8. Screening of KO cell lines.	111
Figure 5.1 Schematic representation of Cre-Loxp combination system working principles.	114
Figure 5.2 The diagram of generating vectors for gene targeting.....	116
Figure 5.3 Schematic representation of target arm loci on <i>UHRF1</i> genomic DNA.	117
Figure 5.4 The generation of Acp24 cell line.....	119
Figure 5.5 The schematic representation of primer design used for screening modified <i>UHRF1</i> genomic DNA and endogenous <i>UHRF1</i> genomic DNA in DT40 cells.....	120
Figure 5.6 The screening of PC7 cell line with conditional expression of <i>UHRF1</i>	122
Figure 5.7 <i>UHRF1</i> downregulation caused upregulated sensitivity to MMC.	125

List of tables

Table 1 Summary of studies suggesting UHRF1 as diagnostic and prognostic biomarker in various cancer	50
Table 2.1 List of reagent supplier	59
Table 2.2 List of solution/buffer recipe.	61
Table 2.3 Antibiotics and drugs used in this study. All solutions involved in the selection for DT40 cells were filtered by 0.45µm filter before use.....	61
Table 2.4 List of primary antibodies.	62
Table 2.5 List of secondary antibodies.....	62
Table 2.6 Primer sequences used in PCR reactions.	64
Table 2.7 The scheme of DNA ligation system.	66
Table 2.8 The reagents and volumes used for the reverse transcriptase master mix.	69
Table 2.9 The reagents and volumes used for generating cDNA from RNA.....	70
Table 2.10 The reagents and volumes used in PCR master mix.....	70
Table 2.11 The cycling instruction for each target fragment used in PCR reactions.	71

Abbreviation

APE	Annurca polyphenol extract
BER	Base excision repair
BRBs	Base excision repair
CDKs	Cyclins Dependent Kinases
CDT1	CDC10-dependent transcript 1
CRISPR	Clustered regularly interspaced short palindromic repeats
DDK	DBF-dependant kinase
DNMTs	DNA methyltransferases
DSBs	DNA double-strand breaks
dsRNA	Double strand RNA
E2F1	E2F transcription factor 1
E2F8	E2F transcription factor 8
ECGG	Epigallocatechin-3-gallate
Eme1	Essential meiotic endonuclease 1
HATs	Histone acyltransferases
HDACs	Histone deacetylases
HKMT	Histone lysine methyltransferase
HMTs	Histone methyltransferase

HR	Homologous recombination
ICLs	Interstrand crosslinks
LSD1	Lysine-specific demethylase 1
MBDs	Methyl-CpG binding proteins
miRNA	microRNA
MPG	N-methylpurine DNA glycosylase
mRNA	Messenger RNA
Mus81	Methyl methansulfonate UV sensitive clone 81
NHEJ	Non-homologous end joining
NSCLC	Non-small cell lung cancer
ORC	Origin recognition complex
PARP	Poly ADP-ribose polymerase
PBR	Polybasic region
PCNA	Proliferating cell nuclear antigen
PHD	Plant Homeo Domain
PML	Promyelocytic leukemia
PPARG	Peroxisome proliferator-activated receptor gamma
pre-IC	pre-initiation complex
pre-RC	pre-replication
PRMT	Protein arginine methyltransferase

PTMs	Post-translational modifications
RFC	Replication factor C
RFTS	Replication foci targeting sequence
RIF1	Replication timing regulatory factor 1
RING	Really Interesting New Gene
RISC	RNA-inducing silencing complex
RNAi	RNA interference
RPA	Replication protein A
RWPs	Red wine proteins
SAM	S-adenosylmethionine
siRNA	Small interfering RNA
SP1	specificity protein 1
SRA	Set and RING Associated
ssRNA	Single-stranded RNA
T3	Thyroid hormone 3
TD	Terminally differentiated
TQ	thymoquinone
TR	Thyroid hormone receptor
TSG	Tumour suppressor gene
TTD	Tandem Tudor Domain

UBL	Ubiquitin-like Domain
UHRF1	Ubiquitin-like with PHD and RING finger domain containing protein 1
UIM	Ubiquitin-interacting motif
UPAT	UHRF1 Protein Associated Transcript
USP7	Ubiquitin-specific-processing protease 7
YY1	Yin Yang transcription factor 1

Chapter 1 Introduction

Cancer, as one of the top causes of mortality worldwide, is regarded as rising from the cooperative and inheritable alterations on genetic sequence and their epigenetic codes. Genetic alterations may occur in the promoter region or the coding region of a specific gene, which affects its expression level and the function or the stability of its expression products, respectively. Epigenetic alterations refer to the relevant modifications, including DNA methylation, histone modification and RNA interference (RNAi), on gene expression without changes on underlying DNA sequence constitution. Among the epigenetic modulators, UHRF1, also known as inverted CCAAT box-binding protein of 90 KDa (ICBP90) or nuclear protein of 90KDa (NP95), was found to be critical for cancer development as it coordinates DNA methylation and histone modification and drives the occurrence of tumorigenesis. UHRF1 is also involved in the DNA repair that makes the cells resistant to chemotherapeutic drugs or irradiations. Therefore, the understanding of the molecular mechanism of UHRF1 in epigenetic regulation and DNA repair would help the therapeutic development of cancer. In this literature review, we will focus on the epigenetic mechanism underlying UHRF1 in the regulation of gene expression and the involvement of UHRF1 in DNA repair.

1.1 Epigenetic regulation

1.1.1 DNA methylation

DNA methylation is now widely acceptable as an inheritable and stable epigenetic marker of transcription repression and indirectly increasing chromatin condensation in context dependent manner. The patterns of DNA methylation and levels of global/local DNA methylation are essential for X chromosome inactivation,

imprinting, heterochromatin maintenance, development control, tissue specific expression control and disease progression in mammalian system (Li 2002), as shown in **Figure 1.1**. Mechanistically, DNA methylation mainly happens on the cytosine residues in CpG dinucleotides catalyzed by DNA methyltransferases (DNMTs), among which DNMT3a and DNMT3b are responsible for the establishment of new DNA methylation patterns and DNMT1 maintains the methylation status of DNA by copying existing DNA methylation patterns following DNA replication. DNMT3L is homologous to DNMT3a and DNMT3b and stimulates the catalytic activities of DNMT3a and DNMT3b (Gopalakrishnan, Van Emburgh et al. 2008).

Consistently with this, DNMT3a null mice showed normal development but died at four weeks of age, while DNMT3b null mice were not viable (embryonic lethality), suggesting the importance of *de novo* methylation in mammalian development (Li 2002). Mice null in DNMT3L showed global demethylation as well as developmental and imprinting defects, suggesting the essential role of DNMTs in DNA methylation (Goll and Bestor 2005).

Besides, methylated CpG dinucleotides of DNA can be read by methyl-CpG binding proteins (MBDs) followed by the binding of MBD2, an integral role of nucleosome remodelling and histone deacetylation complex (Wood and Zhou 2016).

DNA demethylation also plays an important role in maintaining DNA methylation status, while the mechanism about it is little known. Recent study found reduced expression of UHRF1 and bi-methylated histone H3 lysine 9 (H3K9me2) significantly impaired the status of DNA methylation, providing some insights for the demethylation process (Leitch, Surani et al. 2016).

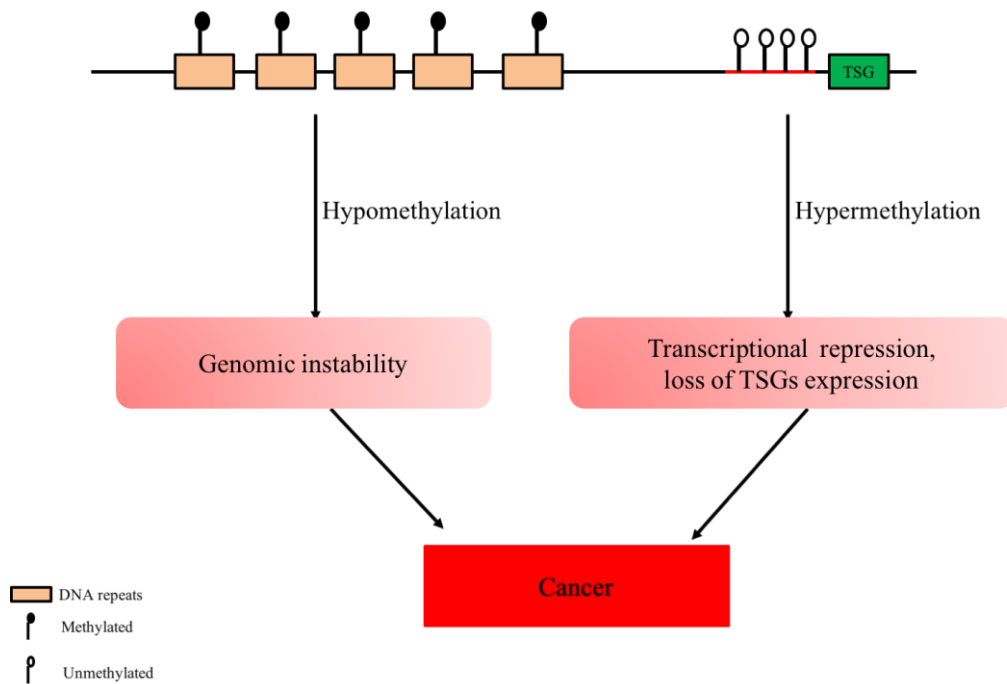


Figure 1.1 The schematic relationship between DNA methylation and cancer.

This diagram showed a representative region of genomic DNA in a normal cell, containing repeat-rich hypermethylated pericentromeric heterochromatin and hypomethylated CpG islands on the promoter region of tumour suppressor gene (TSG) (indicated in green). In cancer cells, heterochromatin was hypomethylated through mitotic recombination resulting in the genomic instability, while CpG islands were hypermethylated resulting in the transcription inactivation. These alteration events on DNA methylation occurred at the early stages of tumourigenesis.

1.1.2 Histone modifications

Following DNA methylation, post-translational modification (PTMs) of histones was also found to be involved in tumorigenesis by controlling the accessibility of chromatin and transcriptional activities inside a cell (Fullgrabe, Kavanagh et al. 2011). As shown in **Figure 1.2**, the nucleosome is consisted of a histone octamer core, containing two copies of each histones (H2A, H2B, H3 and H4), and 146 base pair of DNA that is wrapping around the histone core. The linker histone H1 binds to the entry and exit sites of wrapping DNA, thereby locking the nucleosome in place. The modification of histones occurs on the N-terminus tail which could also penetrate from their own nucleosome into adjacent nucleosomes, thereby affecting the inter-nucleosomal interaction and the overall structure of chromatin.

PTMs of histones could also regulate the open/close conformation of chromatin by recruiting specific proteins, including transcription factors, chromatin remodelers or chromatin structure proteins, thereby regulating the manipulation and the expression of DNA (Bannister and Kouzarides 2011). Therefore, in the following section, we will review the manners of histone modification, mainly focusing on the histone methylation, acetylation, phosphorylation and ubiquitination.

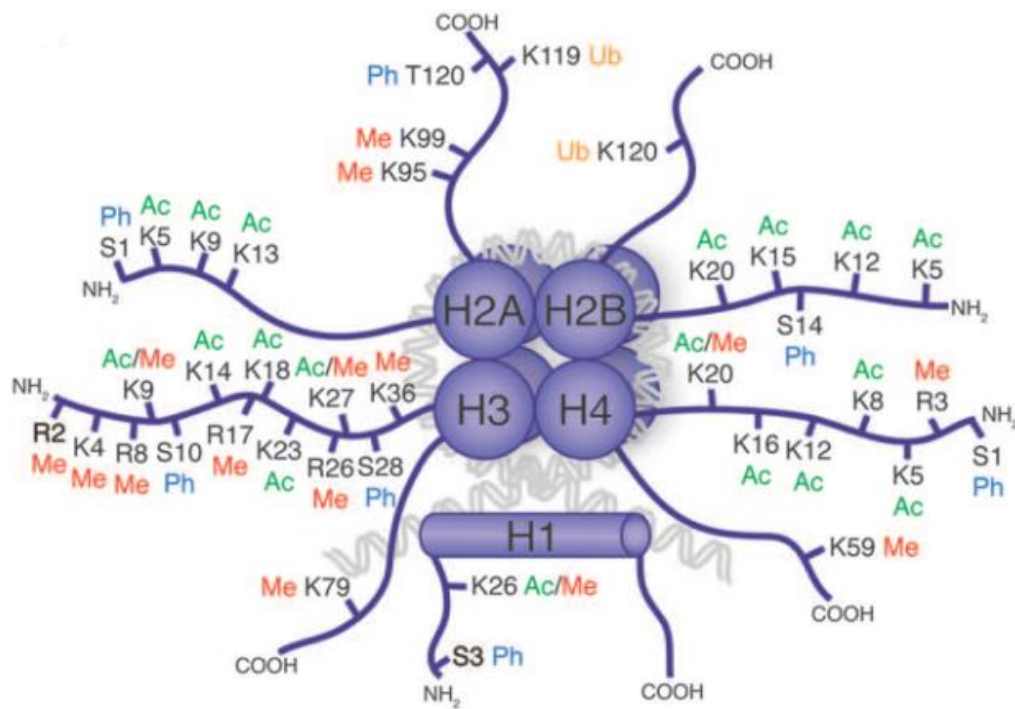


Figure 1.2 Schematic representation of histone post-translational modifications

Currently known covalent modifications were highlighted on the N and C terminals of histones. **Me in red indicated methylation**; **Ac in green indicated acetylation**; **Ph in blue indicated phosphorylation**; **Ub in orange indicated ubiquitination**. This image is adopted with permission from (Y. Q. Zhao et al., 2013).

Histone methylation

Histone methylation is a reversible process mediated by histone methyltransferase (HMTs) or demethylase respectively, and mainly occurs on the side chains of lysine (K) and arginine (R) residues without alteration on the charge of histone proteins. The consequence of histone methylation can induce the activation or silencing of gene transcription depending on the methylated residues and the amount of transferred methyl groups of various histones.

The methylation of lysine residues is catalysed by histone lysine methyltransferase (HKMT) mainly at N-terminus tail by enzymes with SET domains except for Dot1 enzyme catalysing methylation on H3K79 at a globular region of histone H3, thereby activating transcription activities (Bannister and Kouzarides 2011). HKMTs catalysed the transfer of 1 or 2 or 3 methyl group/groups from S-adenosylmethionine (SAM) to a lysine's amino group depending on the lysine binding pockets of catalytic domains of HKMTs and resulting in the mono-, bi- or tri-methylated histones (Bannister and Kouzarides 2011).

The methylation of arginine was mainly catalysed by protein arginine methyltransferase (PRMT) through transferring 1 or 2 methyl group/groups to the arginine residues within a variety of substrates (Bannister and Kouzarides 2011). Lysine-specific demethylase 1 (LSD1) and enzymes with JmjC domains determines the demethylation from H3K4me_{1/2} and all the three states of the methylated lysine residues, respectively (Shi, Lan et al. 2004, Mosammaparast and Shi 2010), similar to arginine demethylase mediated by enzymes with JmjC domains (Walport, Hopkinson et al. 2016).

Histone acetylation

Histone acetylation is another reversible regulating mechanism on lysine by adding negatively charged acetyl group to positively charged lysine residues, thereby weakening the binding of acetylated histones and negatively charged DNA resulting in the transcription activation and chromatin relaxation. The acetylation of lysine is highly dynamic and controlled by opposing actions catalysed of two major classes of enzymes: histone acyltransferases (HATs) and histone deacetylases (HDACs), responsible for transcription repression and restoration by adding and removal acetyl groups, respectively (Verdin and Ott 2015).

Histone phosphorylation

The phosphorylation of histones is also highly dynamic by adding or removing the negatively charged phosphate group from the residues of serines, threonines and tyrosines, predominantly, but not exclusively, and is catalysed by kinases and phosphatases. These marks functions as platforms for recruitment, assembly or retention of various chromatin associated factors during various chromatin based events including transcription, DNA repair and chromatin condensation during cell division and apoptosis (Bannister and Kouzarides 2011).

All the previous modification of histones described above results in the relatively small addition or removal of residues to the side chains of histones. However, the polyubiquitination of histones results in the attachment of a 76-amino acid polypeptide to the lysine residues through the sequential actions of E1-activating, E2-conjugating and E3-ligating enzymes. Until now, two well characterised ubiquitinated histones lie in H2AK119ub1 and H2BK123ub1, responsible for regulating gene

silencing and transcriptional initiation and elongation, respectively (Cao and Yan 2012).

1.1.3 RNA interference

RNAi is the posttranscriptional modification through neutralizing the targeted messenger RNA (mRNA) by small RNA molecules, central to which is small interfering RNA (siRNA) and microRNA (miRNA). Both of siRNA and miRNA can be regulated by DNA methylation and histone modification, while siRNA and miRNA themselves can repress the expression of key enzymes that drive the epigenetic remodelling, and bind to the complementary sequence of the gene promoter, thereby regulating chromatin conformation and gene expression.

The pathway of RNAi is initiated by the enzyme Dicer, which leaves long double-strand RNA (dsRNA) into short non-coding fragments of ~20 base of siRNA or ~22 base of miRNA. The dsRNA is subsequently unwound into two single-stranded RNAs (ssRNA), that is, the passenger strand RNA and the guide strand RNA. The passenger strand is subsequently degraded, while the guide strand is incorporated into RNA-inducing silencing complex (RISC). This is followed by the cleavage of targeted RNA by catalytic component Argonaute2 in RISC complex (Song, Smith et al. 2004).

Similarly, miRNAs are encoded by the genome and are transcribed by the RNA polymerase II (pol II) into primary miRNAs and processed into nucleus by the microprocessor complex into the precursor miRNAs, which are further processed into mature miRNAs by another RNase III Dicer in the cytoplasm. miRNAs can bind to the targeted mRNAs with complete complementarity leading to their degradation, and

bind to the RNA targeted mRNAs with incomplete complementarity, mainly at 3'UTR sequence leading to the translational suppression (Chuang and Jones 2007).

1.2 The structure of UHRF1

Initially, UHRF1 was identified as a transcription factor regulating the expression of topoisomerase II α (TopoII α) through binding to the inverted CCAAT box (ICB2) in the promoter region (Hopfner, Mousli et al. 2000). Later, UHRF1 was found to participate in various epigenetic processes through its five recognisable domains, namely Ubiquitin-like Domain (UBL), Tandem Tudor Domain (TTD), Plant Homeo Domain (PHD), Set and RING Associated (SRA), and Really Interesting New Gene (RING) domains, as shown in **Figure 1.3**. These five domains allow UHRF1 to actively regulate the DNA methylation, chromatin modifications, cell proliferation and DNA repair. Therefore, this section will demonstrate the specific functions of each domain.

1.2.1 UBL

The N-terminus UBL domain of UHRF1 is 35% identical to ubiquitin, a protein regulating protein activation, degradation, location and interaction with other proteins. The function of UBL domain is less known, but the structure and sequence homology reveals that UBL domain has ubiquitin function and could bind to the ubiquitin-interacting motif (UIM) subunits of proteasome and transport proteasome to the destination sites, providing insights for UHRF1 as bridge molecule linking proteasome degradation and histone modification (Heir, Ablasou et al. 2006).

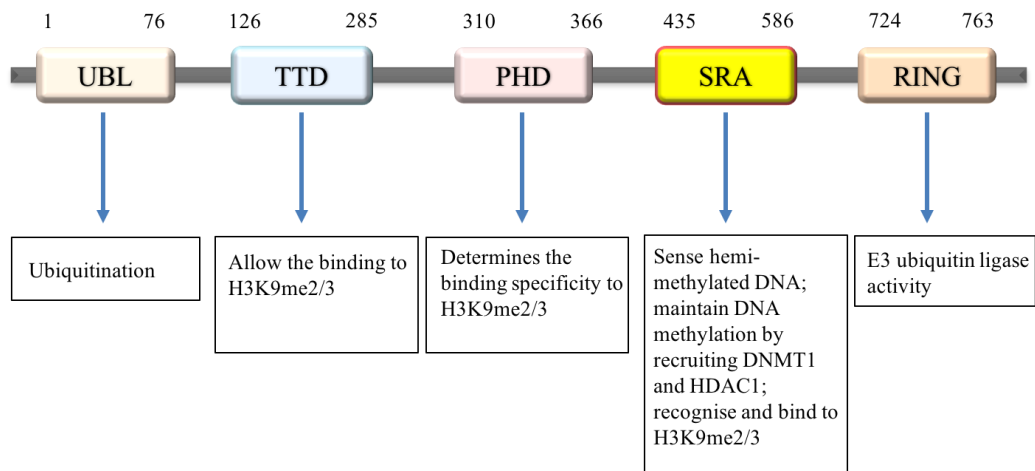


Figure 1.3 Schematic representation of human UHRF1 domain structure.

Domain boundaries are defined as the positions of their starting and ending amino acids. UBL domain at N-terminus plays ubiquitination activity, TTD recognises and binds to di-/tri-methylated histone H3 lysine 9 (H3K9me2/3), PHD determines the binding specificity of UHRF1 to histone H3 arginine 2 (H3R2) and H3K9me2/3, SRA domain facilitates the maintenance of DNA methylation and histone modifications by recruiting DNMT1 (DNA methyltransferase-1) and HDAC1 (histone deacetylase 1), respectively, and RING domain at C-terminus shows intrinsic E3 ligase activity towards histones and non-histone proteins.

1.2.2 TTD

TTD is composed of two tightly packed subdomains TTD_N and TTD_C and plays an important role in DNA methylation. An aromatic cage formed by residues of F152, Y188 and Y191 in TTD_N allows UHRF1 to recognise and bind to the bi/tri-methylated histone H3 lysine 9 (H3K9me_{2/3}), which is an essential part of DNA methylation and known to be associated with heterochromatin formation and the subsequent transcription suppression (Weake and Workman 2008, Liu, Gao et al. 2013). The peptide binding groove formed by TTD_N and TTD_C ensures the tight and specific contact to unmodified histone H3 arginine 4 (H3K4me₀) (Nady, Lemak et al. 2011, Tauber and Fischle 2015). Another study using TTD mutant, which is deficient in binding to H3K9me₃ or H3K4me₀, found the altered localization of UHRF1 to heterochromatin, indicating the role of TTD in mediating UHRF1 binding to heterochromatin (Nady, Lemak et al. 2011).

1.2.3 PHD

PHD is identified as a binder of unmodified histone 3 arginine 2 (H3R2). This is because PHD mutants abrogates the binding to H3R2 and its following repression on targeted genes, although no effects were found on its localization onto euchromatic targets (Rajakumara, Wang et al. 2011). The binding of PHD to H3R2 could be abrogated by the methylated H3R2 or the intramolecular binding between PHD and SRA domain of UHRF1, but is largely unaffected by the methylation of H3K4 and H3K9 (Fang, Cheng et al. 2016). Besides, PHD cooperates with TTD in the recognition of H3K9me₃, which can be promoted by the hemi-methylated DNA and be inhibited by the binding of C-terminus Spacer region (located between SRA and RING domain) to TTD (Fang, Cheng et al. 2016). Moreover, both of TTD and PHD

mutants of UHRF1 show complete abolition of hemi-methylated CpG or H3K9me2/3 binding in UHRF1^{-/-} cells, while TTD or PHD mutant of UHRF1 could partially rescue the association with hemi-methylated CpG or H3K9me2/3 respectively, suggesting the binding of UHRF1 to hemi-methylated CpG or H3K9me2/3 works in cooperative manner and in preparation for the following DNMT1 recruitment (Liu, Gao et al. 2013).

1.2.4 SRA domain

SRA domain occurs only in the UHRF family and plays a fundamental role in the sensing of hemimethylated DNA CpG islands (high-density CpG regions) and recruiting UHRF1 to these sites, aiming at maintaining the methylation status of DNA (Avvakumov, Walker et al. 2008, Hashimoto, Horton et al. 2008, Zhao, Zhang et al. 2016). The binding of SRA domain to the hemimethylated DNA does not induce the distortion of DNA but facilitates the recruiting of DNA methyltransferase-1 (DNMT1) to the hemimethylated DNA through interacting with the replication foci targeting sequence (RFTS) domain of DNMT1 (Bashtrykov, Jankevicius et al. 2014, Greiner, Kovalenko et al. 2015, Kilin, Gavvala et al. 2017). Furthermore, SRA domain could cooperatively recognise the presence of di- and tri- methylated lysine 9 of histone 3 (H3K9) with the help of TTD (Karagianni, Amazit et al. 2008, Hashimoto, Horton et al. 2009, Nady, Lemak et al. 2011).

The overall interaction between DNA and SRA domain could be described as a hand grasping DNA helix with a methylcytosine-binding pocket, and two loops corresponding to a thumb (444–449 residues) and NKR finger (483–496 residues), which are responsible for CpG recognition and base flipping respectively through penetrating into the minor and the major grooves of DNA helix (Hashimoto, Horton et

al. 2009). R496 residue in NKR finger replaces the flipping 5- methylcytosine (5mC) which binds to the pocket of SRA domain, while N489 residue within the NKR finger loop acts as a selective filter and prevents the symmetric C5 base from flipping out of the DNA duplex, which therefore allows the discrimination between fully and hemimethylated DNA strands for ensuring faithful methylation patterns (Avvakumov, Walker et al. 2008). Another conformational study found SRA domain could recognise hydroxymethylcytosine bringing new insight to DNA methylation (Frauer, Hoffmann et al. 2011).

1.2.5 RING domain

It is known that ubiquitination is required for transcription initiation, elongation, suppression. RING finger domain is the only domain of UHRF1 showing E3 ubiquitin ligase activity towards histone H3, and therefore providing a docking site for DNMT1 binding (Nishiyama, Yamaguchi et al. 2013). In *Xenopus* egg extracts, histone H3 ubiquitination was found to be coupled with DNA methylation as DNMT1 deletion increased the accumulation level of UHRF1 dependent histone H3K23 ubiquitination (Nishiyama, Yamaguchi et al. 2013). The ubiquitination of histone H3 disrupted by the downregulation of endogenous UHRF1 cannot be restored by the mutation in the RING finger domain (C713A/C715A/C716A) and the SRA domain (D474G/R489A), but can be restored by the wild type mouse UHRF1. Following immunohistochemical experiments, it was found that both RING finger mutants and SRA mutants failed to recruit DNMT1. Collectively, these finding suggests that the RING finger domain and the consequent ubiquitination of histone H3 is required for DNMT1 recruitment to the DNA replication sites (Nishiyama, Yamaguchi et al. 2013). Similarly, another study established mutation on the PHD (H346G) and the RING finger domain (H730A) to

prevent the binding of zinc ions by zinc-finger motif, and found that the RING (H730A) mutant significantly reduced the level of histone H3 ubiquitination, confirming the role of RING finger domain in the ubiquitination of histone H3 (Qin, Wolf et al. 2015). Additionally, both mutants of the SRA domain and the RING finger domain displayed impaired localization of UHRF1 on hemi-methylated DNA, suggesting the role of SRA domain on recognising hemi-methylated DNA (Qin, Wolf et al. 2015).

Using mass spectrometry, a UIM motif was separated from N-terminus of DNMT1 which binds to the ubiquitinated histone H3 and is regarded as essential for DNA methylation. Considering the binding of PHD to H3R2 was required for DNA methylation following histone H3 ubiquitination, it was suggested that there are manifold regulatory mechanisms in controlling DNMT1 in the process of the DNA methylation and the histone modifications (Qin, Wolf et al. 2015). Additionally, UIM deficient cells failed to show the association between DNMT1 and ubiquitinated histone H3 ubiquitinated H2AK119, which are catalysed by the RING finger domain, providing new insights for future study in the recruitment of DNMT1 to hemimethylated DNA sites (Qin, Wolf et al. 2015).

1.2.6 Intramolecular interaction of UHRF1

The structural basement of UHRF1 in the maintenance of DNA methylation during S phase is dependent on its adjustable close/open forms, being controlled by the absence or the presence of hemi-methylated DNA and the binding to some histones (Gelato, Tauber et al. 2014). Between SRA C-terminus and RING finger domain, there is a polybasic region (PBR) defined as Spacer that was recently reported. Before binding to the hemi-methylated DNA, UHRF1 adopts a closed conformational shape with

Spacer binding to the groove of TTD and SRA binding to PHD. This inhibits the recognition of H3K9me3 and unmethylated H3R2 respectively, because the function of TTD-PHD linker is inhibited. Upon binding to the hemi-methylated DNA in CpG sites, the closed conformation of UHRF1 is opened, which promotes the binding to H3K9me3, thereby allowing the following binding of SRA domain to the hemi-methylated DNA and the recruitment of DNMT1, as shown in **Figure 1.4** (Fang, Cheng et al. 2016).

The dynamic conformation of UHRF1 is also influenced by the interaction with ubiquitin-specific-processing protease 7 (USP7), a deubiquitinase enzyme of Spacer region. The association of USP7 with Spacer region disrupted the binding of Spacer region to TTD and thus opening the UHRF1 conformation (Zhang, Rothbart et al. 2015).

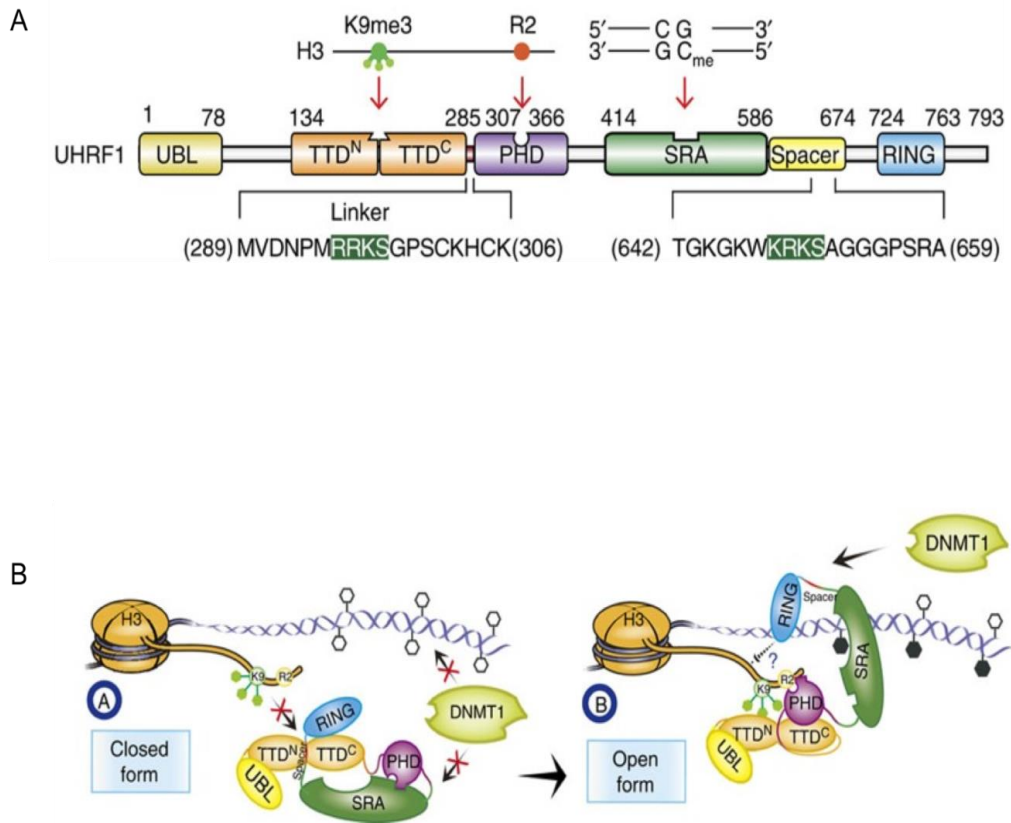


Figure 1.4 Spacer region indication and UHRF1 dynamic conformation.

(A): Spacer locates at C-terminus of SRA and is indicated in yellow colour. The conserved motif of Spacer (residues 587–674) binds to TTD in the similar manner as TTD-PHD linker (residues 286–306) to TTD. (B): Changeable forms of UHRF1 being controlled by hemimethylated DNA. The images were adopted from (Fang, Cheng et al. 2016) with permission.

1.2.7 Molecules interacting with UHRF1 in DNA methylation

The maintenance of the pattern of hemimethylated CpG dinucleotides at the DNA replication fork is the key event to the faithful mitotic inheritance of DNA methylation. Among its functional molecules, UHRF1 was found to play an important role in the maintenance of both global and local DNA methylation *in vitro/vivo* with preferential affinity to hemimethylated DNA. This is similar to DNMT1, whose preference for hemi-methylated to symmetrically methylated DNA is up to 30 to 40-fold greater *in vitro*. UHRF1 also interacts with proliferating cell nuclear antigen (PCNA), a cofactor of DNA polymerase in DNA replication, aiding the synthesis of leading strand of DNA helix. Therefore, the complex of UHRF1/DNMT1/PCNA was studied together and was found to be responsible for heterochromatin condensation. The disruption of UHRF1/DNMT1/PCNA complex was found to cause global DNA hypomethylation, which was an inducer of tumorigenesis. High level of hypomethylation induced by the complex disruption or DNMT1 inhibitor (5-aza) was required for the tumorigenesis, while the low level of hypomethylation by partial UHRF1 or DNMT1 deletion fails to induce tumorigenesis (Pacaud, Brocard et al. 2014).

The mechanism of heterochromatin formation associated with UHRF1 in DNA replication is proposed to occur in the following order: First, UHRF1 binds to PCNA and recognises the hemi-methylated DNA through its SRA domain. Next, UHRF1 recruits G9a, a catalase which is located near the methylated promoter of di/tri-methylated H3K9 (a transcription repressor) and binds to the PHD of UHRF1. The binding of UHRF1 to H3K9me3 will further increase the binding ability of UHRF1 to the hemimethylated chromatin. Simultaneously, ubiquitinated H3K18 (H3K18ub) catalysed by RING domain binds to the UIM of DNMT1, and then UHRF1 recruits

DNMT1 to the hemi-methylated DNA and methylate both DNA strands to transfer methylation status. Finally, UHRF1 recruits HDAC1 to deacetylate relevant histones, which in turn facilitates the heterochromatin formation, because the charge of histone tail is positive in deacetylated status, thereby increasing the binding force between deacetylated histone and negatively charged DNA strand (Unoki, Brunet et al. 2009, Sidhu and Capalash 2017), as shown in **Figure 1.5**.

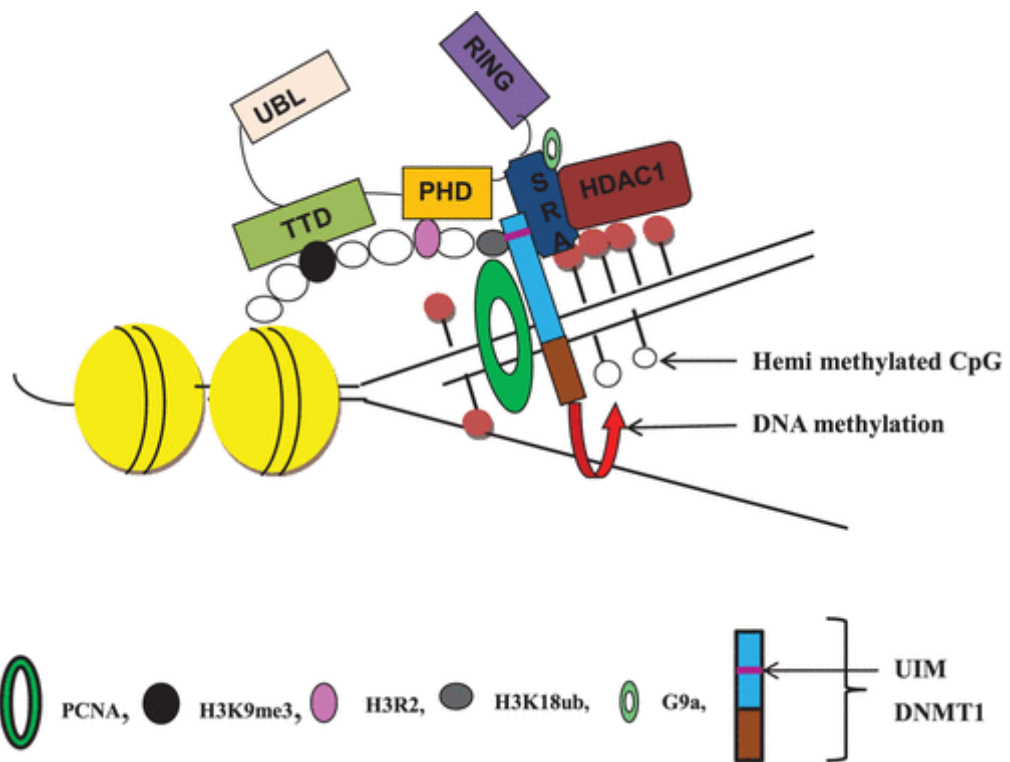


Figure 1.5 Working principle of UHRF1 with its interactive partners in DNA methylation and histone modification.

Red ball means methylated CpG islands and white ball means unmethylated CpG islands.

Yellow ball means helixed DNA. This image was adopted from (Sidhu and Capalash 2017)

with permission.

1.3 The control of UHRF1 expression

1.3.1 cell cycle and checkpoint response

The cell cycle is a series of highly ordered processes that transmits genetic material to the two duplicated daughter cells in discrete but unidirectional manner at precise time under the control of cell cycle checkpoints. Checkpoints also ensure the high fidelity of cellular events, such as DNA replication, chromosome segregation, genome surveillance and repair mechanisms by providing time, and inducing relevant gene expression in the presence of DNA replication block, spindle damage and DNA damage. Currently, there are three widely accepted checkpoints, the G1 checkpoint (also known as the restriction or start checkpoint), the G2/M checkpoint and the metaphase checkpoint (also known as spindle checkpoint), controlled by the specific Cyclins Dependent Kinases (CDKs). CDK1 can bind to cyclins A/B, CDK2 to cyclin A/E and CDK4/6 to cyclins D. These CDKs proteins are activated by binding to Cyclin proteins in cell cycle phase specific manner and terminated by the separation. Therefore, the checkpoints ensure the sequential progression of cell cycle under the control of CDK/Cyclin complex, as shown in **Figure 1.6**.

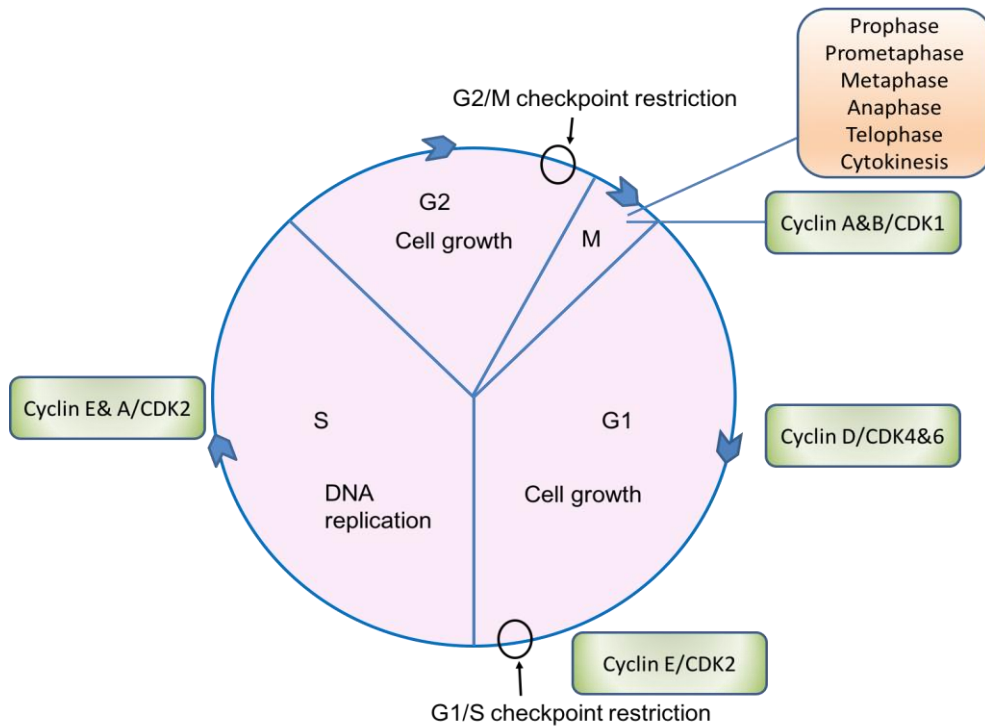


Figure 1.6 The schematic representation of cell cycle and checkpoints.

In the proliferation cells, there are 4 cell cycle phases, the G1, S, G2 and M phase. The M cell cycle phase when chromosomes are condensed, sorted and distributed into two daughter cells can be further divided into prophase, prometaphase, metaphase, anaphase, telophase and cytokinesis. Cells can also enter replicative dormancy G0 quiescence phase.

1.3.2 The involvement of UHRF1 in checkpoint response

UHRF1 is highly expressed in proliferating cells, while no UHRF1 can be found in fully differentiated tissues. The level of UHRF1 proteins is therefore regarded as positively correlated with the proliferative potential of cells (Hopfner, Mousli et al. 2000). In the observed cancer cells, UHRF1 was highly and continuously expressed through all stages of cell cycle, while in the corresponding normal cells, UHRF1 expression was cell cycle dependent with the peaks in the late G1 and G2/M phase (Mousli, Hopfner et al. 2003).

In G1 phase, the ATM kinase plays an early and pivotal role in detecting DSBs by phosphorylating itself at Serine 1981 and subsequently phosphorylating γ H2AX. *p53* could be phosphorylated by both of ATM/ATR and CHK2/CHK1 at serine 15, threonine 18 and serine 20 within the same domain. The downstream target of *p53* is cyclin E/CDK2, which can be inhibited by *p21CIP1/WAF1* proteins. This will consequently induce the sustainable G1 block by the continuous activation of pRb/E2F transcription inhibiting factors and the inhibition of CDC25a (Kastan and Bartek 2004), as shown in **Figure 1.7**.

In the intra-S phase, DNA damage induces the reversible delay of DNA replication firing by inhibiting the expression of CDK2 and the loading of pre-replication (pre-RC) complex on chromatin. The G2/M checkpoint activation is maintained by BRCA1, *p53* and the following expression of CDK inhibitors. Moreover, cells defective of other checkpoints, such as *p53* induced G1/S checkpoint loss, will selectively accumulate at G2/M boundary, indicating the activation and maintenance of G2/M checkpoint is independent of *p53*, as reviewed in (Kastan and Bartek 2004) and the schematic representation in **Figure 1.7**.

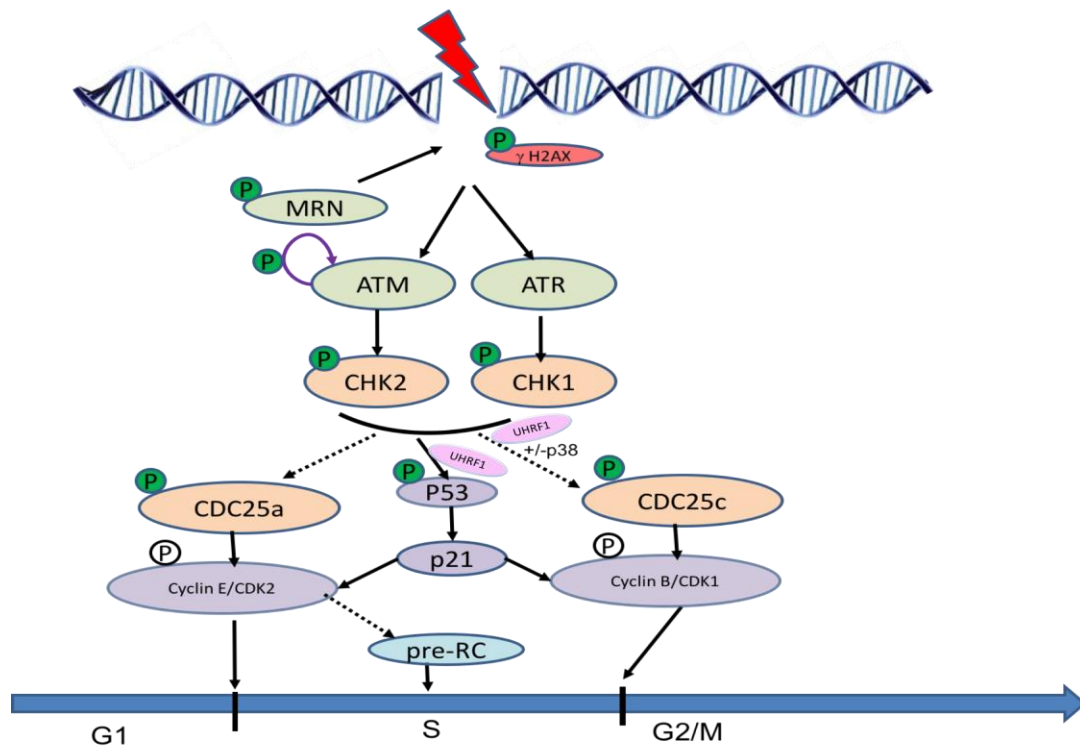


Figure 1.7 Schematic representation of G1/S and G2/M checkpoint response to DNA damage.

Green colour of p indicates phosphorylation, while white p indicates de-phosphorylation. Upon the damage of DSBs, ATM is phosphorylated by itself and MRN complex, which sequentially induces the G1/S checkpoint activation through ATM/ATR-CHK2/CHK1-CDC25a-Cyline E/CDK2 pathway. Meanwhile, UHRF1 was found to activate G1/S checkpoint in *p53/p21* dependent pathway (Arima, Hirota et al. 2004). The G2/M checkpoint signals through ATM/ATR-CHK2/CHK1 –with or without p38 kinase, UHRF1-CDC25s-Cyclin B/CDK1 at the boundary of G2/M phase (Bulavin, Higashimoto et al. 2001).

In HeLa cells, downregulation of UHRF1 activates G1/S checkpoint in *p53/p21Cip1/WAF1* dependant pathway and arrests cell cycle at S phase (Arima, Hirota et al. 2004). Consistent with this, in NIH-3T3 embryonic cells, UHRF1 was found to be essential for the S phase entry as its depletion by RNAi inhibited the replication of pericentromeric heterochromatin via hyper-acetylation on the histone of H4K8/12/16 (Papait, Pistore et al. 2007). Similarly, in terminally differentiated (TD) cells where UHRF1 expression is undetectable, the introducing of UHRF1 and Cyclin E/CDK2 expression (not alone of each) is sufficient to induce the S phase entry and initiate cell proliferation (Bonapace, Latella et al. 2002). All these evidences suggest the role of UHRF1 in the control of G1/S checkpoint.

Moreover, the expression of UHRF1 was found to be related to the activation of G2/M checkpoint, which is in parallel to its expression peak. In lung cancer H1299 cells, downregulation of UHRF1 induces cell cycle arrest at G1 and G2/M phase (Jenkins, Markovtsov et al. 2005). Inhibiting the expression of UHRF1 by shRNA in HeLa cells found hypersensitivity to γ -radiation and cell arrest at G2/M phase (Mistry, Tamblyn et al. 2010). In agreement with this, depletion of UHRF1 in HCT116 cells induces G2/M arrest and caspase 8 dependent apoptosis by the phosphorylation of γ -H2AX Ser139, CHK2 Thr68, CDC25 Ser216 and CDK1 Tyr15 regardless of the deficiency of *p53* (Tien, Senbanerjee et al. 2011). All these evidences of UHRF1 in cell cycle control indicates its essential role in cell proliferation and tumorigenesis.

Recently, overexpression of UHRF1 was found to induce both global and local DNA hypomethylation, and drives the occurrence of hepatocellular carcinoma in transgenic zebrafish cells. UHRF1 is therefore regarded as a tumour promoter (Mudbhary, Hoshida et al. 2014). Research using zebrafish model found UHRF1 overexpression processed hepatic cells into p53-mediated senescence with reduced liver size and

DNA hypomethylation through destabilizing and delocalizing DNMT1. When senescence was passed, the overexpression of UHRF1 drove the occurrence of hepatocellular cancer, suggesting the role of *UHRF1* as oncogene (Mudbhary, Hoshida et al. 2014).

After identifying the role of UHRF1 in tumorigenesis, it is important to clarify the regulation of UHRF1 expression and control them at the normal level. As the expression of proteins can be controlled at mRNA transcription level, protein translation level and protein degradation level, the abnormal regulation of UHRF1 expression is therefore discussed in promoter inhibition, *UHRF1* mRNA stability and reduced UHRF1 protein degradation.

1.3.3 The regulation of *UHRF1* promoter

At the *UHRF1* promoter binding level, the transcription of *UHRF1* is reported to be upregulated by the factors of E2F transcription factor 1 (E2F1), E2F transcription factor 8 (E2F8), specificity protein 1 (SP1), FOXM1 and NF- κ B. However, the expression of G9a and Yin Yang transcription factor 1 (YY1) were found to be able downregulate the expression of *UHRF1*, as shown in **Figure 1.8**.

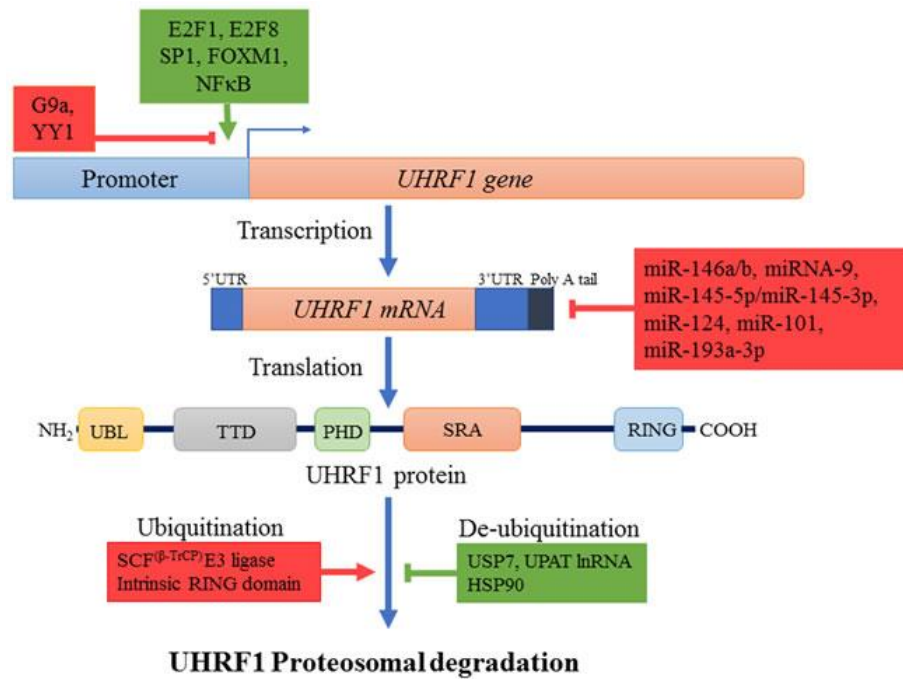


Figure 1.8 The regulation of UHRF1 expression.

Transcription factors E2F1, E2F8, SP1, FOXM1 and NF- κ b (indicating in green colour) upregulate the transcription of *UHRF1*, while G9a and YY1 (indicating in red colour) downregulates the transcription of *UHRF1*. Many microRNA, including miR-146a and miR-146b, miR-9, miR-145-5p and miR-145-3p, miR-124, miRNA-101, miR-193a-3p and miR-34a (indicating in red colour), decrease the expression of *UHRF1* by destabilizing *UHRF1* mRNA and binding to the 3'-UTR of *UHRF1*. SCF β -TrCP1/2 and intrinsic RING finger domain of UHRF1 (indicating in red colour) catalyze UHRF1 ubiquitination and proteasomal degradation, while USP7, UPAT lncRNA and HSP90 (indicating in green colour) stabilize UHRF1 by catalysing deubiquitination of UHRF1. This image was adopted from (Ashraf, Ibrahim et al. 2017) with permission.

E2F1 was the earliest *UHRF1* promoter regulator being reported in 2003 after finding there were several E2F binding sites in the promoter region of *UHRF1*. Through comparing the effect of E2F1 overexpression on normal cells and cancer cells, E2F1 overexpression was found to upregulate the expression of *UHRF1* by 10-fold and 38.1% in IMR90 and WI38 normal cells, whereas 20.9% and 13.3% in U2OS and SaOs cancer cells respectively, indicating the upregulating role of E2F1 to *UHRF1* with an efficiency depending on the cancer status of cell lines (Mousli, Hopfner et al. 2003). Another E2F transcription factor E2F8 was found overexpressed in tumour tissues comparing with normal tissues. Downregulating the expression of E2F8 by siRNA reduced UHRF1 expression by 60% to 70% through binding to the promoter region of *UHRF1* in lung cancer A549 cells. Moreover, co-downregulating the expression of E2F1 and E2F8 displayed no additive effect on the inhibiting of UHRF1 expression, indicating that E2F8 is directly regulating the expression of UHRF1 in the same pathway as E2F1 (Park, Platt et al. 2015).

Thyroid hormone (T3) and its receptor (TR) plays important role in the tumour suppressing and their abnormal expression is related to the tumour transformation. As aberrant epigenetic regulation of tumour suppressor genes also promotes cancer progression, T3/TR and UHRF1 were therefore studied together and found T3 negatively regulates the expression of UHRF1 both *in vitro* and *in vivo*. The negative regulation of T3 on UHRF1 was indirect and mediated by Sp1 which binds to the promoter region (2664/2505) of *UHRF1*. Additionally, the downregulation of UHRF1 by T3/TR results in the induction of tumour suppressor gene *p21* and the inhibition on cell proliferation in HepG2 hepatic cancer cells, suggesting T3/TR signalling inhibits hepatic cancer cell growth via repressing UHRF1 and activating *p21* expression (Wu, Cheng et al. 2015).

FOXM1 is a member of Forkhead family of transcription factors and plays an important role in many cellular processes through silencing or activating specific transcription pathways. In HeLa and HEK293 cells, UHRF1 was found enriched together with FOXM1 on inverted CCAAT motifs, indicating the possible role of UHRF1 in providing genomic binding sites for FOXM1 (Sanders, Gormally et al. 2015).

Finally, CD47, an integrin-associated protein on the cell surface, is overexpressed in cancer cells which consequently enables cancer cells to escape the invasion from macrophage and survive. Therefore, CD47 were used to investigate the role of UHRF1 in cancer occurrence. In astrocytoma cell line, it was observed that CD47 could upregulate the expression of UHRF1 via the activation of NF- κ B transactivation and downregulate the expression of *p16INK4A* (a tumour suppressor gene). In contrast, inhibiting CD47 resulted in the downregulation of UHRF1 and re-expression of *p16INK4A*, suggesting CD47 as potential target for cancer therapy functions via decreasing *UHRF1* and increasing *p16INK4A* expression (Boukhari, Alhosin et al. 2015).

UHRF1 can recognise and bind to H3K9me_{2/3} via the cooperative work of TTD and PHD, thereby allowing the binding to hemimethylated DNA via SRA domain. Therefore, it is important to know relationship between UHRF1 and H3K9 methyltransferase (HMTase) G9a mediated transcription repression. Using H1299 lung cancer cells, *UHRF1* is found to be transcriptionally repressed by G9a by directly binding to promoter region of *UHRF1*. Further study about YY1 found the effects of transcription repression on *UHRF1* are in order of G9a and YY1, YY1 alone and G9a alone, suggesting YY1 functions as a direct inhibitor of *UHRF1*

transcription and as a mediator recruits G9a to *UHRF1* promoter region (Kim, Son et al. 2015).

1.3.4 The regulation of *UHRF1* mRNA by miRNA

miRNA, as noncoding sequence, binds to the 3'-untranslated region (3'-UTR) of their target mRNA resulting in the destabilizing of mRNA or the inhibited translation activities. As *UHRF1* is abnormally highly expressed in cancer cells, it is speculated that most *UHRF1* mRNA experienced abnormal miRNA regulation. Until now, known miRNAs contributing to the repression of *UHRF1* mRNA include miR-146a and miR-146b, miR-9, miR-145-5p and miR-145-3p, miR-124, miRNA-101, miR-193a-3p and miR-34a, as shown in **Figure 1.8**.

miR-146a and miR-146b, tumour suppressor genes in gastric cancer, were found to repressing function on the expression of *UHRF1* through simultaneously binding to the 3'-UTR of *UHRF1*. In GC9811-P gastric cancer cells, overexpression of wild type miR-146a and miR-146b show significantly reduced expression of *UHRF1* mRNA and proteins, whereas no significant changes were found in 3'-UTR with mutant binding sites of miR-146a and miR-146b, indicating that miR-146a and miR-146b suppressed the *UHRF1* expression through directly binding to the 3'UTR of *UHRF1*. miR-146a and miR-146b were also found to be negatively related to gastric cancer metastasis and invasion through inhibiting *UHRF1* and reversing the promoter methylation status of metastasis related genes (*Slit3*, *CDH4*, and *RUNX3*). Conversely, silencing the expression of miR-146a or miR-146b enhances the expression of *UHRF1*. Tissue study found significantly downregulated expression of miR-146a and miR-146b and upregulated expression of *UHRF1* in gastric cancer tissues comparing with adjacent non-tumour tissues, further confirming the role of

miR-146a and miR-146b in negatively regulating the expression of UHRF1 in gastric cancer. (Zhou, Zhao et al. 2013).

miR-9, a tumour suppressor gene in colorectal cancer, was found to be negatively related to the expression of UHRF1 in colorectal cancer tissues. The upregulated expression of miR-9 was found to inhibit colorectal cancer cell proliferation and promote cell apoptosis through binding to 3'-UTR of *UHRF1* and decreasing its expression. (Zhu, Xu et al. 2015).

In the same way, miR-145-5p and miR-145-3p are tumour suppressor gene in bladder cancer. miR-145-5p is the guide-strand of miR-145 which binds to the target RNA and induces gene silencing, whereas miR-145-3p is the passenger strand which will be degraded. Both of miR-145-5p and miR-145-3p can downregulate the expression of UHRF1 by directly bounding to the specific sites of 3'-UTR of *UHRF1* mRNA, whereas no synergistic effects were found between miR-145-5p and miR-145-3p. miR-145-5p and miR-145-3p were also found to significantly suppress cancer cell growth, migration and invasion, and induce cell apoptosis as opposed to the effects of UHRF1. (Matsushita, Yoshino et al. 2016) Another bladder cancer gene suppressor, miR-124 was found to be inversely expressed with UHRF1 in bladder cancer tissues and the overexpression of mi-124 inhibits cancer cell proliferation, migration, invasion and vasculogenic mimicry *in vitro* similar as the phenotype in *UHRF1* knockdown cells. miR-124 could also repress the expression of *UHRF1* mRNA by directly binding to 3'-UTR of *UHRF1*. Consistent with this, overexpression of UHRF1 could reverse the inhibitory effect of miR-124 on cell proliferation, migration, invasion and vasculogenic formation (Wang, Wu et al. 2015).

miR-101, as tumour suppressor gene, showed the most dramatic downregulation in renal cancer tissues among 232 miRNA candidates and the inhibitory effect of miR-101 on cell proliferation, migration and invasion *in vitro* as the phenotype of *UHRF1* knockdown cells could be restored by the introducing of exogenous miR-101. MiR-101 was also found to downregulate the expression of UHRF1 in both mRNA and protein levels by directly binding to the 3'-UTR of *UHRF1*. Knockdown *UHRF1* also suppressed the pathway of nucleotide excision repair and mismatch repair (Goto, Kurozumi et al. 2016).

miR-193a-3p, a tumour suppressor gene of non-small cell lung cancer (NSCLC), inhibited the metastasis of NSCLC by downregulating the expression of several tumour related proteins including UHRF1, but the interaction between miR-193a-3p and UHRF1 remains to be elucidated (Deng, Yan et al. 2015).

In addition, miR-34a, a tumour suppressor gene in many cancers, is suggested to decrease the expression of UHRF1 with the help of TQ (thymoquinone), the most biologically active component in black cumin oil. This is because TQ could increase the expression of miR-34a and inhibiting the expression of UHRF1 in *p73* dependant pathway in *p53* deletion cells (Alhosin, Omran et al. 2016).

1.3.5 The regulation of UHRF1 protein

The regulation of UHRF1 proteins is controlled by the coordination of enzymes functioning in ubiquitination and deubiquitination, which subsequently activates or silences the degradation by proteasomes. Until now, known molecules regulating the degradation of UHRF1 include SCF β -TrCP1/2 E3 ligase, Ubiquitin Specific Peptidase 7 (USP7), UHRF1 Protein Associated Transcript (UPAT) and 90-kDa heat-shock protein (HAP90).

The first 300 amino acids of UHRF1, which involves the elements of DSG degron (a portion of protein regulating degradation), are observed to be essential for UHRF1 stability rather than its intrinsic activity to ubiquitinate itself by RING finger domain or UBL domain. Further study found the phosphorylation of Ser108 of UHRF1 within the DSG degron determines the interaction between UHRF1 and SCF β -TrCP1/2 E3 ligase, which is a mediator of UHRF1 proteasomal degradation by ubiquitination without effects on the *UHRF1* mRNA (Chen, Ma et al. 2013).

Deubiquitinase USP7 was found to interact with UHRF1 by maintaining its deubiquitinated status and preventing it from auto-ubiquitination by its RING domain or the degradation by proteasome (Felle, Joppien et al. 2011). Later study found the activity of deubiquitination between UHRF1 and USP7 can be abolished by the mutants of UHRF1 (K659E), indicating the site determining USP7-UHRF1 interaction is at Spacer region of UHRF1. Further study found the phosphorylation of UHRF1 Ser652 (inside Spacer region), catalysed by CDK1-cyclin B, was essential for disrupting the interaction between USP7-UHRF1 and subsequently decreasing the stability of UHRF1 comparing with the group with phosphorylation resistant Ser652 of UHRF1 (Ma, Chen et al. 2012), indicating the effect of USP7 in maintaining the dynamic balance of UHRF1 between ubiquitinated and deubiquitinated statuses. Conformational study of USP7-UHRF1 found the interaction of USP7-UHRF1 opens the closed conformation of UHRF1 by separating the association of Spacer region and TTD within UHRF1 and allowing histone H3K9me3 binding. Consistently, the introduction of USP7 interaction defective mutants to UHRF1 significantly reduces the association of UHRF1 to chromatin (Zhang, Rothbart et al. 2015), indicating the role of USP7 in mediating UHRF1 to chromatin through the readout of histone codes.

UPAT is one member of long noncoding RNAs (lncRNAs) and was required for the tumorigenesis of colorectal cancer cells. Study found UPAT could interfere β -TrCP1/2 E3 ligase mediated ubiquitination at Lys-663 of UHRF1, consequently stabilizing UHRF1. However, whether the epigenetic characteristics are required for the formation of USP7-UHRF1 remains unknown. Consistent with this, the growth defects caused by UPAT deficiency can be partially rescued by overexpression of UHRF1, indicating UHRF1 is one of target genes of UPAT. However, many genes were found to be regulated by UPAT in an UHRF1-independent manner, indicating UPAT may have other important target molecules (Taniue, Kurimoto et al. 2016)

HSP90 was found to downregulate the expression of UHRF1 in the manner of HSP70 (70-kDa heat-shock protein) dependent ubiquitination and subsequent proteasomal degradation via a post-transcriptional mechanism rather than modifications on *UHRF1* mRNA. The ubiquitination of UHRF1 is independent from UHRF1 RING finger domain and SCF β -TrCP1/2 E3 ligase. It is also suggested that the effect of HSP90 on repressing cell proliferation may be mediated by the degradation effect on UHRF1 (Ding, Chen et al. 2016).

1.3.6 UHRF1 mediated silencing of tumour suppressor genes

After performing the large scale meta-analysis of methylation profiles of cancer and normal cells, it is observed that epigenetic reprogramming contributes to the cancer development by modifying the gene transcription factors (Moarii, Boeva et al. 2015), and the dysregulation of epigenetic codes resulting from genetic mutation or epigenetic modification on themselves allows the abnormal cell survival (Timp and Feinberg 2013). UHRF1, as epigenetic adaptor between DNA methylation and histone modification, has drawn great attention for its functions in regulating gene

transcription, maintaining target gene and its own epigenetic state. The localization and stabilization of UHRF1 on TSGs retains them in a repressive state through the coordination with DNMT1 caused demethylation and HDAC1 caused histone acetylation. In this section, the effects of UHRF1 on TSGs will be demonstrated.

In colorectal cancer, the high expression of UHRF1 was found to be closely related to the low expression of *PPARG* (Peroxisome proliferator-activated receptor gamma). UHRF1 promoted cell proliferation and migration through silencing the *PPARG*, which was an important step for colorectal cancer progression. Ectopic expression of UHRF1 could induce the methylation of *PPARG* promoter and the negative histone marks, while downregulation of UHRF1 induces *PPARG* promoter demethylation and activates histone modification (Sabatino, Fucci et al. 2012).

PML (promyelocytic leukemia) protein was originally identified as a tumour suppressor in acute promyelocytic leukemia and was later found to be related to tumorigenesis in many cancers. The ubiquitination driven degradation of PML was found to be mediated by the RING finger domain of UHRF1 which binds to the N-terminus of PML proteins. Furthermore, the effects of UHRF1 downregulation on cancer cell migration and capillary tube formation was found to be related to the increased accumulation of PML proteins (Guan, Factor et al. 2013).

Carcinogenesis of non-small cell lung cancer is also related with the silencing of tumour suppressor genes, including *RASSF1*, *CYGB*, and *CDH13*. In A549 cells, downregulation of *UHRF1* was observed to consistently reduce the methylation of the promoters of *RASSF1*, *CYGB*, and *CDH13*, while these promoters were originally frequently hyper-methylated. Moreover, downregulation of *UHRF1* showed no change on the expression levels of *DNMT1* and *DNMT3A* other than *DNMT3B*. The

direct or selective advantage of DNMT3B on taking over cell population remains unknown. Therefore, it is suggested that the incomplete hypomethylation on promoters of *RASSF1*, *CYGB*, and *CDH13* were maintained by DNMTs in the presence of low abundance of UHRF1 protein (Daskalos, Oleksiewicz et al. 2011).

3OST2, as tumour suppressor gene, could be silenced by the promoter methylation in many cancers. In hepatic cancer tissues, *3OST2* is frequently methylated comparing with respective non-cancerous tissues. This frequent methylation of *3OST2* could be completely reversed through decreasing the binding the UHRF1 to *3OST2* promoter upon the combatant treatment of 5-Aza-CdR (DNA methylation inhibitor) and trichostatin A (HDAC inhibitor), providing new insight for *3OST2* related cancer therapy (Chen, Zhang et al. 2015).

In gastric cancer cells, inhibition of UHRF1 by siRNA reversed the promoter methylation status of TSGs, including *Slit3*, *CDH4*, and *RUNX3* (Zhou, Zhao et al. 2013). Further study by this group about UHRF1 downregulation found the reactivation of another 6 TSGs, including *CDX2*, *CDKN2A*, *PPARG*, *BRCA1*, *FOXO4*, and *PML* in gastric cancer cells (Zhou, Shang et al. 2015).

1.4 Role of UHRF1 in genomic stability

1.4.1 Involvement of UHRF1 in DNA repair

Base excision repair (BER) is the primary DNA repair machinery underlying DNA damage caused by alkylating and oxidative agents and/or by deamination resulting in the base modification. This base modification can be mutagenic and/or cytotoxic depending on the interaction with the template DNA during the processes of DNA replication and DNA transcription. MPG (N-methylpurine DNA glycosylase), the first

enzyme involved in the BER pathway, is responsible for the recognition and excision of damaged bases through generating an apurinic/aprimidinic (AP) site and activating the downstream proteins. Interestingly, MPG overexpression or underexpression both could increase the risk of cancer occurrence, suggesting other proteins are involved in maintaining the dynamic balance of MPG (Jacobs and Schar 2012). Using co-immunoprecipitation assay and mass spectrometry (IP/MS), UHRF1 was found to co-localize with MPG in different cancer cells rather than non-cancer cells in p53 independent manner, suggesting the critical role of UHRF1 in BER (Jacobs and Schar 2012).

DNA double-strand breaks (DSBs), a serious hazard to cell viability and genomic integrity, are mainly repaired by non-homologous end joining (NHEJ) and homologous recombination (HR). NHEJ is regarded as the error-prone repair pathway in repairing the blunt end of broken DNA without homologous DNA as template, whereas HR is considered to be the error free mechanism underlying DSBs repair which employs homologous DNA in the sister chromatid as template to repair and restore genomic integrity. The occurrence of NHEJ or HR was cell cycle dependent, with NHEJ functioning throughout the cell cycle and HR in S and G2 phases (Fragkos, Ganier et al. 2015).

In G1 phase, RIF1(replication timing regulatory factor 1) prevented 5'end excision of broken DNA by binding to the DSB sites and interacting with 53BP1 and promoted NHEJ. In S/G2 phase, RIF1 was removed in BRCA1-dependent manner and thereby promoted HR by antagonizing 53BP1-dependent NHEJ (Escribano-Diaz, Orthwein et al. 2013, Zimmermann, Lottersberger et al. 2013). UHRF1 was identified as a deciding factor for the choice between NHEJ and HR through interaction with BRCA1 and 53BP1. Mechanistically, in S phase of HEK293T cells, UHRF1 was

phosphorylated by CDK2/cyclin A at Ser674 and was subsequently recruited to the DSBs sites through the recognition of Ser674p by BRCT domain of BRCA1. Subsequently, RIF1 was ubiquitinated by UHRF1 and disassociated from 53BP1, thereby switching DNA repair from NHEJ to HR (Zhang, Liu et al. 2016).

UHRF1 was also found to participate in the Ku heterodimer protein complex (Ku70/Ku80) catalysed NHEJ pathway. In ESCC TE-1 cells, downregulating the expression of UHRF1 increased cell radio-sensitivity and apoptosis, and alleviated G2/M phase arrest caused by irradiation. Mechanistically, UHRF1 inhibition increased the level of γ -H2AX after irradiation rather than initial γ -H2AX through further downregulating the expression of DNA repair proteins of Ku70/Ku80, comparing with the decreased expression of Ku70/Ku80 proteins before irradiation (Li, Meng et al. 2011, Yang, Wang et al. 2013).

Interstrand crosslinks (ICLs) of DNA helix is another type of DNA lesion that is extremely toxic to the genome. Repair of ICLs also has two distinct pathways: during S phase when the replication fork encountering with ICL, HR is initiated to repair the damaged double strand break of ICLs with the help of the sister chromatid as template, while during G0/G1 phase or S phase, repair mechanism of ICLs contains nucleotide excision repair and lesion bypass syntheses, as shown in **Figure 1.9**.

UHRF1 was found to act as the scaffold for the recruitment of ICL repair nuclease to the DNA damage sites by directly binding to the ICLs sites under the sensing of SRA domain. This function of UHRF1 in ICLs repair was in parallel to the FA pathway (Liang, Zhan et al. 2015, Tian, Paramasivam et al. 2015). Additionally, the downregulation of UHRF1 reduced the localization of FANCD2 on ICLs sites,

suggesting the binding of UHRF1 with chromatin was essential for the recruitment of FANCD2 and the initiation of the following repair events (Liang, Zhan et al. 2015).

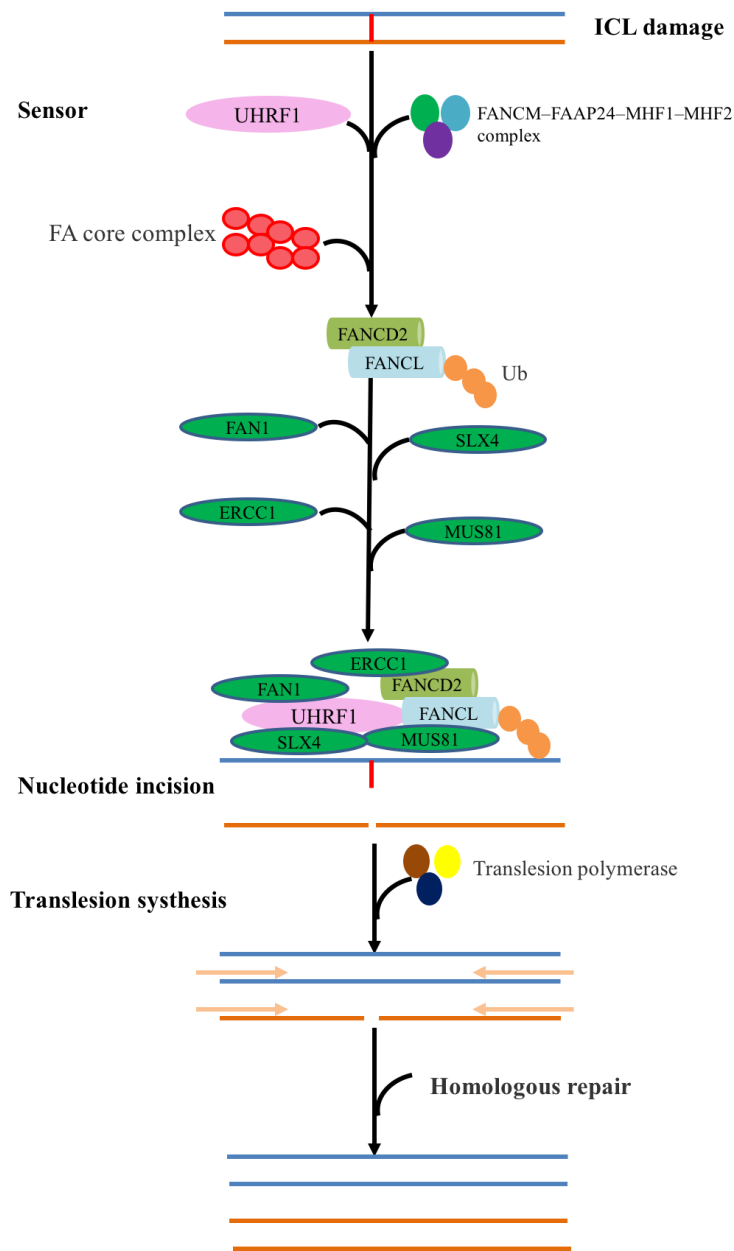


Figure 1.9 Schematic signal pathway of ICL repair.

ICL damage is recognised by FANCM-FAAP24-MHF1-MHF2 complex and UHRF1 with the following activation of FA core complex and mono-ubiquitination of FANCD2-FANCL heterodimer. The loading of ubiquitinated FANCD2 on ICL region works as a platform for the recruitment of SLX1, FAN1, ERCC1 and MUS81 resulting in the nucleotide incision. The unhooked DNA is repaired by translesion synthesis polymerase through lesion bypass, extension and ligation. The restored DNA double strand serves as a template for HR (Ceccaldi, Sarangi et al. 2016)

1.4.2 Involvement of UHRF1 in DNA replication

Heterochromatin formation is critical for the suppression of transcription, segregation of chromosomes and the maintenance of genome stability. A key event of heterochromatin formation is the underacetylated status of histone H4, binding of which is essential for maintaining the compacted and silenced regions of heterochromatin. The activation of DNA origin can be explained by **Figure 1.10**.

The licensing of replication origins is restricted in G1 phase and is dependent on the sequential loading of pre-RC complex in the order of ORC, CDC6, CDT1 (CDC10-dependent transcript 1 and MCM (mini-chromosome maintenance) helicase complex, which contains six subunits of MCM2-7.

The activation of origin involves the formation of pre-IC (pre-initiation complex) and the activation of MCM complex. Activation of pre-IC is triggered in G1/S phase transition by DDK (DBF-dependant kinase) and CDKs resulting in the occurrence a function replisome in S phase. The DDK and CDKs could promote their own binding by phosphorylating the replication factors of MCM10, CDC45, RECQL4 (ATP dependent DNA helicase Q4), treslin, GINS, TOPBP1 and DNA polymerase ϵ (Pol ϵ). The DDK and CDKs could also activate the residues of MCM complex by phosphorylation, resulting in the activation of these helicases and the unwinding of DNA. UHRF1 is required for maintaining the binding of pre-RC at DNA replication origins until after the initiation of DNA replication (Taylor et al., 2013).

The firing of origins happens in S phase. Activated MCM hexamer divides into two hexamers moving to two replication forks at replication origins. The activation of MCM helicase complex induces the recruitment proteins including RFC (replication

factor C), PCNA, RPA (replication protein A) and other DNA polymerases. This recruitment is

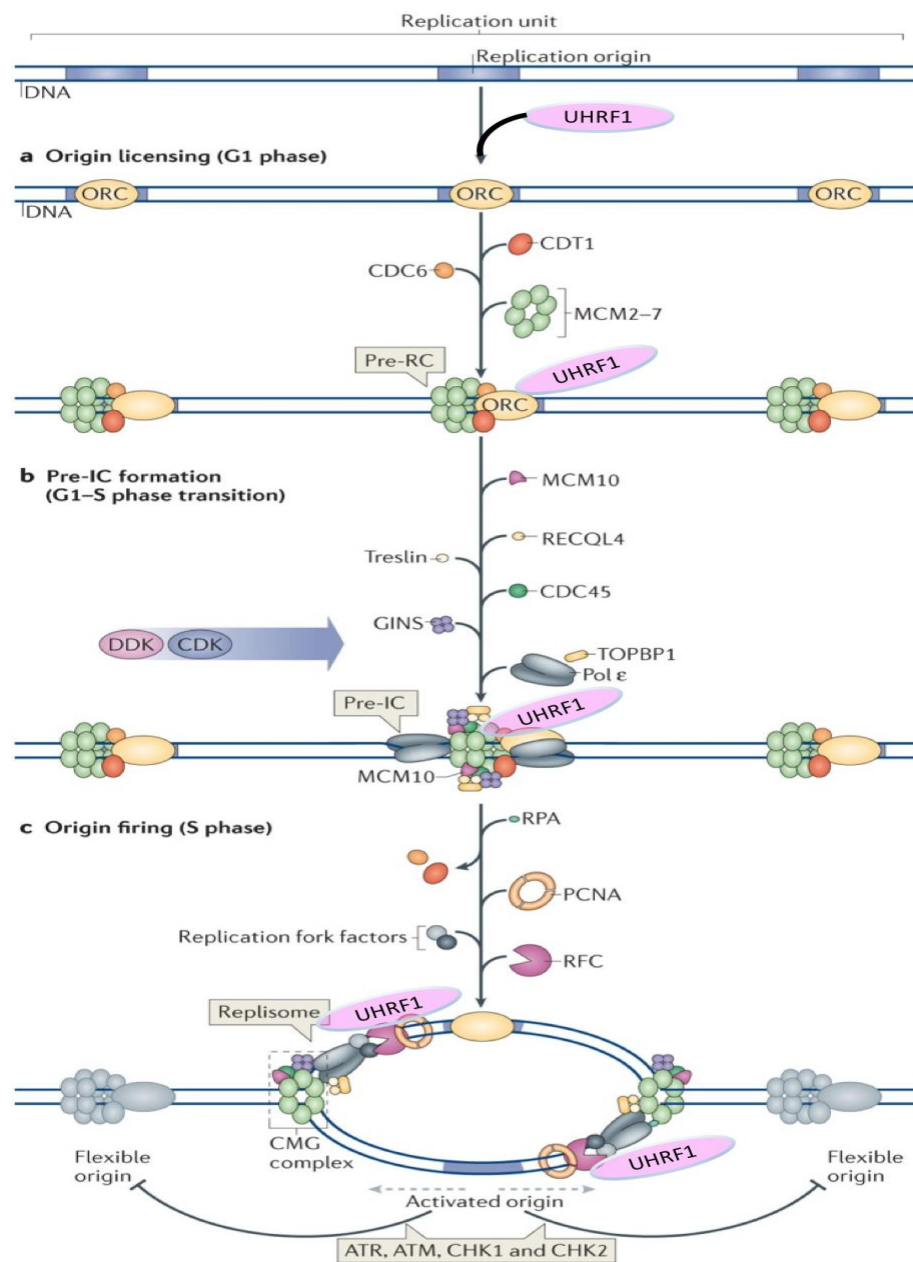


Figure 1.10 Schematic representation of DNA replication origin activation.

(a). Origin licensing and DNA helix loading. (b). Origin activation and DNA helix loading and activating, resulting in the unhooking of DNA. (c). The firing of origins and the formation of replisome fork. This image is modified from (Fragkos, Ganier et al. 2015) with permission.

essential for the convert of conformational alteration of pre-IC into two functional replication forks in opposite direction from the activated origins with the replisome at each replication fork. The functional helicase at replication forks are CMG complex (CDC45, MCM hexamer and GINS complex). There are only 1-3 replication flexible origins being activated on average within one replication unit, the replisome is therefore only formed in the activated origins. The inhibition of adjacent origins within one replisome is partially controlled by ATM/ATR-CHK1/CHK2. However, the selection, activation or silencing of flexible origins remain unknown (Fragkos, Ganier et al. 2015).

In NIH-3T3 cells, knockdown of UHRF1 caused hyperacetylation of histone H4K8/12/16 and increased pericentromeric major satellite transcription levels, indicating the critical role of UHRF1 in heterochromatin formation. Furthermore, downregulation of UHRF1 inhibits heterochromatin replication in mid-S phase and blocks cells at the early S phase of cell cycle (Papait, Pistore et al. 2007), suggesting a role of UHRF1 in inducing a more open chromatin conformation (Papait, Pistore et al. 2008). As little effect of *UHRF1* knockdown on euchromatin can be found comparing with significantly suppression on heterochromatin (Papait, Pistore et al. 2007), it is, therefore, possible that the function of UHRF1 is confined to heterochromatin instead of euchromatin, or low level of UHRF1 is still sufficient to maintain the less compacted regions of the genome in the early S phase (Taylor, Bonsu et al. 2013).

To further study the involvement of UHRF1 in DNA replication, UHRF1 was studied using *Xenopus laevis* egg extract system, a model that is absent from transcriptional events. Depletion of UHRF1 inhibited the initiation of chromatin DNA replication, indicating that UHRF1 was required before replication licensing for the recruiting and loading of chromatin replication proteins, including ORC (origin recognition

complex). Further study found, UHRF1 depletion also affected the chromatin DNA replication after origin licensing, indicating a role of UHRF1 in maintaining the association of replication required components and chromatin (Taylor, Bonsu et al. 2013).

1.5 Clinical usage of UHRF1

1.5.1 Modulation of UHRF1 by natural polyphenols

The extracts of natural compounds targeting the epigenetic codes in cancer cells had been applied into clinical work for preventing or treating cancer, mainly as complementary or alternative medication. So far, only one UHRF1 direct inhibitor (NSC232003) was reported. NSC232003, a uracil derivative, could structurally fit in the 5-methylcytosine pocket in the SRA domain of UHRF1 and reduce the interaction between DNMT1 and UHRF1 by 50%. NSC232003 was also reported to induce the global DNA demethylation, possibly through blocking the recognition of SRA domain to hemimethylated DNA (Myriantopoulos, Cartron et al. 2016). Further study is required to clarify the molecular mechanism of NSC232003 in epigenetic regulation and its side effects on normal cells.

There are also natural polyphenols targeting UHRF1, possibly non-specifically through TSGs dependant pathway, including shikonin, naphthazarin, ECGG (epigallocatechin-3-gallate), luteolin and RWPs (red wine proteins), resulting in the inhibition of cancer development.

Shikonin, a natural naphthoquinone extracted from Chinese medicine Zi Cao, could downregulate the expression of UHRF1 and the binding of UHRF1/DNMT1/3a/3b complex to *p16INK4A* promoter in MCF-7 and HeLa cells, thereby inducing the

reactivation of *p16INK4A* and cell apoptosis. Shikonin induced apoptosis was also related with the downregulated expression of anti-apoptosis protein Bcl-2 and enhanced cleavage of apoptosis effector caspase 3 (Jang, Hong et al. 2015), which was possibly the downstream targets of UHRF1 in *p53* independent apoptosis (Tien, Senbanerjee et al. 2011).

Similarly, naphthazarin is a natural derivative from lipophilic red pigment with activities in cytotoxic effects in cancer cells. Molecular study found naphthazarin could enhance the disassociation of UHRF1, DNMT1 and HDAC1 from *p21* promoter and cell apoptosis in *p53/p21* dependent manner in MCF-7 cells, indicating the role of naphthazarin as a potential radio-sensitizer in the treatment of breast cancer (Kim, Park et al. 2015).

EECG extracted from green tea was found to prevent skin cancer, molecularly through reactivating the expression of *p16INK4A* and *p73*, thereby inducing G1 phase cell cycle arrest and apoptosis. The upregulation of *p16INK4A* and *p73* by EECG was activated by the downregulation of by SRA domain of UHRF1 (Achour, Mousli et al. 2013), possibly through the counteracted recruitment role of UHRF1 on DNMT1/3/3b and the binding role of UHRF1 to histone H3K9 and H4K5 (Nandakumar, Vaid et al. 2011).

Similar results were found in luteolin and RWPs. Luteolin was another natural compound that is capable in inducing cytotoxicity and cell cycle perturbation in a dose-dependent manner. Mechanistically, luteolin can trigger the cleavage of PARP and inhibit the expression of UHRF1 and DNMT1, which subsequently upregulate the expression of *p16INK4A*, thereby inducing apoptosis of BE colorectal cancer cells (Krifa, Leloup et al. 2014). Consistently, RWPs administrated with diets was found to

have protective effects on colorectal carcinogenesis. Cytological study found RWPs downregulated the expression of UHRF1, followed with the reactivation of the cell cycle regulator of *p21Waf1/Cip1* and TSGs including *p16INK4A*, *p53*, and *p73* (Walter, Etienne-Selloum et al. 2010).

There are also plants extracts that regulate the expression of DNMTs and TSGs in a similar way as UHRF1 inhibitors, although the involvement of UHRF1 remains to be elucidated. Considering the role of UHRF1 in recruiting DNMTs to the promoter of TSGs and subsequent reactivation of TSGs by demethylation, the study of these natural compounds in relating to UHRF1 are worthy to carry out.

Population in Southern Italy with local apples as administrative diet were observed lower incidence of colorectal cancer than elsewhere globally. Therefore, a biological study was conducted to find the molecular mechanism of APE (Annurca polyphenol extract) on cancer prevention. It was found that APE could inhibit the posttranslational expression of DNMT1/3b (slightly weaker than DNMT1 inhibitor 5-aza), while downregulating the methylation of TSGs including p16 INK4A and p14ARF. APE was also found to induce the cell apoptosis but no effect on S phase entry defects was found possibly due to the enhanced expression of *p53* (Fini, Selgrad et al. 2007).

Additionally, a phase I pilot study demonstrated the effect of intaking black raspberries (BRBs) on preventing colorectal cancers by decreasing the expression of DNMT1 and the reactivation of TSG (Wang, Arnold et al. 2011). suggesting the therapeutic potential of UHRF1 in enhancing cell apoptosis by decreasing the recruitment of DNMT to TSGs promoter regions. TQ, the most biologically active component in black cumin oil, could induce *p53/p21Cip1/WAF* dependent G1/S cell

cycle arrest and apoptosis by activating miR-34a and inhibiting the expression of UHRF1 in *p73* dependent pathway (Alhosin, Omran et al. 2016).

1.5.2 UHRF1 as universal biomarker for cancer

Diagnostic detection and monitoring of cancer are essential parts of successful cancer management. The early stage of cancer diagnosis decides the potential for therapeutic interventions but is always delayed due to the asymptomatic characteristics of most cancers, leading to the poor survival outcome of cancer patients. The application of sensitive and specific biomarkers helps the screening, diagnosis, prognosis and monitoring of cancers, but it is still very hard to diagnostic cancer in early stage. UHRF1 had been validated to be significantly increasingly expressed in various cancer tissues with readily quantifiable measurements to estimate the progression and recurrence of cancers (as shown in Table 1), making it a powerful tool as a biomarker in cancer management.

Moreover, in lung cancer tissues, the overexpression of UHRF1 in NSCLC tissues was in coordination with DNMT1/3a/3b and was observed to be together with another 5 survival related genes, *ABCC4*, *ADRBK2*, *KLHL23*, *PDS5A* and *ZNF551* as gene signature to estimate the overall survival of NSCLC patients (Unoki, Daigo et al. 2010, Daskalos, Oleksiewicz et al. 2011, Huang, Cheng et al. 2016).

In breast cancer, there were conflicting reports about the relationship of UHRF1 overexpression with histological grades and PR status (Geng, Gao et al. 2013), which may come from the pathological types or treatment stages of breast cancer. Specially, by subcutaneous injection of MCF-7 cells into 6 to 8-week-old male athymic nude mice, downregulating the expression of UHRF1 was found to enhance the cell sensitivity to cisplatin and inhibit the tumour growth *in vitro* and *in vivo*, indicating

the potential of UHRF1 as treatment target of high efficiency and high specificity in breast cancer cells (Fang, Shanqu et al. 2012) .

Cancer	Potential of UHRF1	overexpression ratio of UHRF1	
Lung cancer	early pathological stage, histological type, gender, smoking history, TNM stage, metastatic status and poor prognostic consequence.	100% of 378	(Unoki, Daigo et al. 2010) (Daskalos, Oleksiewicz et al. 2011) (Huang, Cheng et al. 2016)
Liver cancer	microvascular invasion, higher AFP level, early but not late tumour recurrence and poor 5-year survival period (29.8% vs 81%); distant metastasis, cancer area and HBV infection; tumour differentiation, TNM stage	65% of 71 57.8%:32.7% 68%:36% 75.7% of 70	(Mudbhary, Hoshida et al. 2014) (Liu, Ou et al. 2017) (Liang, Xue et al. 2015) (Wu, Cheng et al. 2015)
Gastric cancer	poor differentiation, local and distant metastasis but not age and sex; deep tissue invasion (T3-T4) and late TNM stage (stages III–IV) but not tumour size and location, poor 5-year survival rate (19% vs 38%)	86% (89/106) 82.4% of 238	(Zhou, Zhao et al. 2013) (Zhou, Shang et al. 2015)
Colorectal cancer	distal metastasis and poor Dukes staging; more in right hemicolon.	65% of 134 (mRNA) 34% vs 9% (protein) 152 of 231 (65.8%) 87.5% adenoma	(Wang, Yang et al. 2012) (Kofunato, Kumamoto et al. 2012)
Breast cancer	differentiated grades, but not ER, PR or menopausal status or age; c-erbB2 and PR status, staging, lymph node metastasis and poor survival, but not the expression of <i>p53</i> , VEGF, EGFR or E-cadherin and tumour histology grade	5%~15% vs <1% 24%~69%	(Mousli, Hopfner et al. 2003) (Unoki, Nishidate et al. 2004) (Geng, Gao et al. 2013)
Oesophageal cancer	poor ESCC cancer cell differentiation and lymph nodes metastasis but not age, gender and tumour location, radio-resistance in 80.30%. poor 5-year survival (25%) but not tumour size, TNM staging or microscopic lympho-vascular invasion	67% of 61	(Yang, Wang et al. 2013) (Nakamura, Baba et al. 2016)
Pancreatic cancer	Poor survival outcome	57.6% of 158 86% vs 20%	(Cui, Chen et al. 2015). (Abu-Alainin, Gana et al. 2016)

Prostate cancer	Survival periods (10.4 vs 12.4 years), 5-year BCR free time in 12.4% vs 51.8%.	50% of 226 mRNA,	(Babbio, Pistore et al. 2012) (Wan, Yang et al. 2016)
Cervical cancer		71.4%~97.6% of 99	(Lorenzato, Caudroy et al. 2005) (Ge, Yang et al. 2016)
Bladder cancer	stage, grade, and disease progression after transurethral resection; mean survival time of 42.59 vs 71.36 months, the recurrence rate of 41/70 vs 29/70	High expression	(Unoki, Kelly et al. 2009) (Yang, Zhang et al. 2012)
Medulloblastoma	poor overall survival and progression free survival rate	100% of 168	(Zhang, Cai et al. 2016)
Gallbladder cancer	advanced stage and lymph node metastasis	63.2%	(Qin, Wang et al. 2014)
Laryngeal carcinomas	cancer histological and pathological stages	100% of 60	(Pi, Lin et al. 2013)

Table 1 Summary of studies suggesting UHRF1 as diagnostic and prognostic biomarker in various cancer

1.6 Conclusion

The overexpression of anti-apoptosis protein UHRF1 had been demonstrated in most, if not all cancer cells, making it a universal biomarker for cancer detection, therapeutic outcome estimation and survival prediction. Through binding to the promoter regions of TSGs, UHRF1 was found to inhibit their transcription and retain them in repressed state via the cooperation between SRA domain and DNMT1 and HDAC1. Furthermore, the RING finger domain of UHRF1 could induce ubiquitination mediated degradation of tumour suppressing proteins. Therefore, future study on UHRF1 induced enhanced cell proliferation could concentrate on the underlying molecular mechanisms of SRA domain and RING finger domain.

By maintaining the pattern of DNA methylation and histone modification through the cooperative work among its intramolecular domains, UHRF1 also recruits DNMT1 and HDAC1 to the hemi-methylated DNA, thereby playing an important role in heterochromatin formation during the mid-S phase. Meanwhile, UHRF1 was also found to be essential for DNA replication initiation and maintenance, including origin licensing, pre-IC formation and origin firing. However, which domain(s) of UHRF1 plays a predominant role in this process remains unknown. As SRA domain was found to be the key to opening closed conformation of itself and maintaining DNA methylation pattern, it is possible that SRA domain is the core of UHRF1 in the function of DNA replication. This hypothesis can be tested by the DNA fibre assay (i.e. DNA coming) with UHRF1 mutants without SRA domain.

1.7 Objectives

UHRF1, a multi-domain protein, demonstrates various functions in many biological processes, such as epigenetic regulation and DNA repair. Observations using *Xenopus* egg extracts demonstrated that UHRF1 was degraded during S-phase in a ubiquitylation-dependent manner and that the efficient depletion of the protein from extracts severely reduced levels of chromosomal DNA replication. However, lower efficiency of UHRF1 depletion allowed some residual DNA replication to occur. The progressive size of replication intermediates with time, suggesting that the loss of UHRF1 protein reduced the number of origins capable of initiating DNA replication. This was supported by the finding that levels of Orc proteins on chromatin were reduced compared to mock-depleted extract (Taylor, Bonsu et al. 2013).

In order to investigate these observations in a higher eukaryote system, I established DT40 cells model in order to generate conditional *UHRF1* knockout cell lines because of the advantages as a tool for reverse genetic study: (i) a remarkably higher efficiency of gene targeting (up to 80% of stably transfected clones) comparing with 10%~20% of that in mammalian cells depending on targeted gene length; (ii) stable karyotypes and phenotypes even after many generations of cell culture allowing the performance of sequential gene targeting into one single cell with different selection marker genes; (iii) rapid proliferation of 8~10 hours per generation making it easy to perform phenotypic analysis; (iv) the cloning efficiency of around 100% in wild type cells; naturally silencing of *p53* gene facilitating the analysis of mutant cells with genomic instability; (v) whole genome sequence available online (Yamazoe, Sonoda et al. 2004). Once generated, this cell line will be used to investigate the role of the epigenetic modulator of UHRF1 in DNA replication and the regulation of cell cycle,

for example, in which stages and what functions of UHRF1 is important for replication progression and the corresponding signalling pathway. Finally, the project plans to explore the involvement of UHRF1 in DNA repair by testing how cells respond to DNA damage reagents in the absence of UHRF1 functions.

Chapter 2 Materials and methods

2.1 Materials

2.1.1 reagent supplier

2-mercaptoethanol	Sigma
30% Acrylamide mix	Sigma
3mm Filter Paper	Whatman
Acetic acid	Fisher
Agar	Formedium
Ammonium Persulfate (APS)	Sigma
Ampicillin	Melford
Benzonase	Sigma
Blasticidin	Sigma
Bovine Serum Albumin (BSA)	Sigma
Calcium chloride	Fisher
Carbenicillin	Melford
Chloroform	Invitrogen
<i>DH5α E coli</i>	Invitrogen
Dimethyl Sulphoxide (DMSO)	Sigma
Dithiothreitol (DTT)	Melford

DNA Gel Loading Dye (6×)	New England Biolabs
DNA Midi Prep Kit	Qiagen
DNA Mini Prep Kit	Qiagen
Ethanol	Fisher Scientific
Ethylenediaminetetraacetic acid (EDTA)	Melford
Foetal Bovine Serum (FBS)	Sigma
Gel purification kit	Qiagen
Glycerol	Fisher
Glycine	Fisher
Hydrochloride acid	Fisher
Hydrogen Peroxide	Sigma
Hygromycin	Sigma
<i>In vitro</i> transcription coupled translation (TnT) reactions	Promega
Indole 3 Acetic Acid (IAA)	Sigma
Isopropyl β-D-1-thiogalactopyranoside (IPTG)	Melford
Kanamycin	Melford
L-Glutamine	Sigma
Luminol	Fluka

Luria Broth	Melford
Manganese Chloride	Melford
Methanol	Fisher
Methylcellulose	Sigma
Nitrocellulose membrane	Osmonics
P-coumaric acid	Sigma
Penicillin/Streptomycin	Invitrogen
pGEM-T Easy Vector kit	Promega
Phenol/Chloroform	Invitrogen
Phosphate Buffered Saline (PBS)	Oxoid
Phusion Polymerase PCR Kit	New England Biolabs
T4 PNK	New England Biolabs
Potassium acetate	BDH
Potassium chloride	Fisher
Potassium hydroxide	Fisher
Proteinase K	Sigma
Puromycin	Sigma
Quick cell proliferation assay kit II	Abcam
Restricted enzyme buffers	New England Biolabs

Restricted enzymes	New England Biolabs
RPMI 1640 media	Sigma
Skim dry milk	Sainsbury's
Sodium acetate solution	Fluka
Sodium Chloride	Sigma
Sodium dodecyl Sulfate (SDS)	Fisher
Sodium hydrogen phosphate	Fisher
Sodium hydroxide	Fisher
Stratagene Accuscript cNDA Synthesis System	Aligent Technologies
T4 DNA ligase	Invitrogen
Tamoxifen	Sigma
Tetramethylethylenediamine (TEMED)	Sigma
Tissue culture plasticware	Nunc
Transient transfection kit (solution T)	Lonza
Triton-X	Fisher
Trizma base	Fisher
TRIzol	Invitrogen
Tween-20	Fisher
Ultrapure agarose	Invitrogen

X-gal	Melford
-------	---------

Table 2.1 List of reagent supplier

2.1.2 Solutions and buffers

Agarose Gel (0.8%): 0.8g ultrapure agarose, 100ml of 1× TBE buffer.
APS (10%): 1g APS powder in 10ml distilled water.
Blocking Buffer: 5g skimmed milk powder, 100ml PBS buffer.
CCMB80 Buffer: 10mM KOAc pH 7, 80mM CaCl ₂ , 20mM MnCl ₂ , 10mM MgCl ₂ , 10% Glycerol.
Cell freezing media (1ml): 100µl of DMSO, 200µl of serum, 700µl of RPMI 1640
Chicken Culture Media: 10% foetal bovine serum, 1% chicken serum, 1% L-Glutamie, 10 ⁻⁵ β-mercaptoethanol, 1% penicillin , 1% streptomycin and RPMI 1640 media
DTT (1M): 3.09g DTT in 20ml of 0.01M Sodium Acetate pH5.2.
Enhanced-Chemi-Luminescence (ECL): hydrogen peroxide (30% solution) 6µl, 90mM p-coumaric acid 50ul, 250mM luminol 100ul, 1M Tris-HCl pH 8.0 2ml, made up to 20ml with distilled water.
Immunoblotting Stripping buffer I: 200mM glycine pH2, 0.1% SDS, 0.1% Tween-20
Immunoblotting Stripping buffer II: 62.5mM Tris-HCl pH 6.8, 2% SDS,

100mM β -mercaptoethanol
IPTG (100mM stock): 0.48g IPTG powder in 20ml distilled water.
LB Agar: 17g Agar powder in 1L of LB medium.
LB medium: 25g LB powder in 1L of distilled water.
Luminol: 250mM in DMSO (1.1g per 25ml).
Lysis buffer: 50mM Tris-HCl pH7.5, 150mM NaCl, 1mM MgCl ₂ , 0.1% SDS, Benzonase 1 μ l/ml
P-coumaric Acid: 90mM in DMSO (0.147g/10ml).
PBS: 1 tablet in 100ml distilled water.
Proteinase K Buffer: 0.025M EDTA, Tris-HCl (pH8.0), 0.1M NaCl
SDS-PAGE (SDS-Polyacrylamide gel electrophoresis) 5% stacking gel: 30% Acrylamide mix, 1.0M Tris-HCl (pH6.8), 10% SDS, 10% APS, 0.1% TEMED.
SDS-PAGE 8% resolving gel: 30% Acrylamide mix, 1.5M Tris (pH8.8), 10% SDS, 10% APS, 0.1% TEMED.
SDS-PAGE running buffer (5\times): 125mM Tris-HCl base, 1.25M glycine, 0.5% SDS.
SDS-PAGE Transfer Buffer (1\times): 5.82g Trizma base, 2.93g glycine, 3.75ml 10% SDS, 200ml methanol, made up to 1L with distilled water.
SDS-PAGE Wash Buffer (PBST): 1 \times PBS with 0.01% Tween-20.
Sodium acetate solution stock (3M): 2.46g sodium acetate powder in 8ml distilled

water, pH to 5.2 and top up to 10 ml.
TBE Buffer (5×): 54g Tris-HCl, 27.5g boric acid, 20ml 0.5M EDTA, made up to 1L with distilled water.
X-Gal (20µg/µl): 0.4g X-Gal powder in 20ml DMSO.

Table 2.2 List of solution/buffer recipe.

2.1.3 Stock solutions of antibiotics and selection drugs

Antibiotic	Stock concentration	Working concentration	Application
Ampicillin	100mg/ml	100µg/ml	Selection for <i>E. coli</i>
kanamycin	100mg/ml	100µg/ml	Selection for <i>E. coli</i>
Carbenicillin	100mg/ml	100µg/ml	Selection for <i>E. coli</i>
Blasticidin	10 mg/ml	20µg/ml	Selection for DT40 cells
Neomycin	200mg/ml	1mg/ml	Selection for DT40 cells
Puromycin	2mg/ml	0.5µg/ml	Selection for DT40 cells
Hygromycin	20mg/ml	1.4mg/ml	Selection for DT40 cells

Table 2.3 Antibiotics and drugs used in this study. All solutions involved in the selection for DT40 cells were filtered by 0.45µm filter before use.

2.1.4 List of antibodies

Primary antibody	Dilution	Company	Lot No.
Rabbit anti-UHRF1	1:1000	Our own laboratory	-----
Mouse anti-GFP	1:500	Roche	11063100

Table 2.4 List of primary antibodies.

Secondary antibody	Dilution	Company	Lot No.
HRP-conjugated anti-mouse antibody	1:5000	DAKO	00094764
HRP-conjugated anti-rabbit antibody	1:5000	DAKO	20007340

Table 2.5 List of secondary antibodies.

2.1.5 List of PCR primer

Primer ID	Application indication	Nucleotide sequence
2x FLAG pEPEX <i>Xho I</i> (Fw)	FLAG tag	ACTCGAGATGGACTACAAGGACGACGATGACAAGCATATCATGG
2xFLAG pEPEX <i>Age I</i> (Fw)	CMV promoter	AACCGGTAATGGACTACAAGGACGACGATGACAAGCATATCATGG
2XFLAG pEPEX <i>Xho I</i> (Fw)	FLAG	ACTCGAGACATGGACTACAAGGACGACGATGACAAGCATATCATGG
3'arm <i>BamHI</i> (Fw)	Chicken UHRF1 3 target arm	AGGATCCTAATTGGCTCTAAACTGCAGTGCTCCATCAATG
3'arm <i>Pst I</i> (Rev)	Chicken UHRF1 3' target arm	GCTGCAGTAACTTCCTTCATTACAAGTATAGTCCACGTTCTTG
5' arm <i>Not I</i> (Fw)	Chicken UHRF1 5' target arm	AGCGGCCGCTAAACACGATGGATGATTTTGAATTGGAG
5'arm <i>Bam HI</i> (Rev)	Chicken UHRF1 5' target arm	CGGATCCTAAGACAGTTCAGTTTTCCATCTCTCCTCAGC
Ch-UHRF1 (Fw)	Chicken UHRF1	ATGGAGACAGTTGCAACACGATGG
Ch-UHRF1 (Rev)	Chicken UHRF1	TCACCGTCCGTTGCCATATCCAGG
Ch-UHRF1 <i>Age I</i> (Fw)	Chicken UHRF1	AACCGGTAATGGAGACAGTTGCAACACGATGG
Ch-UHRF1 <i>BamHI</i> (Fw)	Chicken UHRF1	AGGATCCATGGAGACAGTTGCAACACGATGG
Ch-UHRF1 <i>Nde I</i> (Fw)	Chicken UHRF1	ACATATGATGGAGACAGTTGCAACACGATGG
Ch-UHRF1 <i>Pst I</i> (rev)	Chicken UHRF1	ACTGCAGTCACCGTCCGTTGCCATATCCAGG
Ch-UHRF1 <i>Sal I</i> (Rev)	Chicken UHRF1	AGTCGAC TCACCGTCCGTTGCCATATCCAGG
Ch-UHRF1 <i>Xho I</i> (Fw)	Chicken UHRF1	ACTCGAGATGGAGACAGTTGCAACACGATGG
Ch-UHRF1 <i>Xho I</i> (Fw)	Chicken UHRF1	ACTCGAGGAATGGAGACAGTTGCAACACGATGG
CMV_ <i>Spe I</i> (Fw)	CMV promoter	AACTAGTTAGTAATCAATTACGGGGTC
CRISPR crRNA (Fw)	CRISPR	TCCTTCTCCTTACTCACAGCGTTTT
CRISPR crRNA (Fw)	CRISPR	AGTGACCATCCTCCATCTGCGTTTT
CRISPR crRNA (Rev)	CRISPR	GCTGTGAGTAAGGAGAAGGACGGTG
CRISPR crRNA (Rev)	CRISPR	GCAGATGGAGGATGGTCACTCGGTG

h_UHRF1_ <i>Sal I</i> (Rev)	Human UHRF1	AGTCGACTCACCGGCCATTGCCGTAGCCGG
h-UHRF1 <i>Age I</i> (Fw)	Human UHRF1	AACCGGTAATGTGGATCCAGGTTCCGGACCATGG ATGG
h-UHRF1 <i>Xho I</i> (Rev)	Human UHRF1	ACTCGAGGAATGTGGATCCAGGTTCCGGACCATG GATGG
h-UHRF1 <i>Xho I</i> (Fw)	Human UHRF1	ACTCGAGATGTGGATCCAGGTTCCGGACCATGGA TGG
SV40 <i>KpnI/SpeI</i> (Rev)	SV40	CGGTACCACTAGTTACCACATTTGTAGAGGTTT TACTTGC
SV40 <i>Sal I</i> (Fw)	SV40	AGTCGACCAGACATGATAAGATACATTGATGAG TTTGG

Table 2.6 Primer sequences used in PCR reactions.

Fw indicates primer in forward direction and Rev indicates primer in reverse direction. All forward and reverse primers were ordered from Eurofins MWG Operon. Primers were dissolved in deionized water of different volumes to achieve a final concentration of 100µM (stock) and stored at -20oC. Primers of 10µM were used for PCR reactions.

2.2 Molecular biology

2.2.1 Preparation of chemically competent *DH5 α* *E. coli*

10 μ l competent cells were inoculated in 20ml sterile LB medium and grown at 37°C overnight. The following day, 1ml of starter culture were inoculated into 100ml sterile LB medium and grown at 37°C for 2~4 hours until OD₆₀₀ reached 0.3 to 0.5 (not higher than 0.5). Cells were pelleted in pre-cooled centrifuge tube by spinning at 5000g for 10min at 4°C. Supernatant were discarded and cells were re-suspended in 32ml pre-cooled sterile CCMB80 buffer. Cells were afterwards kept on ice for 20min. Subsequently, cells were centrifuged as above and re-suspended gently in 4ml CCMB buffer. 50 μ l aliquots of cells were stored at -80°C.

2.2.2 Purification of PCR product

PCR product was purified using the manufacturer's protocol involved in the Gel purification kit. Briefly, 5 volumes of PB buffer were added to 1 volume of PCR sample and applied to the column for centrifuge. Afterwards, DNA was washed with 750 μ l PE buffer and eluted with 30 μ l EB buffer. Purified DNA was stored at -20°C. The concentration of purified PCR product was quantified by NanoDrop 2000c/2000 UV-Vis Spectrophotometer (Thermo Scientific).

2.2.3 DNA fragment purification

Digested DNA fragment was purified following the manufacturer's protocol involved in the Gel purification kit. Briefly, digested DNA reaction system was added to 0.8% agarose gel and run at 100V for electrophoresis until expected bands were separated.

DNA of expected bands was visualised under UVP Dual-Intensity Trans-illuminator and excised by slice. Sliced gel was transferred to a new Eppendorf tube and weighed on the scale. 3 volumes of buffer QG were added to the excised gel and incubated at 55°C until gel was thawed completely (about 10min). 1 volume of isopropanol was added to the melt gel mixture and applied to the column for centrifuge. Finally, 750µl PE buffer was applied for washing and 50µl EB buffer for elution. Purified DNA fragment was stored at -20°C. The concentration was quantified as above.

2.2.4 DNA agarose gel electrophoresis

Digested DNA sample was prepared by adding 1 volume of 6x DNA loading buffer to 5 volumes of DNA samples. Agarose gel was run in 1x TBE buffer within Fisher Brand gel electrophoresis tank. Voltage was set at 100V and time was set depending on the size of expected DNA. DNA bands were visualized and imaged by Image Lab™ software 4.0 (BioRad).

2.2.5 DNA Ligation

A ligation calculator (in silico) was used to determine the amount of vector and insert required to achieve an insert: vector ratio of 3:1. Ligation was left at 4°C overnight before transforming into competent cells.

50ng (Xµl) of vector
X µL of insert
5µl of 2X Rapid Ligase Buffer
1 unit of T4 DNA ligase
Using Milli Q water to top up the final volume to 10 µl

Table 2.7 The scheme of DNA ligation system.

2.2.6 Transformation into *DH5 α* *E. coli*

For each reaction, 5 μ l of ligation reaction was gently added into 50 μ l competent *DH5 α* *E. coli*. The cells and ligated DNA mixture were incubated on ice for 30min followed by the heat-shock at 42°C for 45sec. cells were further incubated on ice for another 2min before the addition of 500 μ l sterile LB medium and the incubation at 37°C for one hour in an orbital shaker. Finally, cell suspension was spread onto LB agar plates with corresponding selective antibiotic. Plates were incubated at 37°C overnight.

2.2.7 Plasmid purification using DNA mini prep Kit

Plasmid was purified following the manufacturer's protocol involved in the DNA miniprep kit. Briefly, single transformed colonies were picked and inoculated into 5ml LB medium containing appropriate selective antibiotic. The bacterial solution was incubated at 37°C in orbital shaker at 150rpm overnight. The next day, the bacteria were pelleted and re-suspended in 250 μ l of buffer P1. 250 μ l of buffer P2 and 350 μ l of buffer N3 were sequentially added, followed by spinning at 13kg for 10min. Finally, DNA was washed with 750 μ l PE buffer and eluted with 50 μ l EB buffer. Purified DNA was stored at -20°C.

2.2.8 Plasmid purification using DNA midi prep Kit

Plasmid was purified following the manufacturer's protocol involved in the DNA midiprep kit. Briefly, single transformed colony was picked and inoculated into 100ml LB medium containing appropriate antibiotic at 37°C overnight in orbital shaker at 150rpm. The following day, bacterial were re-suspended in 4ml buffer P1, 4ml buffer P2 (incubated at room temperature for 5min), 4ml pre-cooled buffer P3

sequentially before incubating on ice for 20min. The pellet was then applied to buffer QBT rinsed column, washed with 10ml of QC buffer and eluted with 5ml of QF buffer. Isopropanol and ethanol were afterwards used to precipitate DNA. Purified DNA was finally eluted in 200 µl of TE buffer and stored at -20°C.

2.2.9 DNA precipitation

1 volume of DNA sample was treated with 1/10 volume of NaOAc and 2~3 volume of 100% ethanol before applying to -20°C for half an hour until overnight. Subsequently, DNA was pelleted and washed with 70% ethanol before dissolving in TE buffer.

2.2.10 Genomic DNA extraction

5×10^7 cells were collected by centrifuging at 1500 rpm for 5min. The cell pellet was washed with PBS buffer and then re-suspended in 500µl of proteinase K Buffer containing 0.1 mg/ml of proteinase K. 12.5µl of SDS (20%) was added and mixed by inverting and spinning down shortly. Afterwards, protein degradation was performed overnight in the incubator of 37°C. The following day, 1 volume of phenol was added into the DNA extract and mixed carefully by gentle shaking before spinning down at 13kg for 5 min. The upper phase was transferred into a new tube and 1 volume of phenol/ chloroform was added. Finally, 300µl of 70% ethanol was applied to precipitate the pelleted DNA. Isolated DNA was dissolved in 100µl of TE buffer by incubating at 55°C for 2h.

2.2.11 RNA extraction

2×10^7 cells were harvested and centrifuged at 1500rpm for 3min. The cell pellet was then re-suspended in 1.5ml of TRIzol reagent and transferred to a new 2ml of Eppendorf tube followed by 5min of incubation at room temperature for complete dissociation from nucleoprotein. Subsequently, 300 μ l of chloroform was added and mixed vigorously for 15sec followed by 3min of incubation at room temperature. After spinning at 13kg for 15min at 4°C, the upper phase solution was transferred to a new 2ml Eppendorf tube followed by the precipitation of 750 μ l of isopropanol and 1ml of 75% ethanol sequentially. The RNA pellet was finally air dried for 5~10min and dissolved in 100 μ l of TE buffer.

2.2.12 cDNA synthesis

cDNA was synthesized following the protocol of Stratagene Accuscript cNDA Synthesis System. Briefly, reaction system was mixed as follows:

10 \times Accuscript RT buffer 2 μ l
dNTP mix (25mM each) 0.8 μ l
oligo dT primers (0.5 μ g/ μ l) 1 μ l
RNA 5 μ g total RNA
dH ₂ O to 16.5 μ l

Table 2.8 The reagents and volumes used for the reverse transcriptase master mix.

The reaction system was then incubated at 65 °C for 5min and cooled down to room temperature for 5 min. Afterwards, this reaction system was added with the following reagents:

2µl of 100Mm DTT
0.5µl of RNase block
1µl of Accuscript RT

Table 2.9 The reagents and volumes used for generating cDNA from RNA.

Finally, the reaction system was incubated at 42°C for 60min, terminated at 70°C for 15min and cooled down at 4°C before storing at -20°C.

2.2.13 PCR

PCR amplification was done following the instruction of Phusion Polymerase PCR kit.

The reaction system was set up with reagents as follows:

10µM forward and reverse primers	1µl of each
50-100µg genomic DNA template	Xµl
DMSO	1.5µl
5x GC buffer	10µl
10mM dNTP	1µl
Phusion polymerase	0.5µl
Distilled water	Add to 50µl

Table 2.10 The reagents and volumes used in PCR master mix.

Afterwards, the standard cycle was proceeded for 35 cycles following the recycling protocol as follows:

Sequence ID	Denaturation	Annealing	Extension

Target arms	98°C for 10sec	65°C for 15sec	72°C for 30sec
<i>UHRF1</i>	98°C for 60sec	55°C for 210sec	72°C for 60sec

Table 2.11 The cycling instruction for each target fragment used in PCR reactions.

Initial denaturation of 95°C for 5min and final extension of 72°C for 5min were given before and after the cycles.

2.2.14 5' phosphate removal

Plasmid DNA was digested with restriction enzyme and incubated at 37°C for 1 hour. Afterwards, 0.5µl CIP was added to the digested DNA and incubated on ice for 2min.

2.2.15 *In vitro* translation of proteins

Recombinant protein was generated via the protocol of TnT system. Briefly, The TnT master mix was thawed rapidly by hand and placed on ice. Other reagents were thawed at room temperature and afterwards placed left on ice. Reaction system was prepared on ice as follows: 40µl of TnT master mix 40µl, 2µl of [³⁵S] methionine, 2µl of DNA plasmid template (0.5µg/µl), nuclease-free water to final volume 50µl. Afterwards, this reaction system was incubated at 30°C for 90~120min before applying to immunoblotting detection.

2.3 Eukaryotic cell culture

2.3.1 Cell culture

The cell line of chicken DT40 B lymphoma cells were a gift from Dr Edgar Hartsuiker (University of Bangor). These cells were cultured in chicken culture

medium in a humidified incubator at 37°C in 95% air: 5% CO₂. The cell density was maintained between 2 x 10⁵/ml and 1 x 10⁶/ml to avoid senescence or apoptosis.

2.3.2 Cell freezing

The cell line of DT40 in culturing T25 flask was gently centrifuged at 500g for 3min using an Allegra™ X-22R centrifuge, Beckman Coulter). Subsequently, the supernatant was removed and the cell pellet was resuspended in cell freezing medium (5ml per T25 flask used). Each 5ml resuspension was divided between 4 labelled cryogenic tubes stored overnight at -80°C freezer in a Mr. Frosty freezing container (VWR) with isopropanol (Fisher Scientific). The next day, the frozen cells were transferred into liquid nitrogen for long-term storage.

2.3.3 Cell resurrection

The cells in cryogenic tubes were taken out from liquid nitrogen and thawed in 37°C water bath quickly by hand shaking. The thawed cells were immediately transferred into 20ml of pre-warmed fresh media and centrifuged at 500g for 3min aiming at remove the DMSO and dead cells. Subsequently, cells were re-suspended in 20ml chicken media and cultured overnight followed by the change of culture medium within 24 hours.

2.3.4 Cell counting

When preparing cells for experiments, cell culture media was first removed and cells were washed twice with fresh media as previously stated. The cell pellet was then resuspended in appropriate volume of complete medium according to the number of cells desired. The number of viable cells (checked by trypan blue) was determined by

the counting using a haemocytometer. The cells in each corner of 4x4 squares was counted followed by the calculation of an average. This value was then multiplied by 10^4 to achieve the number of cells per ml of suspension.

2.3.5 Transient transfection

5×10^6 cells and $5 \mu\text{g}$ of DNA was prepared for each sample. Electroporation was performed via the protocol of Nucleofector™ transfection kit. Briefly, Cells were spun down at 500g for 3min before resuspending within $100 \mu\text{l}$ Nucleofector™ Solution T. Subsequently, $5 \mu\text{g}$ of DNA was applied to cell suspension and transferred to the provided cuvette. The cuvette was inserted into cuvette holder of Lonza Nucleofector™ device followed by the electroporation of Program B023. Immediately after that, the cell solution was transferred into 5ml of pre-warmed fresh complete media and maintained in the humidified incubator at 37°C and 5% CO_2 overnight.

2.3.6 Enrichment of GeneArt CRISPR Nuclease Expressing Cells

Transfected cells were pelleted and washed by 2ml of Buffer I (0.2 micron sterile filtered PBS with 0.1% BSA, 2mM EDTA) for three times followed by the resuspension in $10 \mu\text{l}$ of Buffer I. Simultaneously, the vial of Dynabeads CD4 magnetic beads was mixed well before use. $25 \mu\text{l}$ of magnetic beads was transferred to a sterile 1.5ml Eppendorf tube and washed with buffer I twice followed by the resuspension in $25 \mu\text{l}$ of Buffer I. Subsequently, the mixture of cells and magnetic beads was incubated at 4°C for 30min on the rotator allowing the tilting and rotation of Eppendorf tubes. Next, this mixture was washed three times with $500 \mu\text{l}$ of Buffer I followed by the resuspension in $100 \mu\text{l}$ of Buffer II (0.2 micron sterile filtered RPMI

with 2% FBS). 10 μ l of DETACHBEAD CD4 was then added to this mixture and was incubated on a rotator for 45min at room temperature. Finally, the cells were separate from magnetic beads and transferred to a fresh tube before bringing up to the final volume of 4ml. In order to achieve monoclonal cell CD4 enriched cell line, this enriched cell population was subjected to limiting dilution and incubated in the humidified incubator at 37°C and 5% CO₂ for 10~14 days.

2.3.7 Stable transfection

20 \times 10⁶ DT40 cells of exponential stage was washed with pre-cooled PBS and resuspended in 550 μ l of PBS before mixing with 30 μ g DNA (linearized or not depending the desirable purpose). The cells and DNA mixture was transferred to 4mm cuvette and incubated on the ice for 10min. The electroporation was carried out by one time of pulse at 550V, 25 μ F (using Gene Pulser Xcell™ Electroporation System from BioRad company). Subsequently, the cell mixture was incubated on ice for another 10min before transferring to 5ml of pre-warmed complete media. The next day, cell suspension was washed once and applied to limiting dilution after resuspending in complete media with appropriate selection drugs.

2.3.8 Cell proliferation assay

10⁴ cells were plated on the 96-well plate in a final volume of 100 μ l/well of complete media with or without the addition of tested reagents and incubated in the humidified incubator as stated above for 24 to 96 hours. After the targeted time period, 10 μ l per well of WST solution was added to each well followed by the incubation in the incubator for 1 hour. Finally, the cell absorbance was read by the microtier plate reader at 450nm, 0.1s.

2.3.9 Clonogenic formation assay

To determine cell plating efficiency or cell sensitivity, DT40 cells were plated in 5ml of medium containing 1.5% (by weight) methylcellulose in 6 well plate at the cell number of 5000, 500, 50 per treatment condition. Subsequently, cells were incubated in the incubator as stated above for 2 weeks and visible colonies were counted.

2.4 Protein analysis

2.4.1 Sample preparation

Cells were collected by centrifuge and washed once with PBS. Subsequently, cells pellet was lysed with lysis buffer (100µl per 10^6 of cells) and incubated at room temperature for 10min. The concentration of cell lysate was test before denaturation (at 95°C for 5min) by Bradford protein assay, followed by either the direct use or being stored at -20°C.

2.4.2 SDS-PAGE

7.5µl of molecular weight marker and protein samples were loaded to the gel with 8% of resolving gel. Electrophoresis was run at the voltage of 120V (PowerPac Basic™, BioRad) for the stacking gel and 150V for the resolution gel in Whatman Biometra tank.

2.4.3 Semi-dry transfer

Separated proteins were then transferred onto nitrocellulose membrane at the voltage of 20V for 45min using BioRad semi-dry transfer device. The transfer system was

assembled as follows (from bottom): 2 filter papers, nitrocellulose membrane, gel and 1 filter paper.

2.4.4 Immunoblotting and development

Membranes were blocked with blocking buffer for 1 hour at room temperature before the incubation with primary antibody overnight at 4°C. The next day, the membrane was washed 4 times with PBST followed with the incubation with appropriate secondary antibody for 1 hour at room temperature. Membranes were then washed with PBST for another four times. ECL substrates were used for the development of membranes before exposure using the ChemiDoc™ MP Imaging System (Bio-Rad).

2.4.5 Immunoblotting stripping and re-probing

Mild stripping conditions: the immunoblotted membrane was washed with stripping buffer I for 5min twice at room temperature. Subsequently, the membrane was washed 4 times with PBST.

Harsh stripping conditions: the immunoblotted membrane was submerged in the stripping buffer II at 50°C for 30min. subsequently, the membrane was washed 4 times with PBST.

After stripping using either solution, membranes were incubated in blocking solution (Blotto) as previously described before incubation with primary antibody.

**Chapter 3 Targeting of UHRF1 in
DT40 cells using CRISPR/Cas9
system**

3.1 Introduction of CRISPR technology

CRISPR (clustered regularly interspaced short palindromic repeats) was developed from the system for how bacteria fight virus infection by detecting the viral DNA and destroying it in coordination with Cas9 nuclease. Therefore, CRISPR was regarded as a hallmark for acquired immunity in bacteria. Later, CRISPR/Cas9 system was developed to edit genome sequence by DNA insertion, deletion or mutation in mammalian cells and animals with incredible accuracy, making it a strong gene editing tool for future clinical application (Ran, Hsu et al. 2013). In the CRISPR/Cas9 system, three motifs ensure the precise recognition and cleavage of the targeted nucleotide sequence, which are crRNA, tracrRNA and Cas9 (CRISPR associated 9) nuclease. crRNA functions as guide RNA (gRNA) and leads tracrRNA and Cas9 nuclease to the complementary targeted sequence at the specific loci of the genome. tracrRNA is responsible for recruiting Cas9 nuclease, which creates DSBs and sequentially induces the cells to repair broken DNA and make genomic changes through endogenous DNA repair mechanisms (mainly NHEJ and HR) at the sites of DSBs. The outcome of repair events initiated by CRISPR/Cas9 system may vary among different cells even when DSBs generated are at the same sites. Working principle of CRISPR/Cas9 mediated gene disruption is shown in **Figure 3.1**.

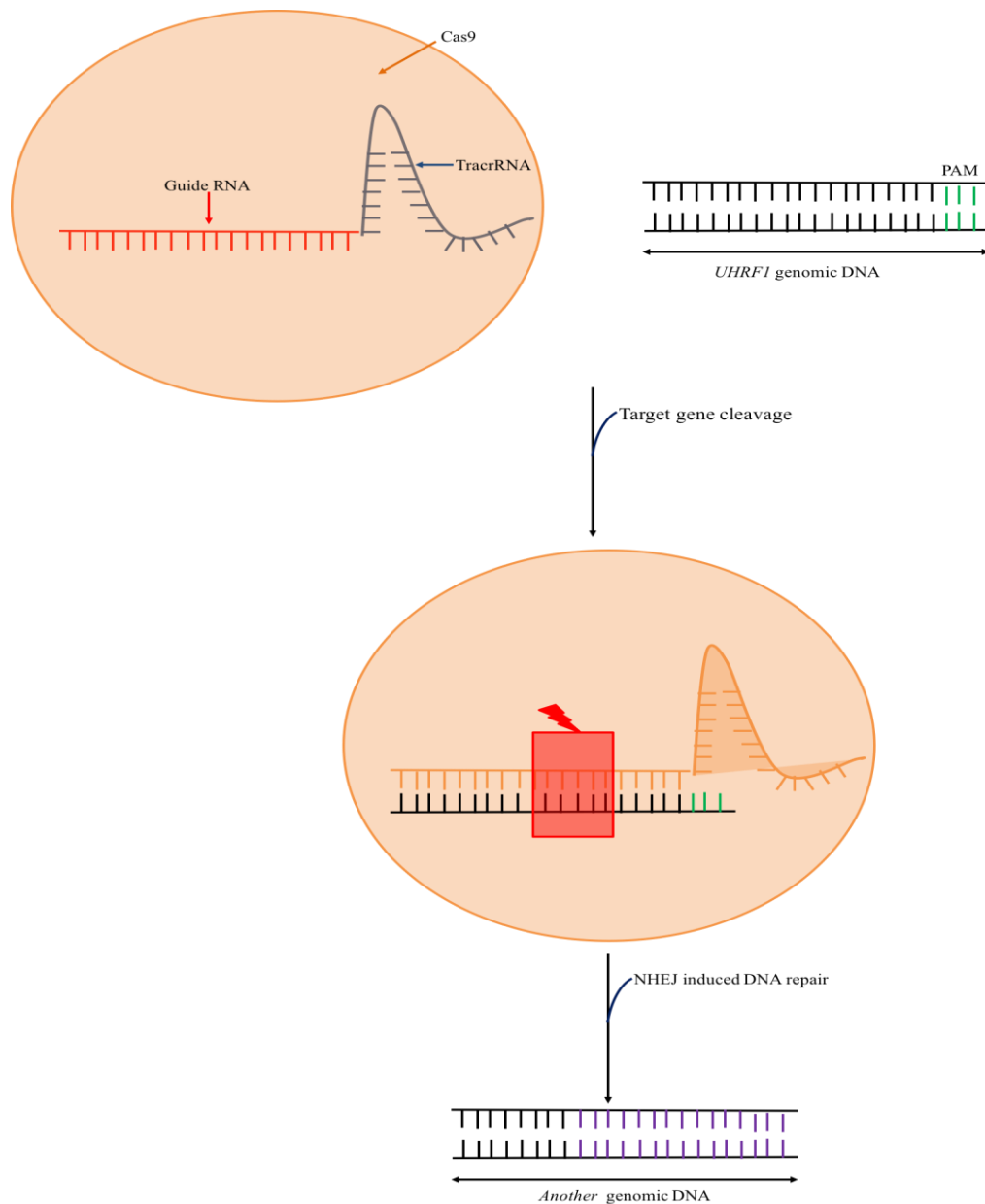


Figure 3.1 Working principle of CRISPR/Cas9 mediated gene disruption.

crRNA and tracrRNA combine as single guide RNA (sgRNA). The recruitment of Cas9 nuclease by sgRNA on the target sequence of *UHRF1* induces the cleavage of *UHRF1* and error-prone NHEJ mediated DNA repair, resulting in the fragment insertion or deletion and ultimately gene disruption.

3.2 Strategy of CRISPR/Cas9 mediated *UHRF1* knockout

In this project, the strategy of CRISPR/Cas9 mediated *UHRF1* knockout was planned to carry out as follows: in order to maximize the chances of disrupting both *UHRF1* alleles, sgRNAs were designed to target the nucleotide sequence in the 1st exon of *chUHRF1* (*UHRF1* in DT40 chicken cells) locus using the website of <http://crispr.mit.edu>, and *chUHRF1* nucleotide sequence generated from cDNA of DT40 cells, as shown in **Appendix 1**.

Two sgRNA were designed and constructed into two independent CRISPR/Cas9 vectors for targeting *UHRF1* genes in separate cell portions. This is used to exclude the potential possibility that the phenotypes of *UHRF1* knockout cell lines are caused by CRISPR/Cas9 off-target effects. The location of sgRNAs on *UHRF1* genomic DNA were shown in **Figure 3.2**.

Subsequently, sgRNAs were established into CRISPR/Cas9 expressing constructs (as shown in **Appendix 2**) and transfected into DT40 cells for gene editing. Transfectants were screened by immunoblotting the expressed *UHRF1* proteins using *UHRF1* antibody.

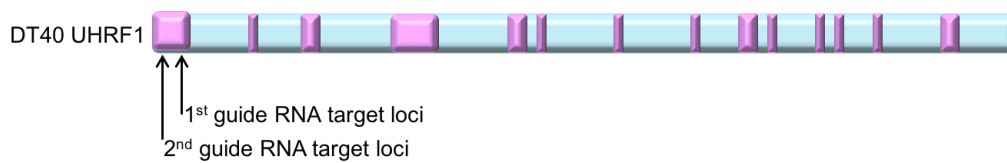


Figure 3.2 CRISPR/Cas9 mediated sgRNA loci and nucleotide sequence for disrupting *UHRF1* in DT40 cells.

The nucleotide sequence of sgRNA1 was TCCTTCTCCTTACTCACAGC and of sgRNA2 was AGTGACCATCCTCCATCTGC.

3.3 Identifying primary antibodies to chicken UHRF1 proteins

One potential issue with the DT40 cell system is the relatively poor availability of UHRF1 antibody reagents directed specifically to chicken UHRF1 proteins or mammalian proteins that have been tested for cross reaction with the chicken homologue. However, due to the high level of the identity between mammalian and chicken homologues as shown in **Figure 3.3**, the cross-reaction between mammalian antibody and chicken proteins is not uncommon.

From the previous work by our laboratory on *Xenopus* UHRF1 proteins, a series of polyclonal antibodies raised to large regions of either the N or C terminal of the protein were available. Comparison of the amino acid sequences of UHRF1 between the species of chicken and *Xenopus* showed a high level of identity of 71.60%, suggesting the possible cross reaction of *Xenopus* UHRF1 antibody to chicken UHRF1 proteins.

A



B

```
human      MWIQVRTMDGRQTHTVDSLRLTKVEELRRKIQELFHVEPGLQRLFYRGKQMEDGHTLFD
Xenopus    MWIQVRTMDGRDTRRIDSLSKLTKVEDLRARIQQIFGVALESQRLFYRGKQMENGHTLFD
DT40       -----METVATRWMILNWRISIEFNDQMI LMLSLQMEDGHSLFD
           : .*          :: : : * :: . ****:***:***

human      YEVRLNDDTIQLLVRQSL-VLPHSTKERDSELSDDTDSGCCLGQSESDKSSTHGEAAAETDS
Xenopus    YSVGLNDIVQLLVRQIPDSVPTK--DKECGISDADSGCGSGQGESDKNSSCGEGATDVDG
DT40       YSVGLNDIVQLLVRQSPAVLPAVSKEKDSELSDDTDSGCSGQSESDKSSHNGEGAMDLEG
           *. * *** :***** :*      ::. :**:* **.* **.* : :.

human      RPAD--EDMWDETELGLYKVNEYVDARDTNMGAWFEAQVVRVTRKAPSRDE-PCSSTRP
Xenopus    QPAGIN---SENVGPSLYKKNLDVARDLNMGAWFEAQIVSVSKRVNPDGMS-AEILDTS
DT40       QSSTAAQADWADPGFLYKIHDLDVARDMNMGAWFEAQVVNVTRKAANESCAVADQQT
           : :          : .*** :: ***** *****:* *:::

human      ALEEDVIYHVKYDDYPENGVVQMNSRDVRRARTIIKWQDLEVGQVVMVLYNPNPNKERG
Xenopus    AASDDIIYHVKYEDYPENGVVQLTYKDVRLRARTTLPWHDLVKGVQVVMVNYNPNDEPKERG
DT40       IPEEDVIYHVKYEDYPENGVVELSSNDVRSRARTILKWHQLEVGQVVMVNYNPNDEPTEG
           .*:*****:*****:.. .*** ** : *::*:*****:*****:*.***

human      FWYDAEISRKRETRTARELYANVVLGD--DSLNDCRIIFVDEVFKIERPEGSPMVDNPM
Xenopus    YWYDAEILRKRETRTIKEIYVKVLLGDAGDSLNDCRIRFVDEIYKIEEPGSAYITTESPQ
DT40       FWYDAEILQKRETKLIREINAKILLGEAGDSLNDCRIIFVDDIYKIEEPGSVCPISARPL
           :***** :****: :*: :::*: ***** **:::***.*. *

human      RRKSGPSCCHKCKDDVNRLCRVCACHLCGGQDPDKQLMCDECDMAFHIIYCLDPPLSSVPS
Xenopus    KRQNGPECKHCKDNPKRACRMACACVYCGGKQDPEKQLLCDECDMAFHIIYCLKPPLSAIPQ
DT40       KRQSGPVCKACKDNPNTCRICACHICGGKQDPDKQLMCDECDMAFHIIYCLNPPLSSIPD
           :*:.* ** ** ***: : : **:*::**:*::**:*::**:*::**:*::**:*::**:*::**

human      EDEWYCPECRNDASEVVLAGEKLRKESKKKAKMASATSSSQRDWKGKMACVGRTECTIVP
Xenopus    DEDWYCPDCRNDASEVVLAGEKLRKESKKKAKMASASSSSQRDWKGKMACVGRSRECTIVP
DT40       DEDWYCPECRNDASEVVLAGEKLRKESKKKQKMASANSSRRDQWKGKMACVGRTECTIVP
           :*:*****:*****:***:***** ***** .***:*****:*****:*****

human      SNHYGPIPGIPVGTMMWRFRVQVSESGVHRPHVAGIHGRSNDGAYSLVLAGGYEDDHDGN
Xenopus    SNHYGPIPGVPVGTMLWKFVQVSESGVHRPHVAGIHGRSNDGYSYSLVLAGGYEDDHDGNS
DT40       SNHYGPIPGIPVGTMMWKFVQVSESGVHRPHVAGIHGRSNDGAYSLVLAGGYEDDHDGN
           *****:****:*.*****:*****:*****:*****:*****:*.**

human      FFTYTGSGGRDLSGNKRTAEQSCDQKLTNTRALALNCFAPINDQEGAEAKDWRSGKPV
Xenopus    EFTYTGSGGRDLSGNKRTAEQSCDQKLTNMRALALNCSAPINDKEGAVAKDWRAGKPV
DT40       SFTYTGSGGRDLSGNKRTAEQSCDQKLTNMRALALNCSAPINDKNGAEAKDWRAGKPV
           *****:***** ***** ***** :* *****:*****
```


3.3.1 *Xenopus* UHRF1 antibody cross-reacted with chicken and human proteins

Several polyclonal antisera raised to different epitopes of *Xenopus* UHRF1 protein were used to probe Western blot of chicken and human cell extracts to determine the cross reactivity. Peptide molecular weight calculation found molecular weight of UHRF1 in *Xenopus* egg extract, DT40 cells and human cells are 84.89KD, 90.4KD and 89.8KD respectively. Among the five available antibodies, the No.59 N-terminus *Xenopus* UHRF1 antibody, generated from the antigen with the similarity of 69.51% to that in DT40 cells (as shown in

Appendix 3), was found to show satisfying cross reaction with UHRF1 proteins in DT40 cells, as shown in **Figure 3.4**. The size of DT40 UHRF1 proteins was slightly smaller than that from *Xenopus* and human cell extracts.

However, it is important to ensure the 85KD band in **Figure 3.4** is not from a non-specific protein. There are also bands smaller or larger than 85KD, which are possibly from degraded or modified UHRF1 proteins or potentially, just unspecific background of the antibody. Therefore, we subsequently adopted the technology of *in vitro* protein translation aiming at confirming the reaction between human and chicken UHRF1 proteins and the *Xenopus* UHRF1 antibody.

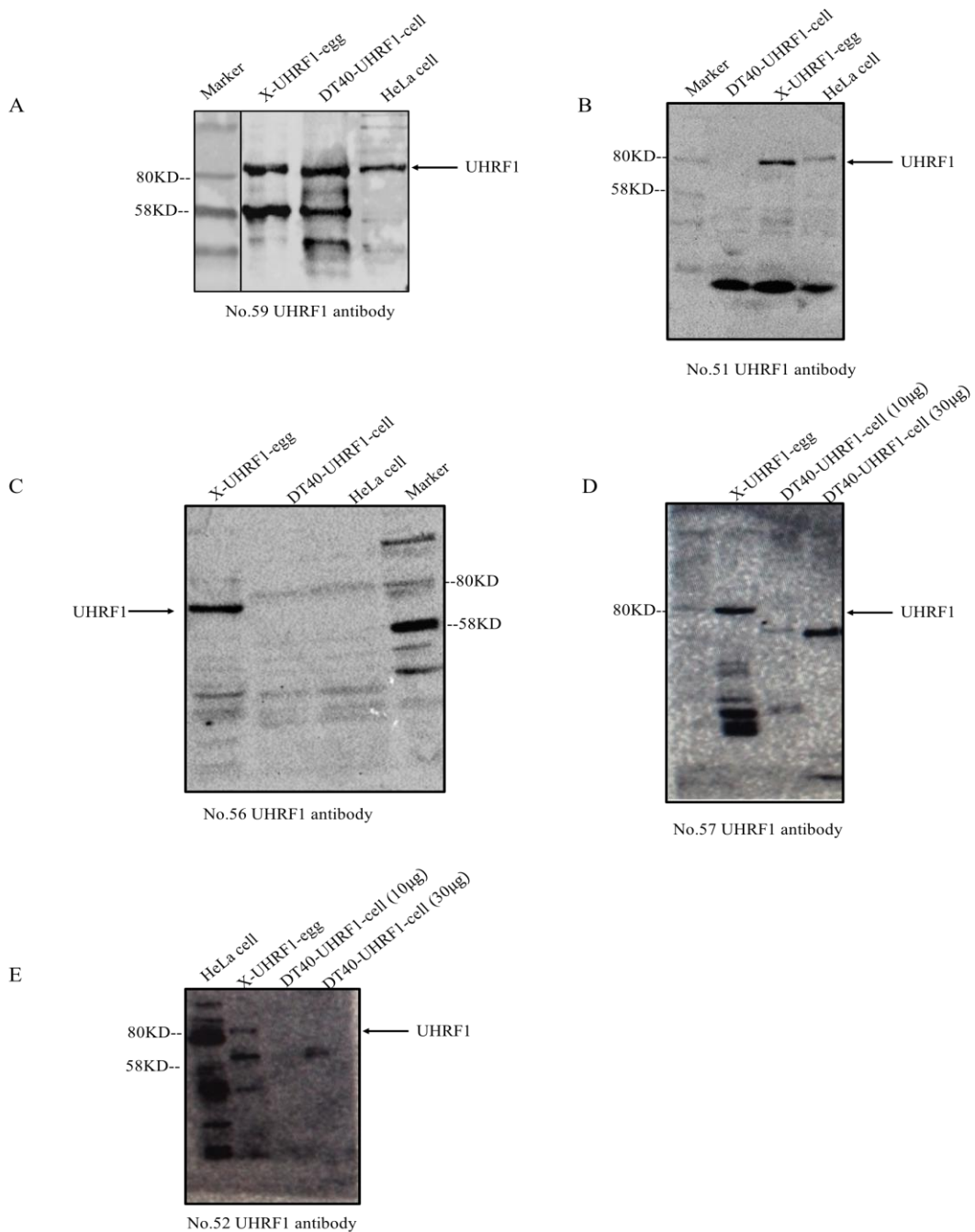


Figure 3.4 Cross reactivity between *Xenopus* antibodies and eukaryotic cell extracted proteins.

Proteins samples were labelled as indicated. 5 antibodies of UHRF1 generated using the first 477 amino acid sequence of *Xenopus* UHRF1 protein as antigen were tested. Equivalent amount of total proteins (30 µg) were loaded if not labelled specially.

3.3.2 UHRF1 antibody cross reacted with DT40 UHRF1 proteins

In order to confirm the major band detected by the UHRF1 antibody used to probe the Western blot of DT40 cell extracts in **Figure 3.4** was generated from the chicken UHRF1 proteins, *in vitro* UHRF1 proteins were produced from DT40 *UHRF1* cDNA using *in vitro* transcription coupled translation (TnT) reactions. The strategy of testing the cross-activity of UHRF1 antibody to UHRF1 proteins in DT40 cells was as follows: Firstly, the *UHRF1* cDNA was generated from the total RNA in DT40 cells and inserted into the *in vitro* translation vector (pEPEX-FLAG). The FLAG tag was added to the N-terminus of the *UHRF1* cDNA by Dr Elaine Taylor and would be translated together with UHRF1. Therefore, the FLAG fused UHRF1 protein would be detectable by immunoblotting using both FLAG and UHRF1 antibodies. Subsequently, *in vitro* translation vectors were introduced into reticulocytes for FLAG fused UHRF1 protein expression. Finally, proteins from reticulocytes were subjected to immunoblotting for the antibody-antigen reaction detection.

The generation of UHRF1 protein expression vector

The cDNA of the *UHRF1* open reading frame was generated by PCR using primers that would insert *Nde I* and *Sal I* restriction sites at the N and C-terminus respectively. The PCR product was inserted into pGEM-T EASY vector for sequencing, as shown in

Figure 3.5. One repeated point difference resulting in amino acid change was found after three independent PCR reactions comparing with the *Gallus UHRF1* cDNA sequence downloaded from Genbank of NCBI website, as shown in **Appendix 4**. Considering the random occurrence of PCR errors and repeated base mutation in *UHRF1* nucleotide sequence of DT40 in **Appendix 4**, it is suggested that the

downloaded *Gallus UHRF1* cDNA sequence was not exactly identical to that of DT40 *UHRF1*. Subsequently, the fragment of our defined *UHRF1* cDNA was inserted into pEPEX expression vector for FLAG fused UHRF1 protein expression, as shown in

Figure 3.5.

Polyclonal antibodies raised against *Xenopus* UHRF1 also recognised the chicken homologues

In order to test the cross reactivity between *Xenopus* UHRF1 primary antibody and DT40 UHRF1 proteins, FLAG fused UHRF1 proteins were generated *in vitro* using TnT Coupled Reticulocyte Lysate System and were subjected to the reaction detection by Western blot, as shown in **Figure 3.6**. From **Figure 3.6A**, it is noticeable that the FLAG antibody reacted well with both FLAG fused *Xenopus* UHRF1 proteins and FLAG fused DT40 UHRF1 proteins translated *in vitro*, while no FLAG antibody reacted with proteins in *Xenopus* egg or DT40 cell extracts. From **Figure 3.6B**, the same size of proteins was found to react with *Xenopus* UHRF1 antibody as those with FLAG antibody, indicating the reactivity of the same proteins to both of the antibodies. The protein samples of X-UHRF1-TnT was degraded during the storage in -20°C.

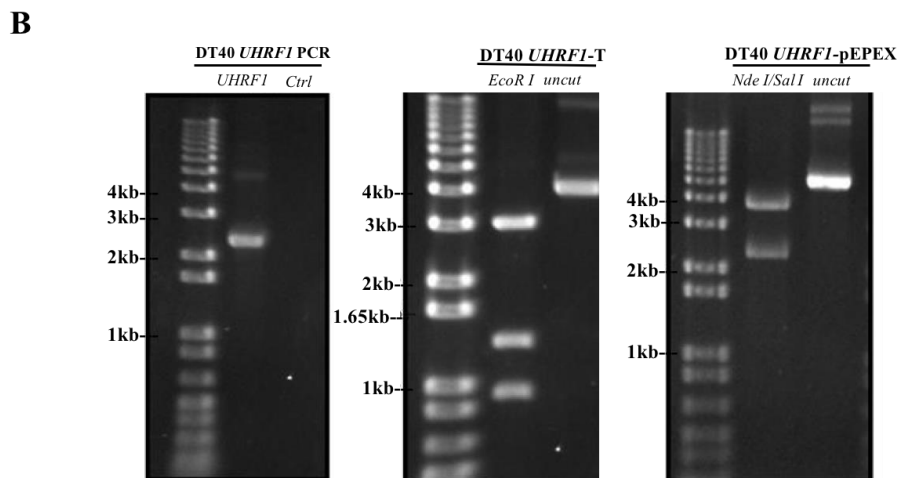
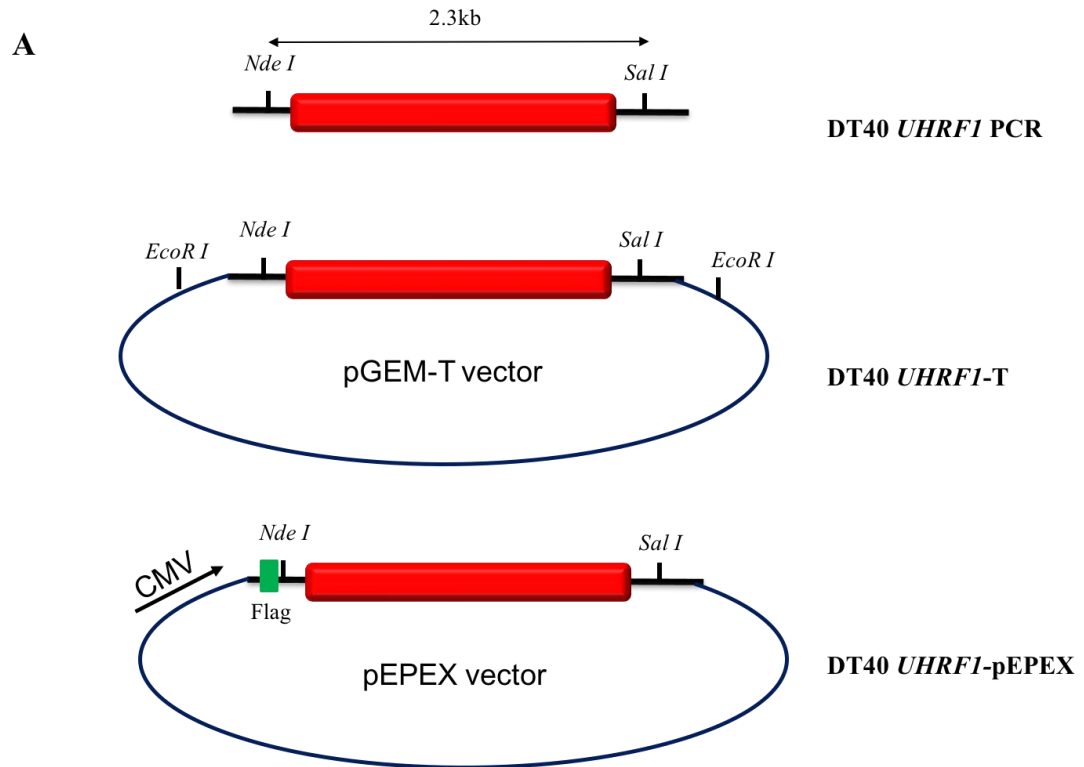


Figure 3.5 The generation of defined *UHRF1* expression vector.

(A). The Strategy of constructing FLAG tag fused *UHRF1* in pEPEX vector. (B). The PCR product of *UHRF1* generated from DT40 cDNA library with expected size of 2.3kb; The DNA constructs of *UHRF1* in pGEM-T EASY vector (*UHRF1*-T) were digested with *EcoRI* with expected bands of 1kb, 1.3kb and 3kb; The DNA constructs of DT40 *UHRF1* in pEPEX vector (DT40-*UHRF1* pEPEX) were digested with *Nde I/Sal I* with expected bands of 2.3kb and 3.8kb. Uncut DNA served as digestion control using water as replacement of restriction enzymes.

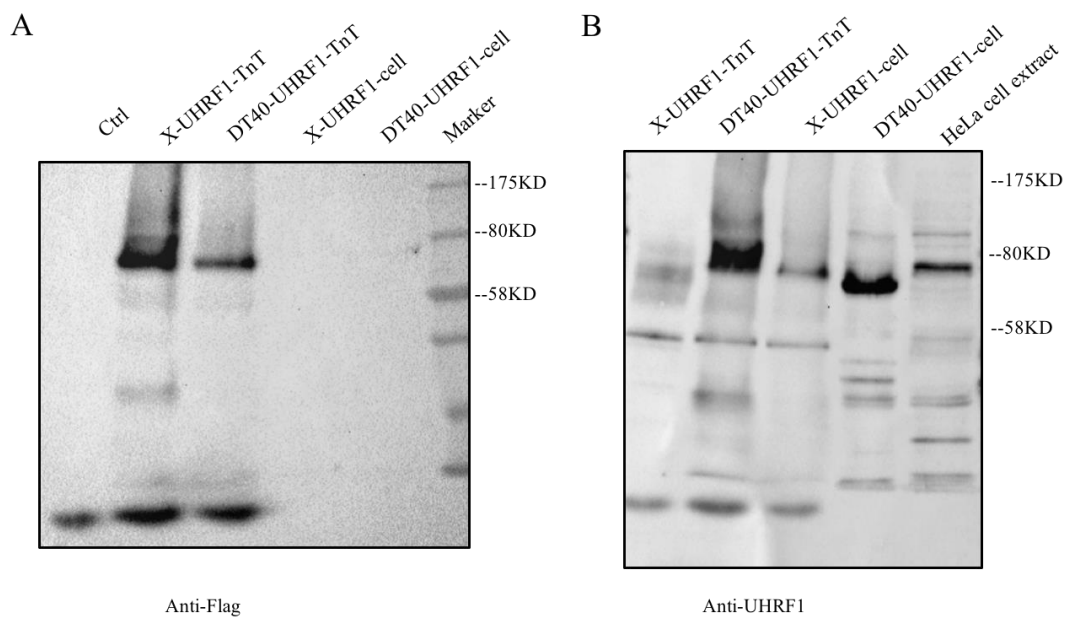


Figure 3.6 Cross reaction of *Xenopus* UHRF1 antibody to DT40 UHRF1 proteins.

(A). *In vitro* translated FLAG-tagged UHRF1 proteins and proteins from cell lysate were immunoblotted with FLAG antibody. (B). *In vitro* translated FLAG-tagged UHRF1 proteins and proteins from cell lysate were immunoblotted with UHRF1 antibody. The size of this sample could be referred to that in the left panel.

3.4 Possibly essential role of UHRF1 for DT40 cell survival

3.4.1 The optimization of CRISPR/Cas9 mediated *UHRF1* disruption

The fragments of two separate sgRNA targeting sequences for the *UHRF1* gene were synthesized by a commercial oligonucleotide synthesis service and inserted into two separate CRISPR/Cas9 vectors. After sequencing, the sgRNA constructs were delivered into two portions of wild type DT40 cells for gene editing by transfection. The transfection efficiency was measured as 45% by GFP signal expression from the control vector provided by the transfection kit. However, the transfection efficiency for CRISPR/Cas9 vector was uncertain.

Initially, no cells were found under the microscope after CD4 enrichment in cell portions with either sgRNA1 or sgRNA2 expression, whereas the control group achieved a significant number of cells, which were technically treated the same as that for *UHRF1* sgRNA. It is possible that CRISPR/Cas9 vector with *UHRF1* sgRNA was contaminated with RNA or nuclease. Alternatively, longer time than that recommended for other proteins is needed for DT40 cells to recover from electroporation damage and *UHRF1* gene disruption. Therefore, CRISPR/Cas9 vectors were then amplified to exclude the possible contamination of salts, proteins and RNA, and another 24 hours were given for cells to recover from the transfection. After changing both factors, 14 cell clones in total were achieved but no *UHRF1* gene deleted cells were found by Western blot.

Subsequently, all the buffer in the process of CD4 enrichment were verified to ensure no harsh wash. However, only few cells were achieved again, indicating the difficulty in having *UHRF1* gene disruption cell line by CRISPR/Cas9 technology may come

from the high efficiency of CRISPR/Cas9 in editing both *UHRF1* alleles simultaneously and the possibly essential role of *UHRF1* gene in DT40 cell survival.

These few CD4 enriched cell clones were screened for the expression status of UHRF1 proteins through immunoblotting with UHRF1 antibody, as shown in **Figure 3.7A**. Interestingly, sample 9 displayed no expression of UHRF1 proteins and was regarded as possible *UHRF1* knockout cells. Cells derived from the colony 9 were slow growing in culture compared to wild type DT40 cells consistent with a significant defect in proliferation. This is consistent with the reduced cell proliferative capacity in the *UHRF* knockdown cells (Tien, Senbanerjee et al. 2011, Jacob, Chernyavskaya et al. 2015, Ma, Peng et al. 2015, Ge, Yang et al. 2016, Jung, Byun et al. 2017, Liu, Ou et al. 2017, Liu, Ou et al. 2017, Xiang, Yuan et al. 2017). However, two weeks later, no proliferative defects were observed in the cell population derived from sample 9 compared with that of the wild type DT40 cells. Cell lysate from sample 9 at various stages were then subjected to immunoblotting for the screening of the UHRF1 protein expression, as shown in **Figure 3.7B**. However, it was found that all the cell populations showed the expression of UHRF1 protein with different levels.

The re-expression of UHRF1 proteins in the *UHRF1* knockout cells was possibly from contamination with wild type DT40 cells. Therefore, an early stock of sample 9 was taken from storage in liquid nitrogen and subjected to limiting dilution with only one cell per well in 96-well plates aiming at achieving monoclonal cell population. However, Western blot of cell extracts derived from these cells showed the presence of UHRF1 protein ultimately, indicating the cell population was not mixed with the wild type DT40 cells or the death of *UHRF1* knockout cells after passaging for a number of generations.

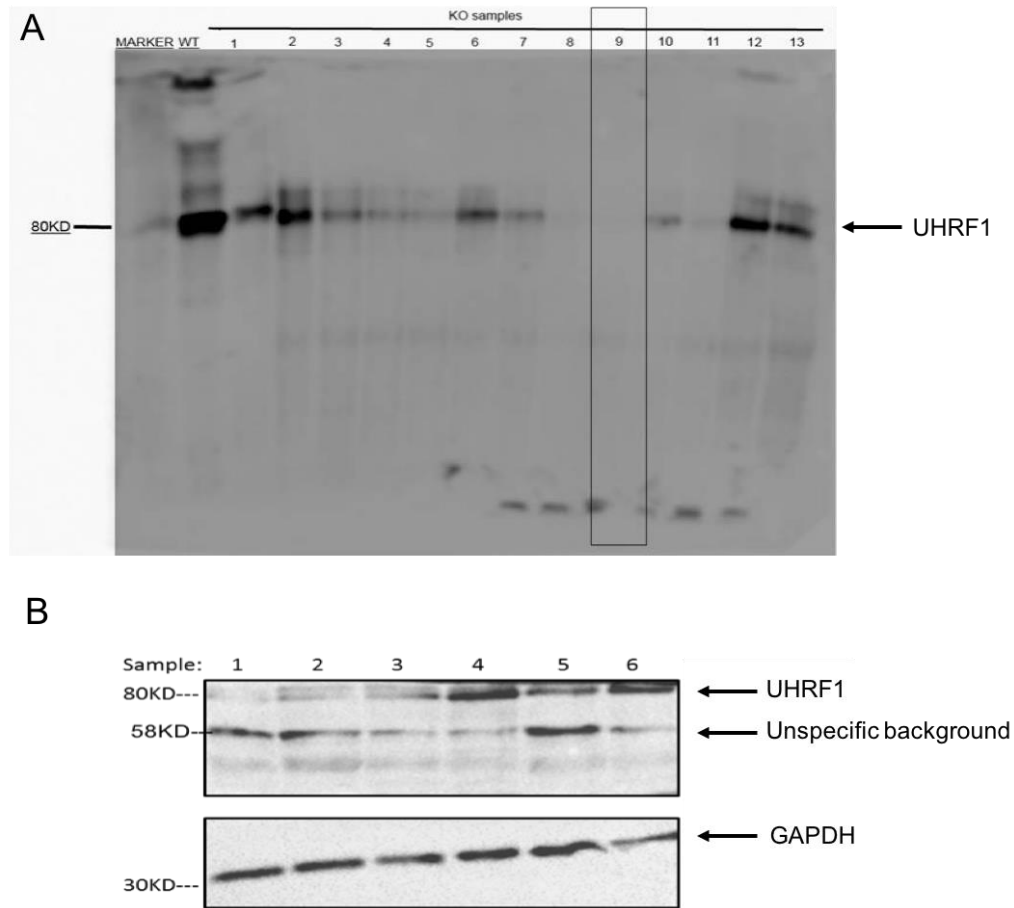


Figure 3.7 Screening of CRISPR/Cas9 mediated *UHRF1* gene deletion.

(A). WT indicated wild type DT40 cells serving as positive control. No.1-13 indicated individual protein samples from cell clones of CRISPR/Cas9 mediated *UHRF1* deletion. *Xenopus* UHRF1 antibody was used to immunoblot DT40 UHRF1 proteins. Equivalent amount of 20 μ g of proteins of were loaded in each lane. (B). Screening of CRISPR/Cas9 mediated *UHRF1* gene deletion. Sample 1-6 were frozen cell lines produced from sample 9.

3.4.2 *UHRF1* was possibly essential for cell survival

In order to know why the UHRF1 proteins in the *UHRF1* knockout cells were re-expressed, we tried to achieve another cell line and observe whether there would be re-expression of UHRF1 proteins in the *UHRF1* knockout cells and the re-expression pattern.

In another round of CRISPR/Cas9 mediated *UHRF1* deletion, longer recovery time after electroporation were given to ensure possibly more newly generated *UHRF1* deletion clones at the early stage. All the clones were treated individually in order to exclude the possibility of mixing with other cell types.

As expected, more cell clones of 64 in total were achieved after CD4 enrichment and were subsequently subjected to screening for the expression status of UHRF1 proteins, as shown in **Appendix 5**. It was found that 11 out from these 64 clones showed no expression of UHRF1 proteins and were regarded as *UHRF1* knockout cells. After culturing these cell lines for another 3 weeks, the re-expression of UHRF1 proteins were found in all these 11 clones, as shown in **Appendix 6**.

All the cell portions of KO cell samples were treated separately from other cell lines in the process of cell culture, and being kept sub-confluent to avoid potential senescence or apoptosis in the absence of UHRF1. However, this significantly reduced cell passing time was abolished after around 3 weeks of cell culture. Therefore, the cell line of KO frozen at the early stages was recovered to know the time points of UHRF1 re-expression. It is found that all the populations of KO cells showed the detectable expression of UHRF1 protein after three weeks of cell culture.

This experiment was repeated for another two times with around 100 clones were screened, but no sustainable *UHRF1* knockout cell line was achieved ultimately. Therefore, it was hypothesized that the difficulty in having *UHRF1* knockout clones was from the biological requirement of UHRF1 for the survival of DT40 cells. CRISPR/Cas9 technology can cause heterozygous or homozygous *UHRF1* allele disruption in cells. The cells with the targeting of only one allele of *UHRF1* will result in the reduced UHRF1 protein levels, as seen in **Figure 3.7** and **Appendix 5**.

If UHRF1 is required for cell viability as indicated by the unsuccessful attempts to isolate DT40 cells where UHRF1 expression has been ablated, then it will be necessary to conditionally express UHRF1 in cells to enable the endogenous loci to be targeted. Therefore, it is strategically planned to introduce exogenous UHRF1, which was conditionally expressed but resistant to *UHRF1* sgRNAs, into wild type DT40 cells and then delete both of the endogenous *UHRF1* alleles by CRISPR/Cas9 mediated gene deletion aiming at generating conditional *UHRF1* knockout cell lines.

**Chapter 4 A system for
conditional expression of UHRF1
in DT40 cells**

AID (auxin-inducible degron) system was developed from the plant species in which SCF E3 ubiquitin ligase and auxin were found to directly induce the rapid degradation of AUX/IAA transcription repressors, mediated by SCF TIR1 and SCF E3 ubiquitin ligase. This AID system was later established in yeast and mammalian cell lines and DT40 cells, in which the rapid and reversible expression of AID tagged protein was observed, thereby providing a powerful tool for studying the essential proteins, as shown in **Figure 4.1** (Nishimura, Fukagawa et al. 2009). However, whether the AID tag could conditionally control the expression of UHRF1 proteins and whether AID tag fused UHRF1 is functional remains unclear.

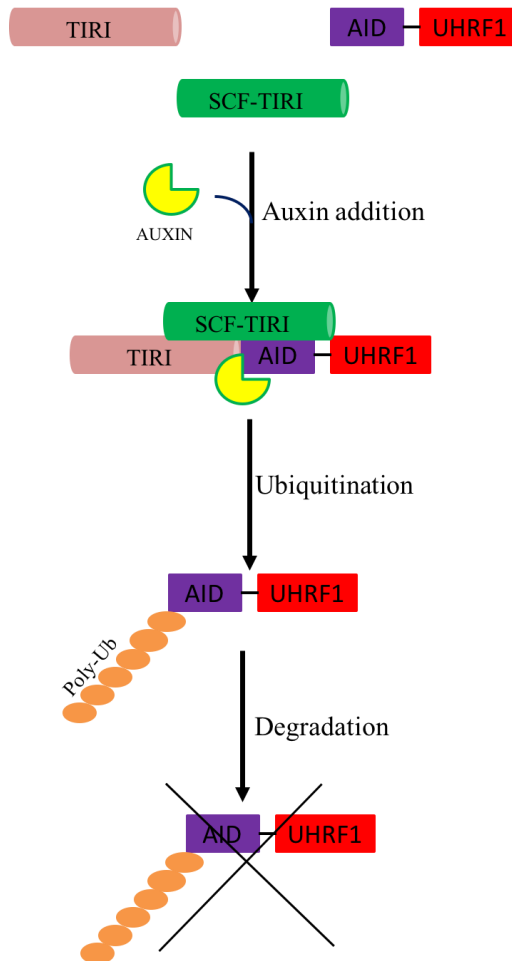


Figure 4.1 Schematic illustration of AID system.

SCF-TIR1 could promote the interaction between TIR1 and AID tagged target proteins. In the presence of auxin, SCF-TIR1 acted as E3 ubiquitin ligase resulting in the polyubiquitylation AID degenon. The degradation of AID tagged target proteins was mediated by proteasomes.

In order to maintain cell viability during the gene targeting of the *UHRF1* loci in DT40 cells, a cDNA encoding the human UHRF1 tagged with the AID degron was introduced into the cells to be targeted. Human *UHRF1* cDNA is resistant to sgRNAs and human UHRF1 proteins are 73.21% identical to that in DT40 cells, as shown in **Figure 3.3**. Once cells have been generated that lack expression of endogenous UHRF1 protein it should be possible to manipulate the levels of hUHRF1 protein in the cells by altering the concentration of auxin in the cell culture media.

4.1 Generation of DT40 cells with conditional expression of exogenous human UHRF1

4.1.1 Generation of constructs with conditional human UHRF1 expression

The cDNA of human *UHRF1* was generated by PCR and was inserted into the pGEM-T easy vector for sequencing. The fragment was then inserted into AID-GFP OSTER2 vector for the fuse to AID-GFP tag, as shown in **Figure 4.2A**. In order to show if AID-GFP tag will affect the expression or the function of UHRF1, the human *UHRF1* cDNA fragment was also cloned into the expressing vectors of AID OSTER2 and PCI-neo in order to tag *UHRF1* with AID and FLAG, respectively, as shown in **Figure 4.2B** and **Figure 4.2C**.

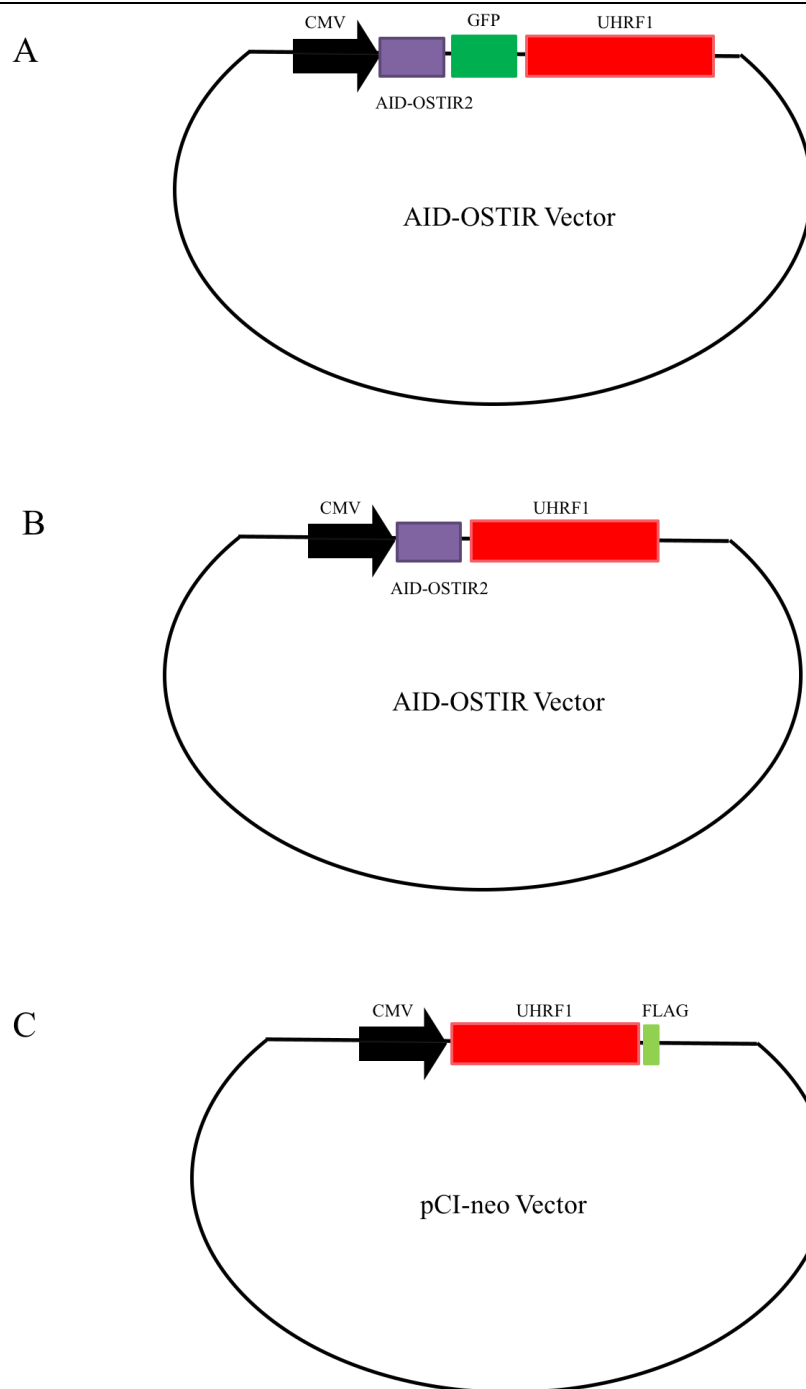


Figure 4.2 Schematic representation of human *UHRF1* in AID-OSTIR2 vector and pCI-neo vector.

(A). AID-GFP tagged human *UHRF1* in AID-OSTIR2 vector. (B). AID tagged human *UHRF1* in AID-OSTIR2 vector. (C). FLAG tagged human *UHRF1* in pCI-neo vector.

4.1.2 Generation of AID-GFP tagged human UHRF1 in DT40 cells

The introduction of AID-GFP tagged human UHRF1 into wild type DT40 cells was carried out by electroporation. Several rounds of transfection were performed and clones were screened by Western blot to find out clones with equivalent expression levels between exogenous and endogenous UHRF1 proteins, aiming at rescuing the loss of endogenous *UHRF1* gene by CRISPR/Cas9 technology. After screening 52 transfectants from three rounds of independent transfection, Ahg4 (clone 4 of AID-GFP tagged human UHRF1 vector transfected cell line) cell line was found to show the closest expression level of exogenous UHRF1 proteins to that being expressed endogenously, as shown in **Figure 4.3**. Similar introduction of AID tagged human UHRF1 (without GFP tag in between) into DT40 cells was performed to clarify the maximal expression level of exogenous UHRF1 proteins, as shown in **Figure 4.3** (clone 7, called Ah7).

Previous study mainly focuses on the effect of UHRF1 downregulation on cell proliferation, while the role of UHRF1 overexpression on cell growth remains unclear. Therefore, we next planned to test whether the introducing of AID-GFP tagged human UHRF1 will affect the proliferation capacity of DT40 cells. Meanwhile, another three UHRF1 expression constructs-----AID tagged human UHRF1, FLAG tagged human UHRF1, FLAG tagged chicken UHRF1 (as shown in **Figure 4.3**)-----were introduced into DT40 cells to exclude the potential influence of the AID-GFP tag or AID-OSTIR2 expression vector backbone on the structure and/or the function of human UHRF1.

From **Figure 4.4**, it is found that the introduction of AID-GFP tagged human UHRF1 or AID tagged human UHRF1 shows no effect on cell survival compared with that for

wild type cells. Together, this indicates that cell survival is not affected by the introduction of exogenous UHRF1 with different tags or from different sources.

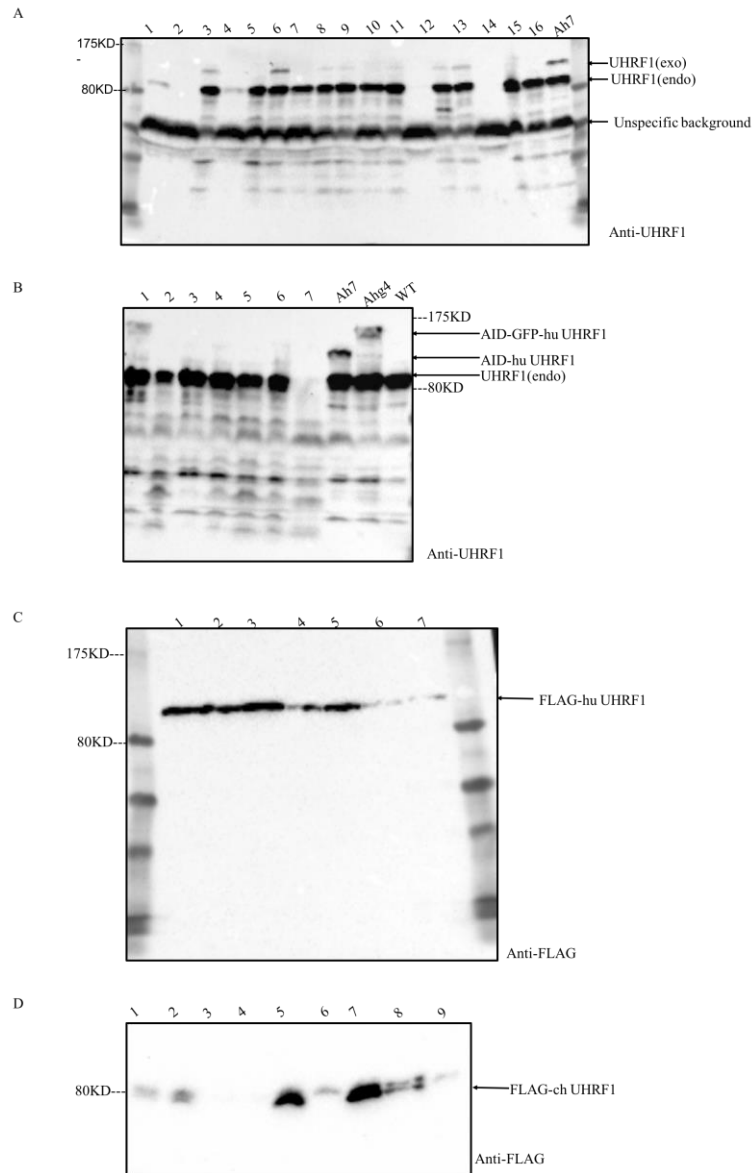


Figure 4.3 Screening of cell clones with cell clones with different tagged UHRF1.

(A). DT40 cells were transfected with AID tagged UHRF1;(B). DT40 cells were transfected with AID-GFP tagged UHRF1; (C). DT40 cells were transfected with FLAG tagged UHRF1 and equivalent amount of 30 μ g total protein was loaded on each lane. Proteins in image A and B were immunoblotted with UHRF1 antibody and image C with FLAG antibody.

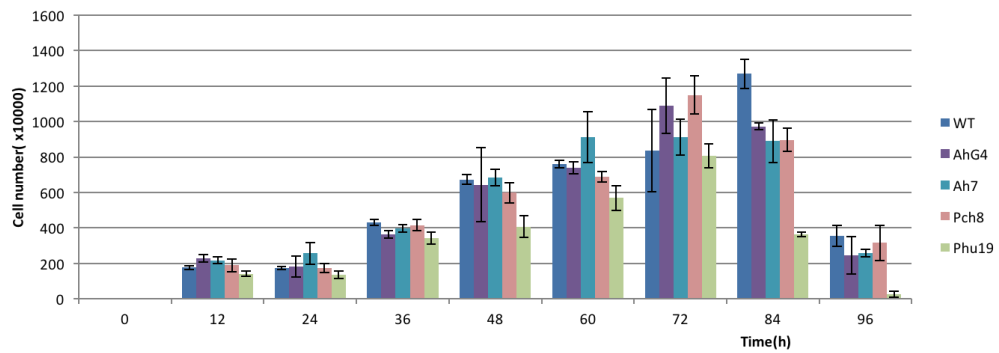


Figure 4.4 Generation of cell lines with exogenous UHRF1 expression.

Cell lines of WT (wild type), Ahg4, Ah7, Pch8 and Phu19 were subjected to cell number counting for every 12 hours with WT cells serving as control.

4.1.3 The conditional expression of AID-GFP tagged human UHRF1 in DT40 cell line

In order to know whether the AID-GFP tag could conditionally control the disruption of UHRF1 proteins in DT40 cells, Ahg4 cell line was then treated with auxin for different time periods. From **Figure 4.5A**, it is found that AID-GFP tagged human UHRF1 was significantly destroyed after 45 minutes of auxin treatment. Subsequently, the reversible expression of AID-GFP tagged human UHRF1 was tested by removing the treatment of auxin after 45min. It was found that on removal of auxin from the DT40 cells, AID-GFP-hUHRF1 protein could be detected after 15 minutes and had returned to “pre-auxin” levels by 45 minutes in **Figure 4.5B**. This demonstrates the rapid and reversible expression of exogenous human UHRF1 in DT40 cells, thereby allowing the subsequent removal of exogenous UHRF1 after the KO of the endogenous alleles.

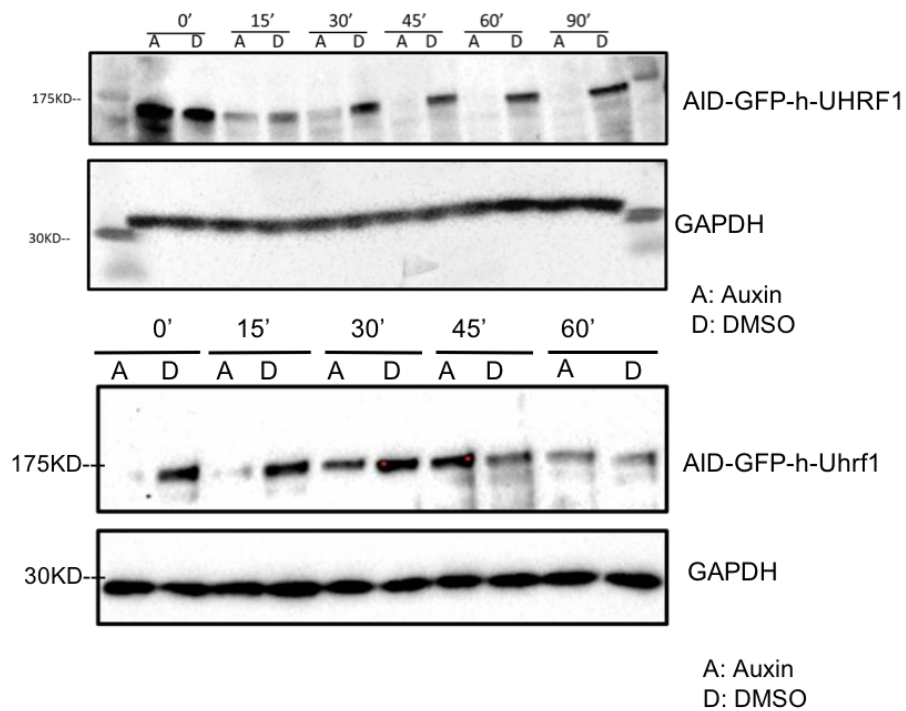


Figure 4.5 Conditional expression of AID-GFP tagged human UHRF1 protein.

(A). Cell lines of Ahg4 was treated with auxin for different time periods: 0min, 15min, 30min, 45min, 60min and 90min. DMSO worked as control solvent for auxin. (B). Ahg4 cell line was treated with auxin for 45min and then incubated in fresh media for different time points: 0min, 15min, 30min, 45min and 60min. Total proteins from different treatment were immunoblotted with UHRF1 antibody by Western blot. GAPDH protein served as loading control. Results presented are representative of three experiments.

4.2 Generation of conditional UHRF1 knockout cell lines

In order to generate conditional UHRF1 knockout cell lines, Ahg4 cell line was treated with CRISPR/Cas9 mediated *UHRF1* disruption following the methodology developed previously in Chapter 3.

588 clones in total were first collected for screening the expression status of UHRF1 proteins by Western blot, as an example shown in **Figure 4.6**. Some of the clones showed both loss of the endogenous and the exogenous UHRF1 protein expression, such as 279, 282, 295, while some clones showed the loss of endogenous UHRF1 protein expression only, such as 290, 291, 292, 293. This suggests both exogenous human UHRF1 and endogenous DT40 UHRF1 can be targeted by sgRNA.

As the aim of this project is to see the effect of UHRF1 loss on cell viability, cell lines of 279, 282, 295 were cultured for large population before using for future cellular events detection. However, re-expression of both endogenous and exogenous UHRF1 were found in all the three clones, consistent with the finding in **Figure 3.7**.

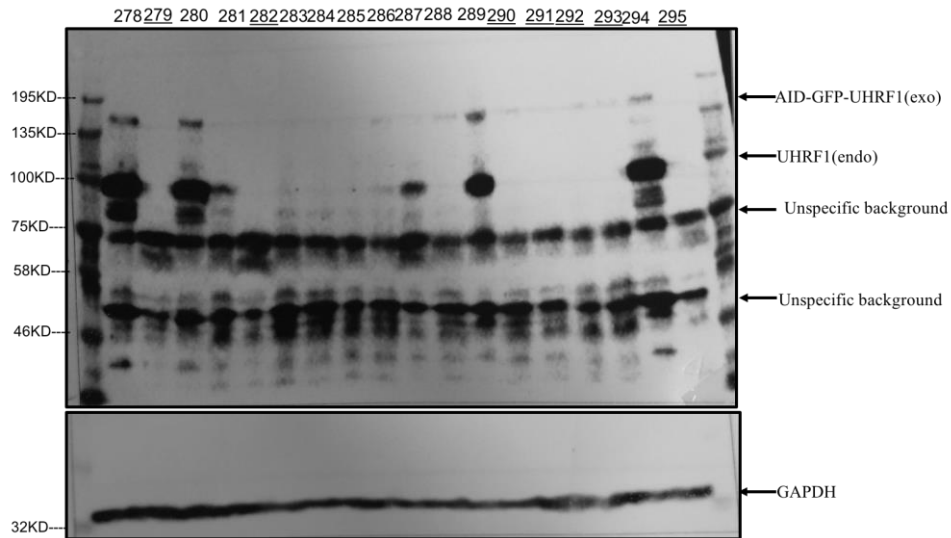


Figure 4.6 Screening of CRISPR/Cas9 mediated *UHRF1* disruption in Ahg4 cell line.

Clone 278-295 were subjected to Western blot for the expression state of UHRF1. UHRF1 antibody was used to immunoblot endogenous and exogenous UHRF1 proteins. GAPDH served as loading control.

4.3 Abolished proliferative capacity of *UHRF1* deleted cells

The experiment of CRISPR/Cas9 mediated *UHRF1* disruption was carried out for another six times with 328 clones being screened in total. Clone 22 (KO) was found to show no expression of both endogenous and exogenous UHRF1, as shown in **Figure 4.7A**. No re-expression of both UHRF1 after growing cells for one week, this cell line was therefore used to test the effect of *UHRF1* deletion on cell viability by cell proliferation assay as shown in **Figure 4.7B**. It is found that the deletion of *UHRF1* completely inhibits the proliferation capacity of DT40 cells.

This cell line of KO22 was also applied into clonogenic formation assay to cell plating capacity, as shown in **Figure 4.7C**. It is found that KO22 shows significantly reduced rather than abolished clonal formation ability comparing with wild type DT40 cells and Ahg4 cells. Therefore, KO cell line was checked for the expression of UHRF1 after culturing in fresh media for the same period. The re-expression of endogenous UHRF1 was found, indicating the formed clones may come from cells with UHRF1 protein expression.

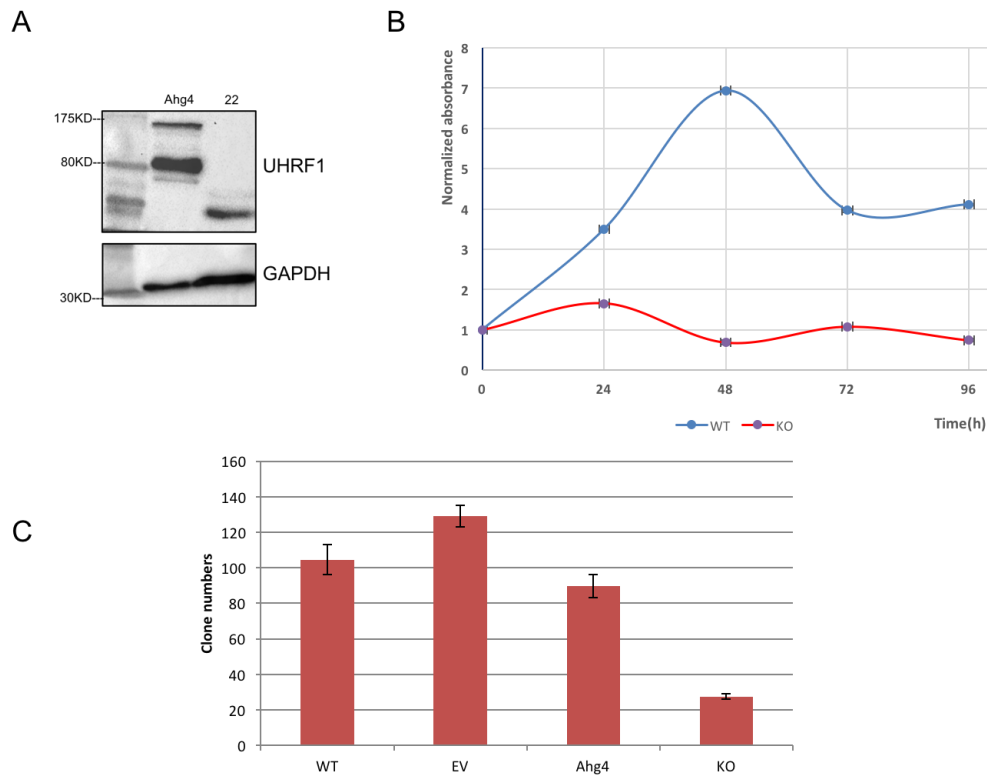


Figure 4.7 The proliferative block of *UHRF1* deleted cells.

(A). The UHRF1 protein expression status of Ahg4 cell line and clone 22 *UHRF1* knockout cell line (KO). UHRF1 antibody was used to immunoblot the expression of UHRF1 proteins and GAPDH serves as loading control. (B) The proliferative capacity was measured by formazan dye cleaved from WST-1 using Absorbance reader at 450nm. 500 of the cell population of KO cells and wild type cells were subject to this experiment. (C) The cell plating efficiency were tested by clonogenic formation assay with 50 cells being seeded in each cell portions. EV indicates AID-GFP OSTIR2 empty vector transfected DT40 cells.

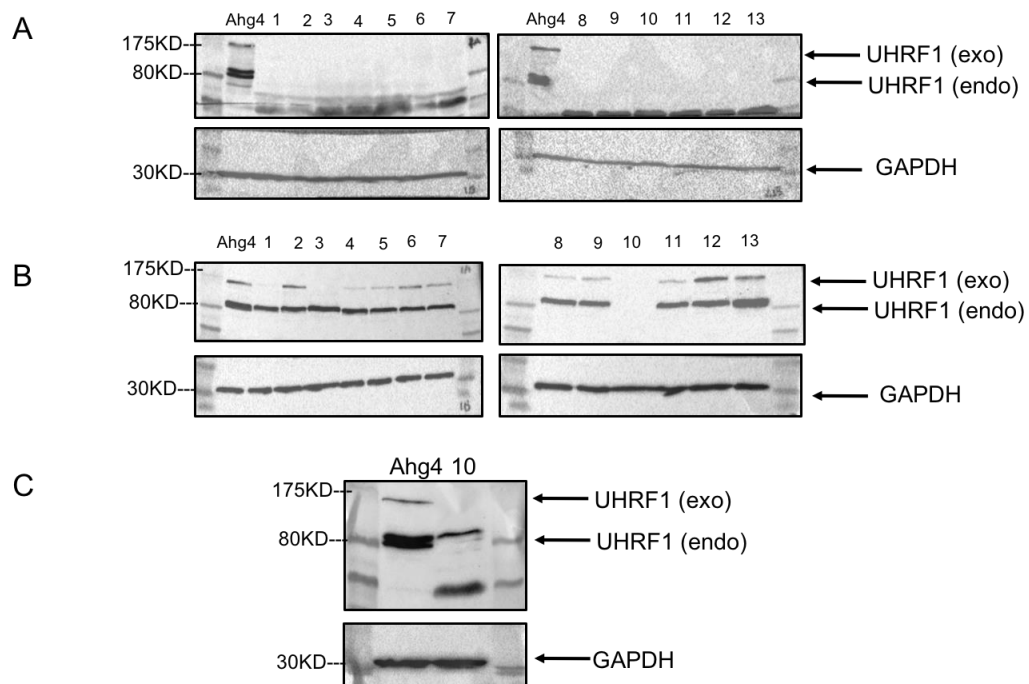


Figure 4.8. Screening of KO cell lines.

(A). Samples from KO samples being cultured for up to 1 week. (B). Samples from KO samples being cultured for up to 2 weeks. (C). Samples from KO samples being cultured for up to 3 weeks. ‘endo’ indicates endogenous proteins and ‘exo’ indicates exogenous proteins.

**Chapter 5 Targeting *UHRF1* gene
by Cre-Loxp combination system**

From chapter 4, we found both the exogenous human *UHRF1* gene and endogenous *UHRF1* gene could be targeted by CRISPR/Cas9 mediated gene deletion, which was fatal to the survival of DT40 cells. As an alternative strategy, we set out to target the endogenous *UHRF1* gene by traditional gene targeting system-----Cre-Loxp combination system with the coordination of conditionally expressed exogenous UHRF1.

5.1 Introduction of Cre-Loxp combination system

The Cre-Loxp combination system consists of Cre recombinase and mutant Loxp sites. Cre recombinase is responsible for reading the 34bp signal sequence of mutant Loxp sites and inducing their recombination, thereby deleting the sequence flanked between them. The newly produced Loxp RE+LE is unlikely to be recognisable by Cre recombinase any longer, as shown in **Figure 5.1**. The activation of Cre recombinase is inducible by the presence of 4-hydroxy tamoxifen, while the inactivation of it is mediated by the heat shock proteins in the absence of tamoxifen, thereby allowing the conditional deletion of the gene flanked by mutant Loxp sites.

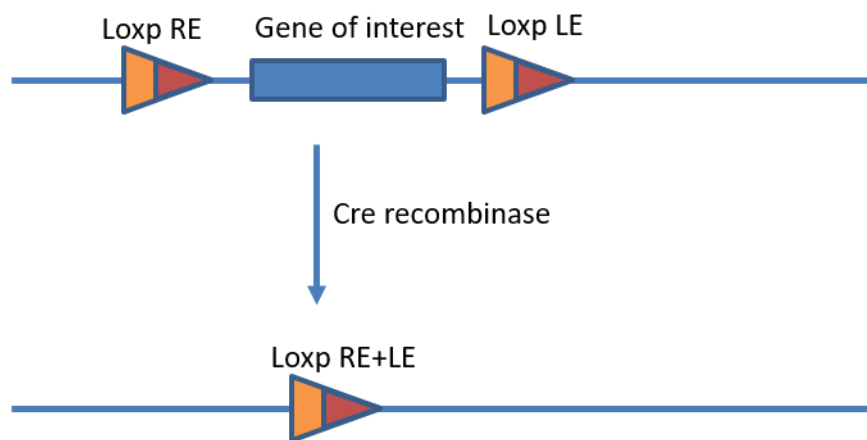


Figure 5.1 Schematic representation of Cre-Loxp combination system working principles.

The Loxp system was shown with mutant Loxp RE and Loxp LE sites for rearrangement. Gene of interest was firstly flanked by Loxp RE and Loxp LE. With the induction of Cre recombinase, for example, the addition of 4-hydroxy tamoxifen, the flanked Loxp RE and Loxp LE would convert into combined Loxp RE+LE, which would be poorly recognised by Cre recombinase, thereby dropping off the interested gene from genome.

5.2 Strategy of targeting *UHRF1* gene by Cre-Loxp system

Strategically, conditionally expressed UHRF1 was to be introduced into DT40 cells, followed by the gene targeting guided by identical target arms of *UHRF1* genomic DNA and the re-arrangement into chromosomes during the process of cell division. The fragment used for gene targeting were generated following the diagram in **Figure 5.2**.

Vectors without *UHRF1* cDNA cassette were used to target one allele of *UHRF1* and vectors with cDNA cassette was used to rescue the *UHRF1* gene expression under the deletion of the other allele. Although using cDNA cassette to rescue both *UHRF1* alleles by two rounds of gene targeting could keep UHRF1 protein expression at higher level before Loxp sites induction than that with only one round of *UHRF1* cDNA cassette, the efficiency of Cre recombinase which ranges from 60% to 100% will induce considerable remaining UHRF1 expression in the cell population, thereby blocking the observation of phenotypes caused by *UHRF1* deletion.

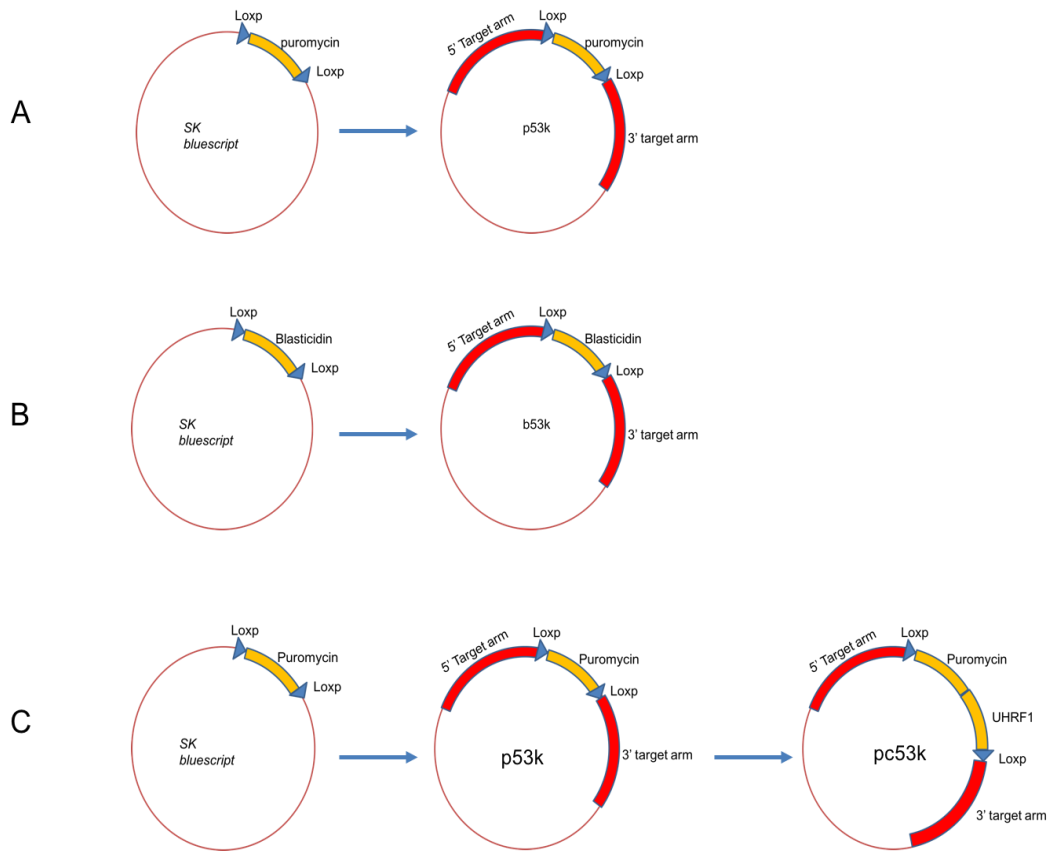
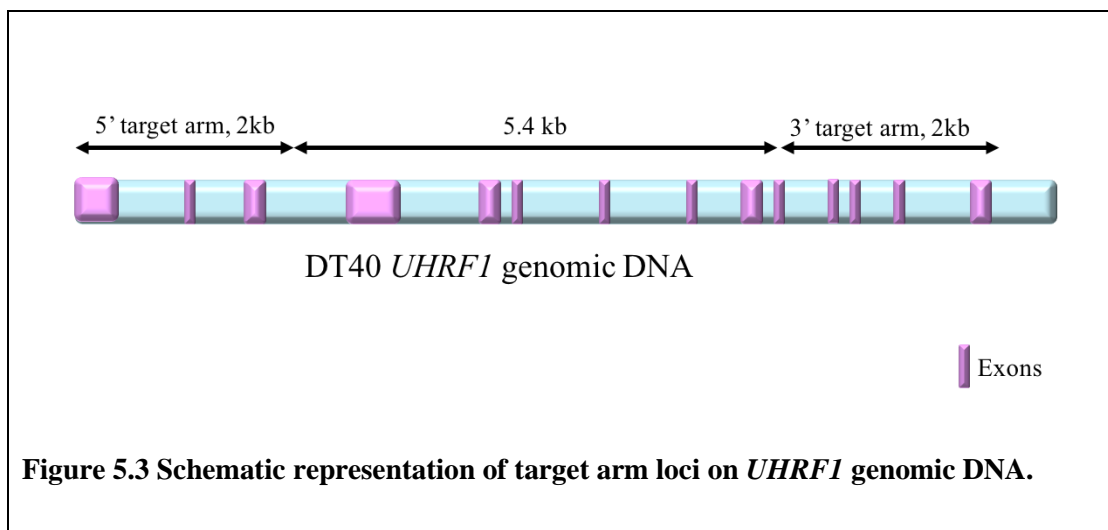


Figure 5.2 The diagram of generating vectors for gene targeting.

(A). *SK Bluescript* vector with the fragment of puromycin flanked by mutant *Loxp* sites served as backbone vector. 5' and 3' target arms of *UHRF1* genomic DNA were generated and assembled at both ends of *Loxp* sites. (B). *SK Bluescript* vector with the fragment of blasticidin flanked by mutant *Loxp* sites served as backbone vector. 5' and 3' target arms were assembled at both ends of *Loxp* sites, making the vector of *b53k*. (C). *UHRF1* cDNA cassette was generated from *PCI-neo* vector for the association with the *CMV* promoter and *SV40* poly A tail and was afterwards assembly into sites between *Loxp* sites in *p53k* vector, thereby making vector of *pc53k*.

Moreover, linearization of these vector was essential before introducing into DT40 cells at the upstream sites of 5' target arms or downstream sites of 3' target arms. The conditionally expressed UHRF1 will be AID-tagged chicken UHRF1, the protein levels of which can be regulated through the concentration of auxin present in the cell culture medium. Alternatively, the controllable expression of UHRF1 can be from a *UHRF1* cDNA cloned into an expression cassette between the *Loxp* sites. Expression from this cassette would be turned off by inducing recombination of the *lox-p* sites by Cre by the addition of tamoxifen.

To balance the requirements of the high transfection efficiency and the unique restriction enzyme sites on the *UHRF1* genomic DNA, the optimal size of the target arms was determined as 2kb and the distance between 5' and 3' target arms in the *UHRF1* genomic DNA was then 5.4kb, as shown in **Figure 5.3**. Stop codons in frame were added to the 3' end of the target arms with the advantage of terminating the sequence translation at the defined position and producing a truncated peptide which is unlikely to be functional.



5.3 Generation of cell lines with conditionally expressed UHRF1

5.3.1 AID system controlled *UHRF1* deletion cell line

Constructs used for exogenous UHRF1 expression and gene targeting (p53k) were generated as shown in **Figure 5.4A** and **Figure 5.4B**. Cell line with the expression of AID tagged chicken UHRF1(Ach) was expected to show 130KD band pattern immunoblotted by UHRF1 antibody, as shown in **Figure 5.4C**. Through the comparison of the signals between the endogenous and the exogenous UHRF1 proteins in Ach cell line, it is found these levels of UHRF1 protein expression are similar to those obtained when expressing the AID tagged human UHRF1 presented in **Figure 4.3**.

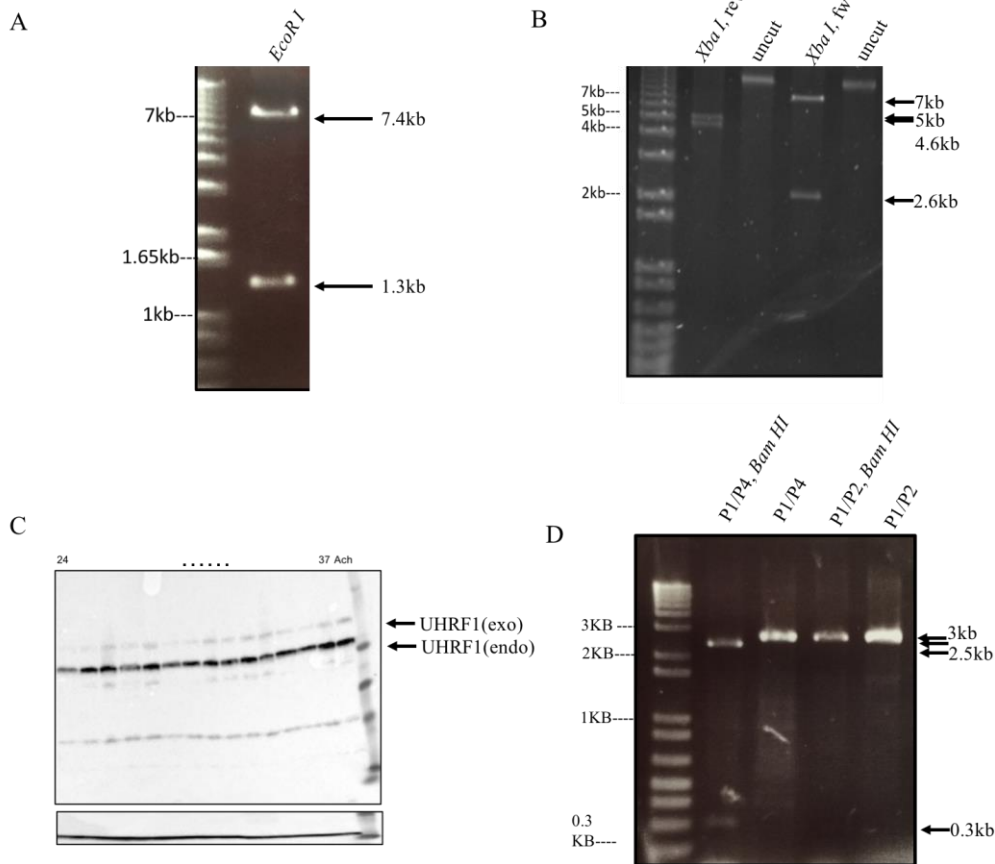
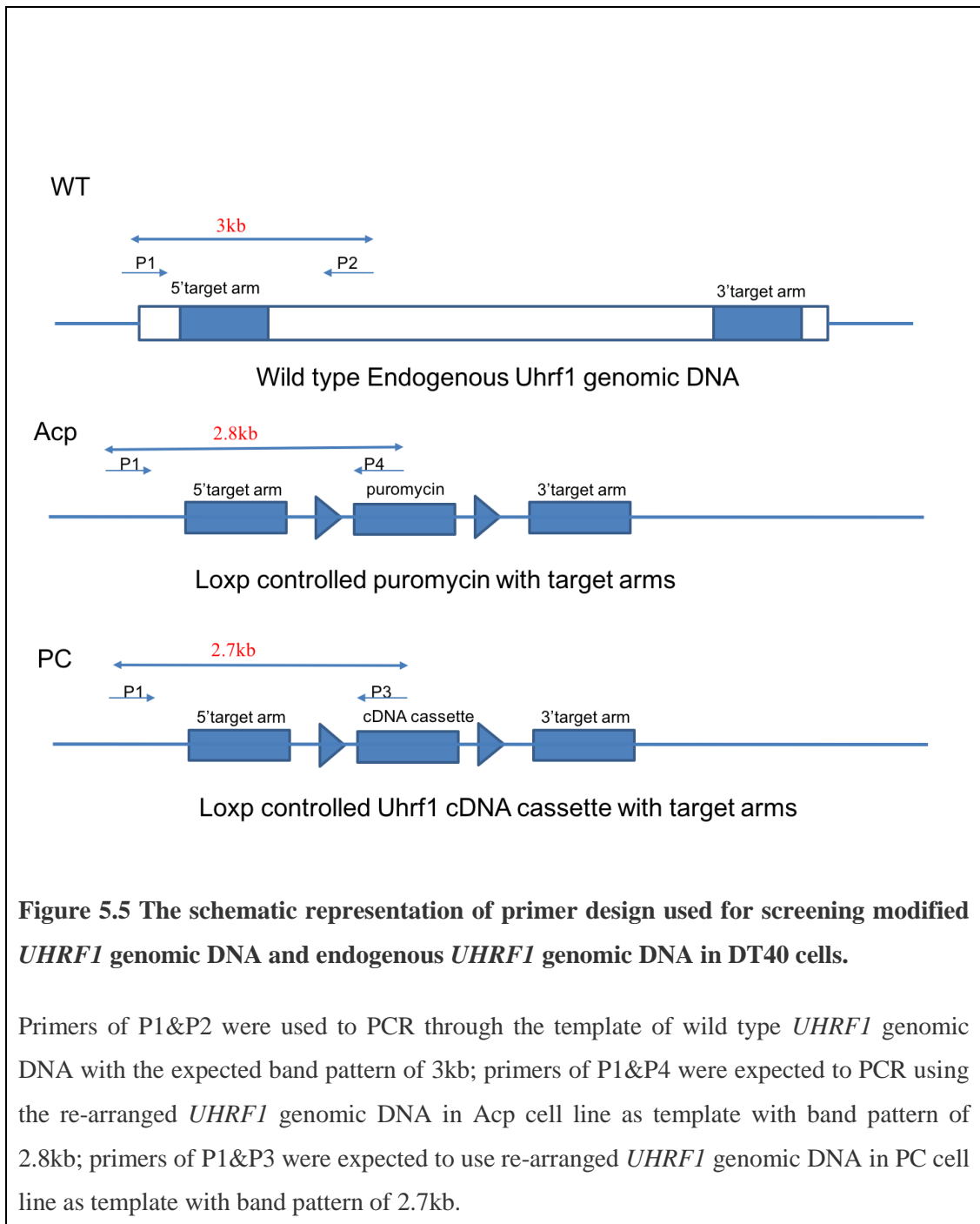


Figure 5.4 The generation of Acp24 cell line.

(A). The vector of Ach was digested with *EcoR I* and expected band pattern was 1.3kb and 7.4kb; (B). Gel analysis of restriction digested vector of p53k. p53k was digested with *Xho I*. *Loxp* puromycin cassette with forward orientation should display 2.6kb and 7kb and with reverse orientation should display 4.6kb and 5kb. (C). The screening of Ach cell line of clone 24 to clone 37 by Western blot immunoblotting with UHRF1 antibody. Cell line of Ach serves as endogenous UHRF1 expression control and GAPDH serves as loading control. (D). PCR products of ACP24 cell line following primer scheme in **Figure 5.5**. Lane 1: PCR product with primer P1&P4 was digested with restriction enzyme *Bam HI*. Expected band pattern is 0.3kb+2.5kb. Lane 2: PCR product of with primers P1&P4 without restriction enzyme digestion. Expected band pattern is 2.8kb. Lane 3: PCR product with primers P1&P2 and was digested with restriction enzyme *Bam HI*. Expected band pattern is 3kb as no *Bam HI* site on the fragment. Lane 4: PCR product with primers P1&P2 without restriction enzyme digestion. Expected band pattern is 3kb.

Subsequently, linearized vector of p53k was transfected into Ach cell line and the screening was done by Western blot and PCR. Targeted *UHRF1* genomic DNA is expected to show the band pattern of 2.8kb in the PCR product using primers of p1&p4, while the wild type allele should display the band pattern of 3kb using primers of p1&p2. The scheme of primer design was shown **Figure 5.5**.



By comparing the endogenous UHRF1 expression levels in Ach and Acp24 cell lines through Western blot, as shown in **Figure 5.4C**, it is found that the disruption of one *UHRF1* allele by gene targeting reduced the total proteins expressed by endogenous UHRF1 to less than 50%. The further PCR screening found clone 24 (called Acp24) showed one allele being targeted by synthetic p53k fragment, while the other allele remains the characteristics of the wild type, as shown in **Figure 5.4D**.

Next, the cell line of Ach24 was subjected to endogenous *UHRF1* gene targeting by b53k vector (as shown in **Appendix 8**) with a different selection marker of blasticidin. However, after three rounds of transfection and screening, no expected cell line was found, indicating the expression level of AID tagged chicken UHRF1 may not be sufficient to compensate the loss of endogenous *UHRF1* alleles.

5.3.2 Cre-Loxp system controlled conditional UHRF1 cell line

Construct of pc53k was generated and identified by restriction enzyme digest, as shown **Figure 5.6A**. Linearized pc53k fragment was used to target *UHRF1* genomic DNA in the wild type DT40 cells and the screening was done by PCR. The targeted genomic DNA is expected to demonstrate the band of 2.7kb on the agarose gel. After screening 76 clones, the cell line of clone 7 (called PC7) was found to show expected band pattern as shown in **Figure 5.6B**.

Subsequently, PC7 cell line was subjected to investigate the effect of the rearrangement of *UHRF1* cDNA cassette into chromosome on cell proliferation, as shown in **Figure 5.6C**. It is notable that there were no significant cell proliferation defects in PC7 cell line comparing with that of the wild type DT40 cells after culturing the cells for 96 hours. Cell proliferation defects are only visible when UHRF1 expression is disrupted to a very low level, as shown in **Figure 4.7**.

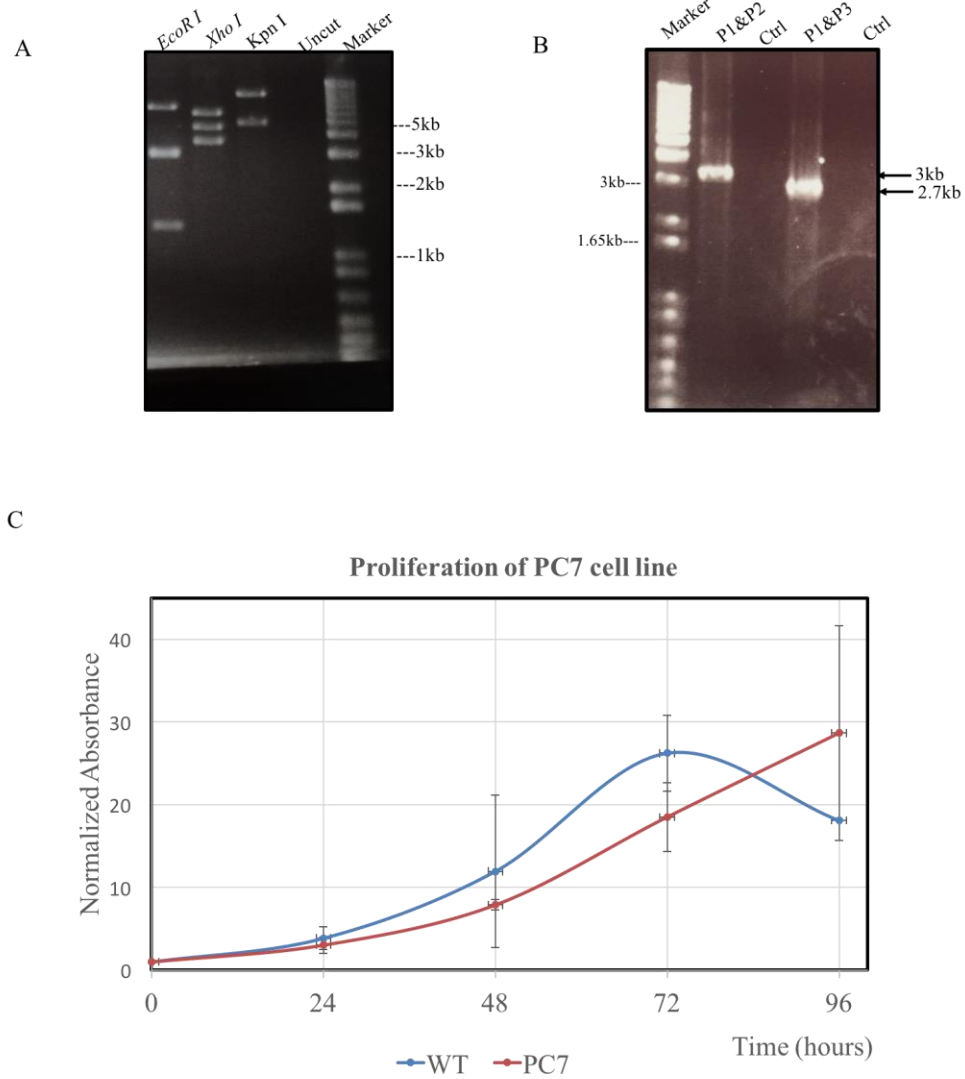


Figure 5.6 The screening of PC7 cell line with conditional expression of UHRF1.

(A) The vector of pc53k was assembled and digested with *EcoRI*, *XhoI*, *KpnI* respectively with expected band pattern. (B). PCR screening of PC7 cell line for conditional expression of UHRF1 (C). The cell proliferation of pc7 cell line. The absorbance at 0h was normalized as 1 and all the other absorbance was normalized to the value at 0h. These experiments were done with triple replicates and repeated three times.

Afterwards, PC7 cell line was transfected with constructs for the inducible expression of Cre recombinase. There was C-terminus FLAG tag of UHRF1 being expressed by the synthetic *UHRF1* cDNA cassette. Therefore, the clones with functional Cre recombinase should induce the Loxp sites combination, thereby abolishing the signal of FLAG when immunoblotted by FLAG antibody. However, no expected clones were found after screening the transfectants from three independent experiments. Subsequently, the PC7 cell line was treated with another construct of b53k aiming at deleting the other endogenous *UHRF1* gene. Unfortunately, no expected clones could be found after screening more than 100 clones in three independent experiments, indicating the UHRF1 protein expressed by the *UHRF1* cDNA cassette was not sufficient to compensate the loss the endogenous *UHRF1* alleles.

5.4 UHRF1 level positively related to cell sensitivity to ICL reagents

In order to know the reason why the other endogenous *UHRF1* allele cannot be targeted, the expression level of UHRF1 protein in PC7 cell line was tested. It was found that the UHRF1 proteins in PC7 cell line in **Figure 5.7A** had been sufficient to support normal cell growth as wild type DT40 cells as shown in **Figure 5.6C**.

Next, the effect of different levels of UHRF1 proteins on the cell sensitivity to MMC was tested by cell proliferation assay. Cell lines of wild type DT40, Ach and PC7 were first treated for different time points with different concentration of MMC, as shown in **Appendix 9**. It was found cells maintained growth characteristics at various concentrations of MMC treatment until culturing for 48 hours. Therefore, 48 hours was treated as the time period for testing cell sensitivity to MMC. It was found that there was positive relationship between UHRF1 protein expression levels and cell resistance to MMC. The overexpression of UHRF1 in DT40 cells enhanced cell viability to ICLs reagent of MMC comparing with the wild type DT40 cells, while the opposite effect can be found in UHRF1 downregulated cell line of PC7.

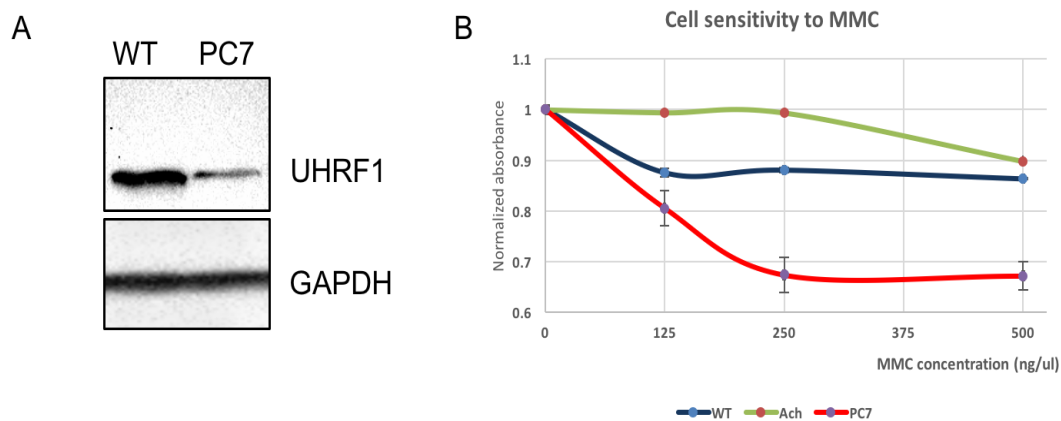


Figure 5.7 UHRF1 downregulation caused upregulated sensitivity to MMC.

(A) The expression of UHRF1 proteins in PC7 cell line. The protein expression of UHRF1 in Ach (AID tagged chicken UHRF1) cell line can be referred to **Figure 5.4C**. UHRF1 antibody was used to immunoblot UHRF1 proteins and GAPDH serves as loading control. (B). The cell sensitivity of cell lines with various expression of UHRF1 to MMC. These three cell lines were seeded with same number of cells and treated with 0 ng/ μ l, 125ng/ μ l, 250 ng/ μ l and 500 ng/ μ l of MMC for 48 hours. The absorbance values were normalized to that with 0 ng/ μ l of MMC treatment. Triple replicates were done for each reaction and this experiment was repeated three times.

Chapter 6 Discussion and future work

6.1 Proliferative block caused by abnormal UHRF1 expression

Epigenetics is a central mechanism for regulating the gene expression and inheriting accurate epigenomic information to the descendent cells. However, the molecular mechanism underlying the cancer cell proliferative block caused by the epigenetic changes still remains unclear.

In the work presented it was found that the homozygous deletion of *UHRF1* in DT40 cells retained the cell proliferation capacity for several generations followed by proliferative block, possibly resulting from senescence or apoptosis, as shown in **Figure 4.8**, indicating the positive relationship between UHRF1 expression levels and cell proliferation potential (Hopfner, Mousli et al. 2000). Similar results were found in zebra fish embryonic development which died by 240 hours after fertilization using embryonic cells with around 15% of normal levels of *UHRF1* mRNA expression (the protein expression level was not published) (Jacob, Chernyavskaya et al. 2015).

Recently, the generation of the cell line with *UHRF1* knockout mediated by CRISPR/Cas9 was achieved in airway basal cells, which demonstrated significantly reduced but countable colony formation efficiency. Further immunofluorescence study found the formed colonies from *UHRF1* knockout cell line were derived from the cells with the expression of UHRF1 (Xiang, Yuan et al. 2017). As Cas9 was transiently transfected into DT40 cells for cleaving the complementary target DNA and inducing the permanent modification of gene expression, the disrupted *UHRF1* gene therefore should allow no expression of UHRF1 proteins. However, the re-expression of UHRF1 protein in CRISPR/Cas9 mediated *UHRF1* knockout DT40 cells was detected after culturing cells for up to 1 to 3 weeks as shown in **Figure 4.8**,

similar to the re-expression of UHRF1 observed in the airway basal cell line (Xiang, Yuan et al. 2017). The reason underlying the protein re-expression of UHRF1 remains to be elucidated.

One possibility of the observed re-expression of UHRF1 protein in CRISPR/Cas9 mediated UHRF1 knockout cells could be due to the off-target effect with the Cas9 targeting a related DNA sequence, and initiating DNA repair events in another location of the genome. UHRF1 knockout cells may have a mutator phenotype due to the loss of UHRF1 function – this might lead to subsequent mutations that restore UHRF1 expression. The selection pressure imposed by genomic stability only allows cells with UHRF1 expression to survive.

Additionally, Cas9 was reported to tolerate the mismatches between guide RNA and target DNA in nucleotide sequence-dependent manner and sensitive to the number of up to 5 (Fu, Foden et al. 2013), position and distribution of mismatches (Hsu, Scott et al. 2013). In this thesis, RNA-target DNA mismatch in the proto-spacer region was found to be seven mismatches, as the demonstration in **Figure 4.8**, where human UHRF1 was targeted by sgRNA1 in DT40 cells. Alternatively, the specificity of guide RNA and DNA remains to elucidate.

Another possibility of UHRF1 to re-express is depending on the choice of sgRNA locus on the genome. In this thesis, sgRNA was chosen using the first exon to maximize the disruption of *UHRF1*. However, there is evidence that targeting the exons at the 3'-end of a gene can also disrupt gene expression successfully (Gillian Dunphy, personal communication). Therefore, more sgRNA may be adopted and selected for UHRF1 knockout.

Technically, the re-expression of UHRF1 in *UHRF1* knockout cell population could rise from the improper cell culture, thereby mixing *UHRF1* knockout cells with other cell lines with UHRF1 expression. However, the knockout cells were treated individually and separately during the maintenance of the cell line. This technique is further emphasized during maintaining the *UHRF1* knockout cells (KO22) the second time. Furthermore, the *UHRF1* knockout cells were subjected to limiting dilution for separating *UHRF1* null cells from UHRF1 positive cells, and only cell population with UHRF1 expression were achieved. Therefore, the re-expression of UHRF1 is more likely due to the biologic requirement of UHRF1 in cell survival as a potentially essential gene and cells without UHRF1 were extinct after several generation of cell division.

Consistently, another study found HCT116 cell line with homozygous *UHRF1* gene deletion via stepwise Loxp/Cre recombinant gene targeting system displayed severe proliferation defects after culturing cells for up to 6 days (Tian, Paramasivam et al. 2015). As the efficiency of Cre recombinase induced Loxp site combination ranges from 60%-100% (Arakawa, Lodygin et al. 2001), the leftover cell viability may rise from uncompleted UHRF1 deletion. Alternatively, UHRF1 deleted mutants maintained cell viability for several generations until senescence or apoptosis.

Moreover, the expression level of UHRF1 required for maintaining cell proliferation capacity may vary among cell species or tissues, as downregulating UHRF1 to the equivalent level as **Figure 5.7A** shows no proliferation defects in DT40 cells (**Figure 5.6C**), but instead demonstrated severe proliferation defects in liver cancer cells (Liu, Ou et al. 2017).

In future, it is important to establish the conditional *UHRF1* knockout cell lines following the procedures: (i) make mutations of chicken *UHRF1* cDNA at the location of sgRNA PAM sequence and tag it with AID-GFP, as the disruption of PAM sequence of sgRNA will abolish the cleavage of CRISPR/Cas9. The introducing of identical exogenous chicken UHRF1 is preferable to the human UHRF1 with the similarity of 73.21% in the rescuing of endogenous loss of *UHRF1* alleles in DT40 cells. (ii) disrupt the endogenous *UHRF1* alleles with sgRNA1 by CRISPR/Cas9 technology. (iii) screening the expression of UHRF1 by immunoblotting. (iv) conditionally control the expression the exogenous UHRF1 by the addition/removal of auxin. (v) test the fate of *UHRF1* knockout cells through TUNEL apoptosis assay or senescence marker of SA- β -GAL. (vi) test the interacting molecules of UHRF1 in the process of senescence or/and apoptosis.

The potential problem under this work is whether the AID-GFP tag will affect the function of chicken UHRF1. Our previous results found AID tagged chicken UHRF1 cannot support the loss the both *UHRF1* alleles in the cell viability, but instead could enhance the cell resistance to ICLs damage. Hopefully, the isolation of GFP tag between AID tag and UHRF1 cDNA, or tagging UHRF1 cDNA with AID-GFP or AID tag at the C-terminus may counteract their interaction. In order to test whether the introduced tagged UHRF1 is function, one feasible way is to test the interaction between UHRF1 and BRCA1 by immunofluorescence for co-localization in response to DNA damage. If the tagged UHRF1 could function with BRCA1 as well as that by the wild type UHRF1, this would provide some indications that the tagged UHRF1 is functional.

If AID-GFP tagged UHRF1 cannot compensate the loss the *UHRF1* alleles, the conditional *UHRF1* knockout cell line can be generated as follows: (i) disrupt one

allele of *UHRF1* by gene targeting using the vectors of p53k. (ii) introduce the AID or AID-GFP tagged UHRF1(with PAM sequence mutation) into that cell line, see if higher level of exogenous UHRF1 can be expressed in the condition of lower level of endogenous UHRF1. Additionally, the CAG promoter which drives much higher expression level of combined target sequence could be used to replace the CMV promoter in the expressing vector. (iii) disrupt the other *UHRF1* allele by CRISPR/Cas9 technology.

6.1.1 The mechanisms underlying UHRF1-dependent proliferative block

The hypomethylation and abnormal DNA replication caused by UHRF1 loss

The mechanism of cell proliferative block induced by the deletion of *UHRF1* was suggested to be proceeded through the global and local hypomethylation (Jacob, Chernyavskaya et al. 2015). Supportive to this, the mutant of UHRF1 could be phenocopied by the mutant of DNMT1, and the knockdown of DNMT1 in UHRF1 mutants enhanced cell proliferation block (Jacob, Chernyavskaya et al. 2015). The induced global DNA hypomethylation by UHRF1 downregulation resulted in the failure of DNA replisome formation (without DSBs lesion) in primary human bronchial epithelial (HBE) cells, followed by G2/M cell cycle arrest and p15 dependent cell senescence (Liu, Ou et al. 2017). The non-apoptotic cell death caused by UHRF1 knockdown was also observed in human liver cancer cells which exhibited G2/M cell cycle arrest and corresponding Cyclins expression (Liu, Ou et al. 2017).

Consistent with this, almost all of the DNA replication was abolished by the depletion of nuclei UHRF1 to less than 1% in *Xenopus* egg extracts (Taylor, Bonsu et al. 2013), although another study found the depletion of UHRF1 in in *Xenopus* egg extracts

placed no effect on DNA replication, but instead the blocking of DNA replication abolished DNA methylation (Nishiyama, Yamaguchi et al. 2013). The abolished effect of UHRF1 depletion on DNA replication observed by the *Nishiyama et al* group may be attributed to the insufficient depletion level of UHRF1 in the former study, which was only enough to abolish the recruitment of DNMT1. This is because depleting UHRF1 to less than 1% in *Xenopus* egg extracts was still sufficient to support around 40% of DNA replication.

In contrast, the DNA hypomethylation caused by UHRF1 loss was found to inhibit the formation of heterochromatin and the replication of pericentromeric heterochromatin (Papait, Pistore et al. 2007), but maintained the conformational structure of euchromatin (Nady, Lemak et al. 2011), thereby allowing the accessibility of origin firing and licensing during DNA replication, which sequentially activating the uncoordinated DNA re-replication (Jacob, Chernyavskaya et al. 2015). The abundant synthetic DNA was supposed to mimic the damaged DNA and activate the G1/S cell cycle arrest and cell apoptosis (Jacob, Chernyavskaya et al. 2015).

The difference between these findings in terms of DNA replication and cell cycle arrest can be interpreted by the lack of checkpoints in *Xenopus* egg extracts or by the function of additional mechanisms to restrict epigenetic damage in the context of the whole organism.

In future, after generating the conditional *UHRF1* knockout cell line, the cell cycle redistribution can be tested by flow cytometry and the effect of UHRF1 on DNA replication will be tested through DNA fibre analysis. If cells can tolerate the treatment of cell cycle synchronization, drugs of geminine, rescovitinone will be used to inhibit the origin licensing and the DNA replication initiation respectively. This

would tell the specific stage of DNA replication that UHRF1 is involved. Afterwards, caffeine, which over-rides the intra-S phase checkpoint and activates the dormant origins, will be used to treat the *UHRF1* knockout cells in order to clarify if the replication block could be overcome and what is the timing for the competent replication origin generation.

Cell apoptosis caused by UHRF1 loss

UHRF1 was found to participate in the initiation of HR in S/G2 phase by being recruited to the DSB sites with coordination of BRCA1, resulting in the polyubiquitination of RIF1 and its disassociation from 53BP1 (Zhang, Liu et al. 2016). Similarly, the repair mechanism of the collapsed DNA replication forks was also found to require the cooperation of UHRF1 and Eme1, a component of endonuclease (Mistry, Gibson et al. 2008). Cells failed to repair the damaged DNA will not be able to bypass the checkpoint but instead will undergo apoptosis. The apoptosis signalling was independent from the expression and the stabilization of *p53* (Tien, Senbanerjee et al. 2011), but instead dependent on the enhanced expression of apoptotic proteins of caspase 3/8/9 and Bax and the reduced expression of anti-apoptosis proteins of Bcl-2 (Tien, Senbanerjee et al. 2011, Ge, Yang et al. 2016).

In contrast, another study using renal carcinoma cells found downregulating the expression of UHRF1 increased the expression of *p53* through markedly enhancing the expression of *p53* transcription factor of *p21*. The E3 ligase activity of UHRF1 RING finger domain promoted the non-degradative ubiquitination of *p53*, thereby inhibiting the transactivation of *p53* and *p53*-dependent apoptosis (Ma, Peng et al. 2015). The different role of *p53* in UHRF1 downregulation induced apoptosis can be

attributed to the failure to transactivate the *p53*-responsive reporters (Gurova, Hill et al. 2004).

Moreover, evidences of G2/M cell cycle arrest by UHRF1 downregulation can also be found in HCT116 colon cancer cells (Tien, Senbanerjee et al. 2011) or Caski cervical cancer cells (Ge, Yang et al. 2016) or with both G1 and G2/M phase in lung cancer H1299 cells (Jenkins, Markovtsov et al. 2005). A number of reasons may interpret the findings for the differences in cell cycle arrest. (i) the requirement for UHRF1 in the propagation of cell cycle may vary depending on the tissue specific cell lines in according to the different mechanisms to bypass the cell cycle arrest. (ii) the cells were synchronized at the certain cell cycle by certain drugs before detecting the cell cycle progression raising the possibility that the arrest may be form an indirect effect. (iii) the variation of UHRF1 downregulation degrees may result in the different cell cycle phenotypes. (iv) the defective checkpoints in cancer cells comparing with matched normal cells.

Cell senescence caused by UHRF1 loss

Comparing with other cell degenerative fates, including apoptosis and necrosis, the development of cell senescence is relatively slow and progressive. In the replicative and oncogene induced senescence cells, significantly repressed mRNA level of UHRF1 was found as early as 18 hours (Xiang, Yuan et al. 2017), possibly through the regulation on its transcription regulators. Similar to another study that identified progressive downregulation of UHRF1/DNMT1 at the early stage of senescence after screening the gene expressing profiles in response to senescence in time serials by bioinformatics.

The inhibited expression of UHRF1 and DNMT1 resulted in the slow accumulation of global hypomethylation and changes in the expression of various genes, which were important for the regulation of cell senescence, thereby initiating senescence (Jung, Byun et al. 2017). Moreover, the induction of senescence was the most effective when both UHRF1 and DNMT1 genes were knocked down, and the knockdown of UHRF1 was more effective than DNMT1 knockdown (Jung, Byun et al. 2017). This implies UHRF1 imposed additional influence on senescence besides its control on DNMT1. For example, UHRF1 was found to be important for the transcription of DNMT1 mediated by *p53/sp1* pathway (Lin, Wu et al. 2010). One downstream target gene of UHRF1/DNMT1 axis was suggested to be *Wnt5A*, which was highly expressed in cells with senescence phenotype (Jung, Byun et al. 2017).

The reactivation of *p16INK4A* caused by UHRF1 loss

As most oncogenes intrinsically inhibit the expression of TSG *p16INK4A* to deregulate the cell proliferation (Asghar, Witkiewicz et al. 2015), the relationship between oncogene *UHRF1* and *p16INK4A* was thereby studied, which ultimately found inverse expression relationship between UHRF1 and *p16INK4A* in colorectal cancer tissues. The downregulation of *UHRF1* by RNAi could markedly increase the expression of *p16INK4A* at both mRNA and protein levels in the colorectal cancer cells, indicating UHRF1 suppression caused cell proliferation block may function through the activation of *p16INK4A* (Wang, Yang et al. 2012).

CD47 was another factor important for the sustainable cell proliferation, the loss of which abolished senescence, enhanced asymmetric cell division and spontaneously activated the formation of multipotent embryonic body-like clusters in primary murine endothelial cells (Kaur, Soto-Pantoja et al. 2013). CD47 was further found to

be involved in the regulation of *UHRF1/p16INK4A* by binding to the promoter region of *UHRF1* and enhancing its transcription. Consistent with this, inhibiting the expression of CD47 downregulated the expression of UHRF1 and reactivated the expression of *p16INK4*, confirming the negative regulating effect of CD47 dependant UHRF1 on *p16INK4A* (Boukhari, Alhosin et al. 2015).

6.1.2 The cell fates caused by UHRF1 overexpression

Overexpression of UHRF1 in zebra fish embryonic cells also caused global hypomethylation by destabilizing and delocalizing DNMT1, but with the withdrawal of cell cycle and with the induction of senescence possibly mediated by TP53 (Mudbhary, Hoshida et al. 2014). This is consistent with our finding about the overexpression of UHRF1 in DT40 cells: only cell lines, with UHRF1 overexpression to that expressed in the wild type DT40 cells as **Figure 4.4**, can be achieved after expressing UHRF1 with different tags and different expressing vectors.

One possibility of the limited UHRF1 overexpression level is that these expressing vectors integrated into the certain locations of the genome. This would suggest that cells expressing endogenous UHRF1 were unable to tolerate much additional expression of UHRF1. It was also suggested that there was a threshold effect of UHRF1 overexpression, in which highest expression of UHRF1 processed cells to senescence, while cells with intermediate overexpression of UHRF1 retained cell proliferation and malignant transformation (Mudbhary, Hoshida et al. 2014). The threshold of UHRF1 overexpression may vary from 70% to 130% depending on the human cancer tissues and pathologic types (Li, Xu et al. 2012, Wan, Yang et al. 2016). Moreover, technically, only CMV promoter driven *UHRF1* overexpression had been committed in DT40 cells, it is, therefore, worth to confirm the highest overexpression

level of UHRF1 by a newly reported constitutive CAG promoter, which drove the transcription of TOPBP1 transgene transcription to 5.8 folds more than that by CMV promoter in DT40 cells (Skouteri, Hochegger et al. 2017).

Mechanistically, the proliferative block caused by UHRF1 overexpression can be attributed the interaction with BRCA1. UHRF1 overexpression facilitated the formation of inhibiting transcriptional complex (UHRF1/HDAC1/DNMT1/G9a) on the BRCA1 promoter, thereby inhibiting the transcription of BRCA1 (Jin, Chen et al. 2010). The deficiency of BRCA1 induced the abnormal cell cycle checkpoints and genomic instability, triggering cellular response to DNA damage and proceeding cells to proliferative block and apoptosis (Deng 2006).

Alternatively, the senescence caused by UHRF1 overexpression is processed through the induction of DNA hypomethylation and the sequentially indirect role on the activation of *p53*, as no change of methylation status of *p53* promoter was observed. The indirect role on *p53* can be increased by DNA damage or genomic instability resulting from the expression of anti-apoptosis protein Bcl-2 (Li, Xu et al. 2012). (ii) the hypermethylation of TSGs and the preservation of them in repressive status by coordination with other epigenetic regulators. It had been found that the overexpression of UHRF1 placed increased suppression on *p53* through the RING finger domain of UHRF1 mediated ubiquitination, thereby inhibiting the occurrence of apoptosis (Ma, Peng et al. 2015).

Therefore, the effect of UHRF1 overexpression on cell proliferation could vary inversely depending on the predominant role between anti-apoptosis and apoptosis/senescence. The DNA hypomethylation caused by both of the UHRF1 downregulation and upregulation was suggested to be mediated through the inverse

epigenetic changes according to the UHRF1 levels, considering UHRF1 had been found to be included into various epigenetic regulations, thereby proceeding cells to different proliferative statuses (Mudbhary, Hoshida et al. 2014).

6.2 AID/OSTIR2 system for conditional expression of UHRF1

In this project, we demonstrated for the first time that the AID/OSTIR 2 system allowed the rapid degradation of UHRF1 proteins upon auxin treatment and efficient complete recovery of UHRF1 proteins upon auxin removal in DT40 cells, as shown in **Figure 4.5**. This finding enables us to study the cellular phenotypes when UHRF1 is removed rapidly as opposed to other systems where the removal of proteins would take up to 24 hours with variable levels of efficiency, for example, 24 hours of target gene deletion by Loxp/Cre combatant system.

From **Figure 5.7**, it was found that the reduced expression of UHRF1 proteins in PC7 cell line was sufficient to support the normal cell proliferation. However, approximately equivalent level of AID tagged chicken UHRF1 to that in PC7 cell line was not able to rescue the cell viability of Acp24 cell line when the other allele of *UHRF1* was disrupted. This implies that the AID tag fused chicken UHRF1 may affect the function of multiple domain protein of UHRF1 within the capacity of cell proliferation. Further study needs to be done to optimize the conditional control of UHRF1 using AID/OSTIR2 system (see future work for details).

6.3 Cell sensitivity to ICL damage positively correlates with UHRF1 levels

Independent from DNA replication, UHRF1 is also involved in DNA repair, as reviewed in section 1.6.1. We therefore studied the relationship between UHRF1 expression levels and cell viability in the presence of ICLs by treating cells with MMC.

My hypothesis was that the overexpression of UHRF1 would enhance the cell resistance to ICLs damages in DT40 cells. In contrast, the significant downregulation of UHRF1 imposed enhanced cell sensitivity to ICL damages comparing with the phenotypes of wild type DT40 cells, as shown in **Figure 5.7**. Compared with the very low level of UHRF1 needed to maintain cell survival under normal conditions, the expression level of UHRF1 required for the response to MMC treatment is relatively tightly regulated. This indicates the essential role of UHRF1 in maintaining genomic stability and possibly explains why *UHRF1* knockout cells are so difficult to achieve.

Mechanistically, as an ICL sensor, UHRF1 directly combined to ICL sites of chromatin within seconds through SRA domain and the coordination of TTD and PHD for additional contacts with histone H3. The binding of UHRF1 provided platform for the following recruitment of FANCD2 and other specific endonucleases, thereby initiating ICL repair (Liang, Zhan et al. 2015). Through protein-protein interaction, UHRF1 was found to interact with XRCC1/XRF and MUS81/Eme1, which were critical for the initiation of incision and unhooking of ICLs (Tian, Paramasivam et al. 2015).

Eme1 (essential meiotic endonuclease 1, also known as MMS4), together with Mus81 (methyl methanesulfonate UV sensitive clone 81) forms a heterodimeric endonuclease, and then play important roles in maintaining genomic stability through responding to the DNA crosslink damage and replication fork collapse. Eme1 was found to co-localize with UHRF1 on the chromatin upon collapsed DNA replication fork after camptothecin (a reagent collapses DNA replication) treatment in UHRF1 RING finger domain-dependent manner, whereas the recruitment of RING finger domain was not due to the ubiquitination of Eme1. This indicates there are other proteins co-localize with UHRF1 on the transiently disrupted DNA replication forks, thereby facilitating the repair machinery (Mistry, Gibson et al. 2008).

Considering the dual functionality of UHRF1 in ICL sites binding and nuclease recruitment, further study was therefore carried to clarify the relationship between UHRF1 and FA pathway (Tian, Paramasivam et al. 2015). It was found that the recognition of ICL sites by UHRF1 promoted the activation of FA pathway. Meanwhile, simultaneous depletion of UHRF1 and FANCL caused an additive increase in cell sensitive to ICL lesions caused by MMC, indicating the non-redundant role of UHRF1 to FANCL. This notion was confirmed by the finding that both downregulation of UHRF1 and SLX4, a main downstream effector of FA pathway, resulted in the even higher enrichment of lesion processing nucleases comparing to the phenotypes in cells with UHRF1 or SLX4 knockdown only (Tian, Paramasivam et al. 2015).

Chapter 7 Conclusion

In summary, this work provides an understanding of the mechanisms affected by the changes in the expression levels of UHRF1 and how this affects cellular proliferation and the cellular response to ICLs damage.

Knocking out the gene UHRF1 resulted in a progressive loss of cell viability over a number of cell cycles in DT40 cells. The underlying mechanism was suggested to be caspase episode dependent apoptosis or DNA hypomethylation induced senescence mediated by tumour suppressor genes. No effect on cell proliferation was observed by significantly downregulating UHRF1 to the level similar to that overexpressed in Ahg4 cells. Besides, there was a threshold for the overexpression of UHRF1 in DT40 cells. Excessively overexpression of UHRF1 induced cell cycle arrest and apoptosis or senescence through the suppression on BRCA1 transcription (Jin, Chen et al. 2010, Mudbhary, Hoshida et al. 2014). Additionally, AID/OSTIR system allowed the rapid degradation and reversible expression of UHRF1 proteins, thereby providing a useful tool for the further study of UHRF1 functions in various epigenetic regulations.

However, this system needs to be optimized before use as it may simultaneous affect the function of UHRF1 in proliferation capacity. Moreover, the expression levels of UHRF1 proteins were related to the cell sensitivity to ICL damages. The overexpression of UHRF1 enhanced cell resistance to ICL damage, while downregulating UHRF1 proteins enhanced cell sensitivity to ICL damage comparing with the phenotypes in wild type DT40 cells. The underlying mechanism was suggested to be that UHRF1 was the sensor for ICL damage and played dual roles in ICL repair except for promoting FA pathway (Liang, Zhan et al. 2015, Tian, Paramasivam et al. 2015). We believe our work, combined with existing evidence that cells lacking UHRF1 are incapable of cell proliferation and more sensitive to DNA

damage agents, provide a basis for investigating UHRF1 as a possible therapeutic target in cancer treatment.

Reference

- Abu-Alainin, W., T. Gana, T. Liloglou, A. Olayanju, L. N. Barrera, R. Ferguson, F. Campbell, T. Andrews, C. Goldring, N. Kitteringham, B. K. Park, T. Nedjadi, M. C. Schmid, J. R. Slupsky, W. Greenhalf, J. P. Neoptolemos and E. Costello (2016). "UHRF1 regulation of the Keap1-Nrf2 pathway in pancreatic cancer contributes to oncogenesis." J Pathol **238**(3): 423-433.
- Achour, M., M. Mousli, M. Alhosin, A. Ibrahim, J. Peluso, C. D. Muller, V. B. Schini-Kerth, A. Hamiche, S. Dhe-Paganon and C. Bronner (2013). "Epigallocatechin-3-gallate up-regulates tumor suppressor gene expression via a reactive oxygen species-dependent down-regulation of UHRF1." Biochem Biophys Res Commun **430**(1): 208-212.
- Alhosin, M., Z. Omran, M. A. Zamzami, A. L. Al-Malki, H. Choudhry, M. Mousli and C. Bronner (2016). "Signalling pathways in UHRF1-dependent regulation of tumor suppressor genes in cancer." J Exp Clin Cancer Res **35**(1): 174.
- Arakawa, H., D. Lodygin and J. M. Buerstedde (2001). "Mutant loxP vectors for selectable marker recycle and conditional knock-outs." BMC Biotechnol **1**: 7.
- Arima, Y., T. Hirota, C. Bronner, M. Mousli, T. Fujiwara, S. Niwa, H. Ishikawa and H. Saya (2004). "Down-regulation of nuclear protein ICBP90 by p53/p21Cip1/WAF1-dependent DNA-damage checkpoint signals contributes to cell cycle arrest at G1/S transition." Genes Cells **9**(2): 131-142.
- Asghar, U., A. K. Witkiewicz, N. C. Turner and E. S. Knudsen (2015). "The history and future of targeting cyclin-dependent kinases in cancer therapy." Nat Rev Drug Discov **14**(2): 130-146.
- Ashraf, W., A. Ibrahim, M. Alhosin, L. Zaayter, K. Ouararhni, C. Papin, T. Ahmad, A. Hamiche, Y. Mely, C. Bronner and M. Mousli (2017). "The epigenetic integrator UHRF1: on the road to become a universal biomarker for cancer." Oncotarget.

Avvakumov, G. V., J. R. Walker, S. Xue, Y. Li, S. Duan, C. Bronner, C. H. Arrowsmith and S. Dhe-Paganon (2008). "Structural basis for recognition of hemi-methylated DNA by the SRA domain of human UHRF1." Nature **455**(7214): 822-825.

Babbio, F., C. Pistore, L. Curti, I. Castiglioni, P. Kunderfranco, L. Brino, P. Oudet, R. Seiler, G. N. Thalman, E. Roggero, M. Sarti, S. Pinton, M. Mello-Grand, G. Chiorino, C. V. Catapano, G. M. Carbone and I. M. Bonapace (2012). "The SRA protein UHRF1 promotes epigenetic crosstalks and is involved in prostate cancer progression." Oncogene **31**(46): 4878-4887.

Bannister, A. J. and T. Kouzarides (2011). "Regulation of chromatin by histone modifications." Cell Res **21**(3): 381-395.

Bashtrykov, P., G. Jankevicius, R. Z. Jurkowska, S. Ragozin and A. Jeltsch (2014). "The UHRF1 protein stimulates the activity and specificity of the maintenance DNA methyltransferase DNMT1 by an allosteric mechanism." J Biol Chem **289**(7): 4106-4115.

Bonapace, I. M., L. Latella, R. Papait, F. Nicassio, A. Sacco, M. Muto, M. Crescenzi and P. P. Di Fiore (2002). "Np95 is regulated by E1A during mitotic reactivation of terminally differentiated cells and is essential for S phase entry." J Cell Biol **157**(6): 909-914.

Boukhari, A., M. Alhosin, C. Bronner, K. Sagini, C. Truchot, E. Sick, V. B. Schini-Kerth, P. Andre, Y. Mely, M. Mousli and J. P. Gies (2015). "CD47 activation-induced UHRF1 overexpression is associated with silencing of tumor suppressor gene p16INK4A in glioblastoma cells." Anticancer Res **35**(1): 149-157.

Bulavin, D. V., Y. Higashimoto, I. J. Popoff, W. A. Gaarde, V. Basrur, O. Potapova, E. Appella and A. J. Fornace, Jr. (2001). "Initiation of a G2/M checkpoint after ultraviolet radiation requires p38 kinase." Nature **411**(6833): 102-107.

Cao, J. and Q. Yan (2012). "Histone ubiquitination and deubiquitination in transcription, DNA damage response, and cancer." Front Oncol **2**: 26.

Ceccaldi, R., P. Sarangi and A. D. D'Andrea (2016). "The Fanconi anaemia pathway: new players and new functions." Nat Rev Mol Cell Biol **17**(6): 337-349.

Chen, H., H. Ma, H. Inuzuka, J. Diao, F. Lan, Y. G. Shi, W. Wei and Y. Shi (2013). "DNA damage regulates UHRF1 stability via the SCF(beta-TrCP) E3 ligase." Mol Cell Biol **33**(6): 1139-1148.

Chen, H., C. Zhang, Y. Sheng, S. Yao, Z. Liu, C. Zhang and T. Zhang (2015). "Frequent SOCS3 and 3OST2 promoter methylation and their epigenetic regulation in endometrial carcinoma." Am J Cancer Res **5**(1): 180-190.

Chuang, J. C. and P. A. Jones (2007). "Epigenetics and microRNAs." Pediatr Res **61**(5 Pt 2): 24R-29R.

Cui, L., J. Chen, Q. Zhang, X. Wang, J. Qu, J. Zhang and S. Dang (2015). "Up-regulation of UHRF1 by oncogenic Ras promoted the growth, migration, and metastasis of pancreatic cancer cells." Mol Cell Biochem **400**(1-2): 223-232.

Daskalos, A., U. Oleksiewicz, A. Filia, G. Nikolaidis, G. Xinarianos, J. R. Gosney, A. Malliri, J. K. Field and T. Liloglou (2011). "UHRF1-mediated tumor suppressor gene inactivation in nonsmall cell lung cancer." Cancer **117**(5): 1027-1037.

Deng, C. X. (2006). "BRCA1: cell cycle checkpoint, genetic instability, DNA damage response and cancer evolution." Nucleic Acids Res **34**(5): 1416-1426.

Deng, W., M. Yan, T. Yu, H. Ge, H. Lin, J. Li, Y. Liu, Q. Geng, M. Zhu, L. Liu, X. He and M. Yao (2015). "Quantitative proteomic analysis of the metastasis-inhibitory mechanism of miR-193a-3p in non-small cell lung cancer." Cell Physiol Biochem **35**(5): 1677-1688.

Ding, G., P. Chen, H. Zhang, X. Huang, Y. Zang, J. Li, J. Li and J. Wong (2016). "Regulation of Ubiquitin-like with Plant Homeodomain and RING Finger Domain 1 (UHRF1) Protein Stability by Heat Shock Protein 90 Chaperone Machinery." J Biol Chem **291**(38): 20125-20135.

Escribano-Diaz, C., A. Orthwein, A. Fradet-Turcotte, M. Xing, J. T. Young, J. Tkac, M. A. Cook, A. P. Rosebrock, M. Munro, M. D. Canny, D. Xu and D. Durocher (2013). "A cell cycle-dependent regulatory circuit composed of 53BP1-RIF1 and BRCA1-CtIP controls DNA repair pathway choice." Mol Cell **49**(5): 872-883.

Fang, J., J. Cheng, J. Wang, Q. Zhang, M. Liu, R. Gong, P. Wang, X. Zhang, Y. Feng, W. Lan, Z. Gong, C. Tang, J. Wong, H. Yang, C. Cao and Y. Xu (2016). "Hemi-methylated DNA opens a closed conformation of UHRF1 to facilitate its histone recognition." Nat Commun **7**: 11197.

Fang, L., L. Shanqu, G. Ping, H. Ting, W. Xi, D. Ke, L. Min, W. Junxia and Z. Huizhong (2012). "Gene therapy with RNAi targeting UHRF1 driven by tumor-specific promoter inhibits tumor growth and enhances the sensitivity of chemotherapeutic drug in breast cancer in vitro and in vivo." Cancer Chemother Pharmacol **69**(4): 1079-1087.

Felle, M., S. Joppien, A. Nemeth, S. Diermeier, V. Thalhammer, T. Dobner, E. Kremmer, R. Kappler and G. Langst (2011). "The USP7/Dnmt1 complex stimulates the DNA methylation activity of Dnmt1 and regulates the stability of UHRF1." Nucleic Acids Res **39**(19): 8355-8365.

Fini, L., M. Selgrad, V. Fogliano, G. Graziani, M. Romano, E. Hotchkiss, Y. A. Daoud, E. B. De Vol, C. R. Boland and L. Ricciardiello (2007). "Annurca apple polyphenols have potent demethylating activity and can reactivate silenced tumor suppressor genes in colorectal cancer cells." J Nutr **137**(12): 2622-2628.

Fragkos, M., O. Ganier, P. Coulombe and M. Mechali (2015). "DNA replication origin activation in space and time." Nature Reviews Molecular Cell Biology **16**(6): 360-374.

Frauer, C., T. Hoffmann, S. Bultmann, V. Casa, M. C. Cardoso, I. Antes and H. Leonhardt (2011). "Recognition of 5-hydroxymethylcytosine by the Uhrf1 SRA domain." PLoS One **6**(6): e21306.

Fu, Y., J. A. Foden, C. Khayter, M. L. Maeder, D. Reyon, J. K. Joung and J. D. Sander (2013). "High-frequency off-target mutagenesis induced by CRISPR-Cas nucleases in human cells." Nat Biotechnol **31**(9): 822-826.

Fullgrabe, J., E. Kavanagh and B. Joseph (2011). "Histone onco-modifications." Oncogene **30**(31): 3391-3403.

Ge, T. T., M. Yang, Z. Chen, G. Lou and T. Gu (2016). "UHRF1 gene silencing inhibits cell proliferation and promotes cell apoptosis in human cervical squamous cell carcinoma CaSki cells." J Ovarian Res **9**(1): 42.

Gelato, K. A., M. Tauber, M. S. Ong, S. Winter, K. Hiragami-Hamada, J. Sindlinger, A. Lemak, Y. Bultsma, S. Houliston, D. Schwarzer, N. Divecha, C. H. Arrowsmith and W. Fischle (2014). "Accessibility of different histone H3-binding domains of UHRF1 is allosterically regulated by phosphatidylinositol 5-phosphate." Mol Cell **54**(6): 905-919.

Geng, Y., Y. Gao, H. Ju and F. Yan (2013). "Diagnostic and prognostic value of plasma and tissue ubiquitin-like, containing PHD and RING finger domains 1 in breast cancer patients." Cancer Sci **104**(2): 194-199.

Goll, M. G. and T. H. Bestor (2005). "Eukaryotic cytosine methyltransferases." Annu Rev Biochem **74**: 481-514.

Gopalakrishnan, S., B. O. Van Emburgh and K. D. Robertson (2008). "DNA methylation in development and human disease." Mutat Res **647**(1-2): 30-38.

Goto, Y., A. Kurozumi, N. Nohata, S. Kojima, R. Matsushita, H. Yoshino, K. Yamazaki, Y. Ishida, T. Ichikawa, Y. Naya and N. Seki (2016). "The microRNA signature of patients with sunitinib failure: regulation of UHRF1 pathways by microRNA-101 in renal cell carcinoma." Oncotarget **7**(37): 59070-59086.

Greiner, V. J., L. Kovalenko, N. Humbert, L. Richert, C. Birck, M. Ruff, O. A. Zaporozhets, S. Dhe-Paganon, C. Bronner and Y. Mely (2015). "Site-Selective Monitoring of the Interaction of the SRA Domain of UHRF1 with Target DNA Sequences Labeled with 2-Aminopurine." Biochemistry **54**(39): 6012-6020.

Guan, D., D. Factor, Y. Liu, Z. Wang and H. Y. Kao (2013). "The epigenetic regulator UHRF1 promotes ubiquitination-mediated degradation of the tumor-suppressor protein promyelocytic leukemia protein." Oncogene **32**(33): 3819-3828.

Gurova, K. V., J. E. Hill, O. V. Razorenova, P. M. Chumakov and A. V. Gudkov (2004). "p53 pathway in renal cell carcinoma is repressed by a dominant mechanism." Cancer Res **64**(6): 1951-1958.

Hashimoto, H., J. R. Horton, X. Zhang, M. Bostick, S. E. Jacobsen and X. Cheng (2008). "The SRA domain of UHRF1 flips 5-methylcytosine out of the DNA helix." Nature **455**(7214): 826-829.

Hashimoto, H., J. R. Horton, X. Zhang and X. Cheng (2009). "UHRF1, a modular multi-domain protein, regulates replication-coupled crosstalk between DNA methylation and histone modifications." Epigenetics **4**(1): 8-14.

Heir, R., C. Ablasou, E. Dumontier, M. Elliott, C. Fagotto-Kaufmann and F. K. Bedford (2006). "The UBL domain of PLIC-1 regulates aggresome formation." EMBO Rep **7**(12): 1252-1258.

Hopfner, R., M. Mousli, J. M. Jeltsch, A. Voulgaris, Y. Lutz, C. Marin, J. P. Bellocq, P. Oudet and C. Bronner (2000). "ICBP90, a novel human CCAAT binding protein, involved in the regulation of topoisomerase IIalpha expression." Cancer Res **60**(1): 121-128.

Hsu, P. D., D. A. Scott, J. A. Weinstein, F. A. Ran, S. Konermann, V. Agarwala, Y. Li, E. J. Fine, X. Wu, O. Shalem, T. J. Cradick, L. A. Marraffini, G. Bao and F. Zhang (2013). "DNA targeting specificity of RNA-guided Cas9 nucleases." Nat Biotechnol **31**(9): 827-832.

Huang, P., C. L. Cheng, Y. H. Chang, C. H. Liu, Y. C. Hsu, J. S. Chen, G. C. Chang, B. C. Ho, K. Y. Su, H. Y. Chen and S. L. Yu (2016). "Molecular gene signature and prognosis of non-small cell lung cancer." Oncotarget **7**(32): 51898-51907.

Jacob, V., Y. Chernyavskaya, X. Chen, P. S. Tan, B. Kent, Y. Hoshida and K. C. Sadler (2015). "DNA hypomethylation induces a DNA replication-associated cell cycle arrest to block hepatic outgrowth in uhrf1 mutant zebrafish embryos." Development **142**(3): 510-521.

Jacobs, A. L. and P. Schar (2012). "DNA glycosylases: in DNA repair and beyond." Chromosoma **121**(1): 1-20.

Jang, S. Y., D. Hong, S. Y. Jeong and J. H. Kim (2015). "Shikonin causes apoptosis by up-regulating p73 and down-regulating ICBP90 in human cancer cells." Biochem Biophys Res Commun **465**(1): 71-76.

Jenkins, Y., V. Markovtsov, W. Lang, P. Sharma, D. Pearsall, J. Warner, C. Franci, B. Huang, J. Huang, G. C. Yam, J. P. Vistan, E. Pali, J. Vialard, M. Janicot, J. B. Lorens, D. G. Payan

and Y. Hitoshi (2005). "Critical role of the ubiquitin ligase activity of UHRF1, a nuclear RING finger protein, in tumor cell growth." Mol Biol Cell **16**(12): 5621-5629.

Jin, W., L. Chen, Y. Chen, S. G. Xu, G. H. Di, W. J. Yin, J. Wu and Z. M. Shao (2010). "UHRF1 is associated with epigenetic silencing of BRCA1 in sporadic breast cancer." Breast Cancer Res Treat **123**(2): 359-373.

Jung, H. J., H. O. Byun, B. A. Jee, S. Min, U. W. Jeoun, Y. K. Lee, Y. Seo, H. G. Woo and G. Yoon (2017). "Senescence-----UHRF1)/DNMT1 Axis is a Primary Regulator of Cell Senescence." J Biol Chem.

Karagianni, P., L. Amazit, J. Qin and J. Wong (2008). "ICBP90, a novel methyl K9 H3 binding protein linking protein ubiquitination with heterochromatin formation." Mol Cell Biol **28**(2): 705-717.

Kastan, M. B. and J. Bartek (2004). "Cell-cycle checkpoints and cancer." Nature **432**(7015): 316-323.

Kaur, S., D. R. Soto-Pantoja, E. V. Stein, C. Liu, A. G. Elkahoun, M. L. Pendrak, A. Nicolae, S. P. Singh, Z. Nie, D. Levens, J. S. Isenberg and D. D. Roberts (2013). "Thrombospondin-1 signaling through CD47 inhibits self-renewal by regulating c-Myc and other stem cell transcription factors." Sci Rep **3**: 1673.

Kilin, V., K. Gavvala, N. P. Barthes, B. Y. Michel, D. Shin, C. Boudier, O. Mauffret, V. Yashchuk, M. Mousli, M. Ruff, F. Granger, S. Eiler, C. Bronner, Y. Tor, A. Burger and Y. Mely (2017). "Dynamics of Methylated Cytosine Flipping by UHRF1." J Am Chem Soc **139**(6): 2520-2528.

Kim, K. B., H. J. Son, S. Choi, J. Y. Hahm, H. Jung, H. J. Baek, H. Kook, Y. Hahn, H. Kook and S. B. Seo (2015). "H3K9 methyltransferase G9a negatively regulates UHRF1 transcription during leukemia cell differentiation." Nucleic Acids Res **43**(7): 3509-3523.

Kim, M. Y., S. J. Park, J. W. Shim, K. Yang, H. S. Kang and K. Heo (2015). "Naphthazarin enhances ionizing radiation-induced cell cycle arrest and apoptosis in human breast cancer cells." Int J Oncol **46**(4): 1659-1666.

Kofunato, Y., K. Kumamoto, K. Saitou, S. Hayase, H. Okayama, K. Miyamoto, Y. Sato, K. Katakura, I. Nakamura, S. Ohki, Y. Koyama, M. Unoki and S. Takenoshita (2012). "UHRF1 expression is upregulated and associated with cellular proliferation in colorectal cancer." *Oncol Rep* **28**(6): 1997-2002.

Krifa, M., L. Leloup, K. Ghedira, M. Mousli and L. Chekir-Ghedira (2014). "Luteolin induces apoptosis in BE colorectal cancer cells by downregulating calpain, UHRF1, and DNMT1 expressions." *Nutr Cancer* **66**(7): 1220-1227.

Leitch, H. G., M. A. Surani and P. Hajkova (2016). "DNA (De)Methylation: The Passive Route to Naivety?" *Trends Genet* **32**(10): 592-595.

Li, E. (2002). "Chromatin modification and epigenetic reprogramming in mammalian development." *Nat Rev Genet* **3**(9): 662-673.

Li, X., Q. Meng, E. M. Rosen and S. Fan (2011). "UHRF1 confers radioresistance to human breast cancer cells." *Int J Radiat Biol* **87**(3): 263-273.

Li, X. L., J. H. Xu, J. H. Nie and S. J. Fan (2012). "Exogenous expression of UHRF1 promotes proliferation and metastasis of breast cancer cells." *Oncol Rep* **28**(1): 375-383.

Liang, C. C., B. Zhan, Y. Yoshikawa, W. Haas, S. P. Gygi and M. A. Cohn (2015). "UHRF1 is a sensor for DNA interstrand crosslinks and recruits FANCD2 to initiate the Fanconi anemia pathway." *Cell Rep* **10**(12): 1947-1956.

Liang, D., H. Xue, Y. Yu, F. Lv, W. You and B. Zhang (2015). "Elevated expression of UHRF1 predicts unfavorable prognosis for patients with hepatocellular carcinoma." *Int J Clin Exp Pathol* **8**(8): 9416-9421.

Lin, R. K., C. Y. Wu, J. W. Chang, L. J. Juan, H. S. Hsu, C. Y. Chen, Y. Y. Lu, Y. A. Tang, Y. C. Yang, P. C. Yang and Y. C. Wang (2010). "Dysregulation of p53/Sp1 control leads to DNA methyltransferase-1 overexpression in lung cancer." *Cancer Res* **70**(14): 5807-5817.

Liu, X., Q. Gao, P. Li, Q. Zhao, J. Zhang, J. Li, H. Koseki and J. Wong (2013). "UHRF1 targets DNMT1 for DNA methylation through cooperative binding of hemi-methylated DNA and methylated H3K9." *Nat Commun* **4**: 1563.

Liu, X., H. Ou, L. Xiang, X. Li, Y. Huang and D. Yang (2017). "Elevated UHRF1 expression contributes to poor prognosis by promoting cell proliferation and metastasis in hepatocellular carcinoma." Oncotarget **8**(6): 10510-10522.

Liu, X., H. Ou, L. Xiang, X. Li, Y. Huang and D. Yang (2017). "tissue. overexpression/inhibition uhrf1 with migration, tissue proliferation.---Elevated UHRF1 expression contributes to poor prognosis by promoting cell proliferation and metastasis in hepatocellular carcinoma." Oncotarget.

Lorenzato, M., S. Caudroy, C. Bronner, G. Evrard, M. Simon, A. Durlach, P. Birembaut and C. Clavel (2005). "Cell cycle and/or proliferation markers: what is the best method to discriminate cervical high-grade lesions?" Hum Pathol **36**(10): 1101-1107.

Ma, H., H. Chen, X. Guo, Z. Wang, M. E. Sowa, L. Zheng, S. Hu, P. Zeng, R. Guo, J. Diao, F. Lan, J. W. Harper, Y. G. Shi, Y. Xu and Y. Shi (2012). "M phase phosphorylation of the epigenetic regulator UHRF1 regulates its physical association with the deubiquitylase USP7 and stability." Proc Natl Acad Sci U S A **109**(13): 4828-4833.

Ma, J., J. Peng, R. Mo, S. Ma, J. Wang, L. Zang, W. Li and J. Fan (2015). "Ubiquitin E3 ligase UHRF1 regulates p53 ubiquitination and p53-dependent cell apoptosis in clear cell Renal Cell Carcinoma." Biochem Biophys Res Commun **464**(1): 147-153.

Matsushita, R., H. Yoshino, H. Enokida, Y. Goto, K. Miyamoto, M. Yonemori, S. Inoguchi, M. Nakagawa and N. Seki (2016). "Regulation of UHRF1 by dual-strand tumor-suppressor microRNA-145 (miR-145-5p and miR-145-3p): Inhibition of bladder cancer cell aggressiveness." Oncotarget **7**(19): 28460-28487.

Mistry, H., L. Gibson, J. W. Yun, H. Sarras, L. Tamblyn and J. P. McPherson (2008). "Interplay between Np95 and Eme1 in the DNA damage response." Biochem Biophys Res Commun **375**(3): 321-325.

Mistry, H., L. Tamblyn, H. Butt, D. Siggoreo, A. Gracias, M. Larin, K. Gopalakrishnan, M. P. Hande and J. P. McPherson (2010). "UHRF1 is a genome caretaker that facilitates the DNA damage response to gamma-irradiation." Genome Integr **1**(1): 7.

Moarii, M., V. Boeva, J. P. Vert and F. Reyat (2015). "Changes in correlation between promoter methylation and gene expression in cancer." BMC Genomics **16**: 873.

Mosammaparast, N. and Y. Shi (2010). "Reversal of histone methylation: biochemical and molecular mechanisms of histone demethylases." Annu Rev Biochem **79**: 155-179.

Mousli, M., R. Hopfner, A. Q. Abbady, D. Monte, M. Jeanblanc, P. Oudet, B. Louis and C. Bronner (2003). "ICBP90 belongs to a new family of proteins with an expression that is deregulated in cancer cells." Br J Cancer **89**(1): 120-127.

Mudbhary, R., Y. Hoshida, Y. Chernyavskaya, V. Jacob, A. Villanueva, M. I. Fiel, X. Chen, K. Kojima, S. Thung, R. T. Bronson, A. Lachenmayer, K. Revill, C. Alsinet, R. Sachidanandam, A. Desai, S. SenBanerjee, C. Ukomadu, J. M. Llovet and K. C. Sadler (2014). "UHRF1 overexpression drives DNA hypomethylation and hepatocellular carcinoma." Cancer Cell **25**(2): 196-209.

Myriantopoulos, V., P. F. Cartron, Z. Liutkeviciute, S. Klimasauskas, D. Matulis, C. Bronner, N. Martinet and E. Mikros (2016). "Tandem virtual screening targeting the SRA domain of UHRF1 identifies a novel chemical tool modulating DNA methylation." Eur J Med Chem **114**: 390-396.

Nady, N., A. Lemak, J. R. Walker, G. V. Avvakumov, M. S. Kareta, M. Achour, S. Xue, S. Duan, A. Allali-Hassani, X. Zuo, Y. X. Wang, C. Bronner, F. Chedin, C. H. Arrowsmith and S. Dhe-Paganon (2011). "Recognition of multivalent histone states associated with heterochromatin by UHRF1 protein." J Biol Chem **286**(27): 24300-24311.

Nakamura, K., Y. Baba, K. Kosumi, K. Harada, H. Shigaki, K. Miyake, Y. Kiyozumi, M. Ohuchi, J. Kurashige, T. Ishimoto, M. Iwatsuki, Y. Sakamoto, N. Yoshida, M. Watanabe, M. Nakao and H. Baba (2016). "UHRF1 regulates global DNA hypomethylation and is associated with poor prognosis in esophageal squamous cell carcinoma." Oncotarget **7**(36): 57821-57831.

Nandakumar, V., M. Vaid and S. K. Katiyar (2011). "(-)-Epigallocatechin-3-gallate reactivates silenced tumor suppressor genes, Cip1/p21 and p16INK4a, by reducing DNA

methylation and increasing histones acetylation in human skin cancer cells." Carcinogenesis **32**(4): 537-544.

Nishimura, K., T. Fukagawa, H. Takisawa, T. Kakimoto and M. Kanemaki (2009). "An auxin-based degron system for the rapid depletion of proteins in nonplant cells." Nat Methods **6**(12): 917-922.

Nishiyama, A., L. Yamaguchi, J. Sharif, Y. Johmura, T. Kawamura, K. Nakanishi, S. Shimamura, K. Arita, T. Kodama, F. Ishikawa, H. Koseki and M. Nakanishi (2013). "Uhrf1-dependent H3K23 ubiquitylation couples maintenance DNA methylation and replication." Nature **502**(7470): 249-253.

Pacaud, R., E. Brocard, L. Lalier, E. Hervouet, F. M. Vallette and P. F. Cartron (2014). "The DNMT1/PCNA/UHRF1 disruption induces tumorigenesis characterized by similar genetic and epigenetic signatures." Sci Rep **4**: 4230.

Papait, R., C. Pistore, U. Grazini, F. Babbio, S. Cogliati, D. Pecoraro, L. Brino, A. L. Morand, A. M. Dechampsme, F. Spada, H. Leonhardt, F. McBlane, P. Oudet and I. M. Bonapace (2008). "The PHD domain of Np95 (mUHRF1) is involved in large-scale reorganization of pericentromeric heterochromatin." Mol Biol Cell **19**(8): 3554-3563.

Papait, R., C. Pistore, D. Negri, D. Pecoraro, L. Cantarini and I. M. Bonapace (2007). "Np95 is implicated in pericentromeric heterochromatin replication and in major satellite silencing." Mol Biol Cell **18**(3): 1098-1106.

Park, S. A., J. Platt, J. W. Lee, F. Lopez-Giraldez, R. S. Herbst and J. S. Koo (2015). "E2F8 as a Novel Therapeutic Target for Lung Cancer." J Natl Cancer Inst **107**(9).

Pi, J. T., Y. Lin, Q. Quan, L. L. Chen, L. Z. Jiang, W. Chi and H. Y. Chen (2013). "Overexpression of UHRF1 is significantly associated with poor prognosis in laryngeal squamous cell carcinoma." Med Oncol **30**(4): 613.

Qin, W., P. Wolf, N. Liu, S. Link, M. Smets, F. La Mastra, I. Forne, G. Pichler, D. Horl, K. Fellingner, F. Spada, I. M. Bonapace, A. Imhof, H. Harz and H. Leonhardt (2015). "DNA methylation requires a DNMT1 ubiquitin interacting motif (UIM) and histone ubiquitination." Cell Res **25**(8): 911-929.

Qin, Y., J. Wang, W. Gong, M. Zhang, Z. Tang, J. Zhang and Z. Quan (2014). "UHRF1 depletion suppresses growth of gallbladder cancer cells through induction of apoptosis and cell cycle arrest." Oncol Rep **31**(6): 2635-2643.

Rajakumara, E., Z. Wang, H. Ma, L. Hu, H. Chen, Y. Lin, R. Guo, F. Wu, H. Li, F. Lan, Y. G. Shi, Y. Xu, D. J. Patel and Y. Shi (2011). "PHD finger recognition of unmodified histone H3R2 links UHRF1 to regulation of euchromatic gene expression." Mol Cell **43**(2): 275-284.

Ran, F. A., P. D. Hsu, J. Wright, V. Agarwala, D. A. Scott and F. Zhang (2013). "Genome engineering using the CRISPR-Cas9 system." Nat Protoc **8**(11): 2281-2308.

Sabatino, L., A. Fucci, M. Pancione, V. Carafa, A. Nebbioso, C. Pistore, F. Babbio, C. Votino, C. Laudanna, M. Ceccarelli, L. Altucci, I. M. Bonapace and V. Colantuoni (2012). "UHRF1 coordinates peroxisome proliferator activated receptor gamma (PPARG) epigenetic silencing and mediates colorectal cancer progression." Oncogene **31**(49): 5061-5072.

Sanders, D. A., M. V. Gormally, G. Marsico, D. Beraldi, D. Tannahill and S. Balasubramanian (2015). "FOXM1 binds directly to non-consensus sequences in the human genome." Genome Biol **16**: 130.

Shi, Y., F. Lan, C. Matson, P. Mulligan, J. R. Whetstine, P. A. Cole, R. A. Casero and Y. Shi (2004). "Histone demethylation mediated by the nuclear amine oxidase homolog LSD1." Cell **119**(7): 941-953.

Sidhu, H. and N. Capalash (2017). "UHRF1: The key regulator of epigenetics and molecular target for cancer therapeutics." Tumour Biol **39**(2): 1010428317692205.

Skouteri, M., H. Hochegger and A. M. Carr (2017). "Characterisation of a stably integrated expression system for exogenous protein expression in DT40." Wellcome Open Res **2**: 40.

Song, J. J., S. K. Smith, G. J. Hannon and L. Joshua-Tor (2004). "Crystal structure of Argonaute and its implications for RISC slicer activity." Science **305**(5689): 1434-1437.

Taniue, K., A. Kurimoto, H. Sugimasa, E. Nasu, Y. Takeda, K. Iwasaki, T. Nagashima, M. Okada-Hatakeyama, M. Oyama, H. Kozuka-Hata, M. Hiyoshi, J. Kitayama, L. Negishi, Y. Kawasaki and T. Akiyama (2016). "Long noncoding RNA UPAT promotes colon

tumorigenesis by inhibiting degradation of UHRF1." Proc Natl Acad Sci U S A **113**(5): 1273-1278.

Tauber, M. and W. Fischle (2015). "Conserved linker regions and their regulation determine multiple chromatin-binding modes of UHRF1." Nucleus **6**(2): 123-132.

Taylor, E. M., N. M. Bonsu, R. J. Price and H. D. Lindsay (2013). "Depletion of Uhrf1 inhibits chromosomal DNA replication in *Xenopus* egg extracts." Nucleic Acids Res **41**(16): 7725-7737.

Tian, Y., M. Paramasivam, G. Ghosal, D. Chen, X. Shen, Y. Huang, S. Akhter, R. Legerski, J. Chen, M. M. Seidman, J. Qin and L. Li (2015). "UHRF1 contributes to DNA damage repair as a lesion recognition factor and nuclease scaffold." Cell Rep **10**(12): 1957-1966.

Tien, A. L., S. Senbanerjee, A. Kulkarni, R. Mudbhary, B. Goudreau, S. Ganesan, K. C. Sadler and C. Ukomadu (2011). "UHRF1 depletion causes a G2/M arrest, activation of DNA damage response and apoptosis." Biochem J **435**(1): 175-185.

Timp, W. and A. P. Feinberg (2013). "Cancer as a dysregulated epigenome allowing cellular growth advantage at the expense of the host." Nat Rev Cancer **13**(7): 497-510.

Unoki, M., J. Brunet and M. Mousli (2009). "Drug discovery targeting epigenetic codes: the great potential of UHRF1, which links DNA methylation and histone modifications, as a drug target in cancers and toxoplasmosis." Biochem Pharmacol **78**(10): 1279-1288.

Unoki, M., Y. Daigo, J. Koinuma, E. Tsuchiya, R. Hamamoto and Y. Nakamura (2010). "UHRF1 is a novel diagnostic marker of lung cancer." Br J Cancer **103**(2): 217-222.

Unoki, M., J. D. Kelly, D. E. Neal, B. A. Ponder, Y. Nakamura and R. Hamamoto (2009). "UHRF1 is a novel molecular marker for diagnosis and the prognosis of bladder cancer." Br J Cancer **101**(1): 98-105.

Unoki, M., T. Nishidate and Y. Nakamura (2004). "ICBP90, an E2F-1 target, recruits HDAC1 and binds to methyl-CpG through its SRA domain." Oncogene **23**(46): 7601-7610.

Verdin, E. and M. Ott (2015). "50 years of protein acetylation: from gene regulation to epigenetics, metabolism and beyond." Nat Rev Mol Cell Biol **16**(4): 258-264.

Walport, L. J., R. J. Hopkinson, R. Chowdhury, R. Schiller, W. Ge, A. Kawamura and C. J. Schofield (2016). "Arginine demethylation is catalysed by a subset of JmjC histone lysine demethylases." Nat Commun **7**: 11974.

Walter, A., N. Etienne-Selloum, D. Brasse, H. Khallouf, C. Bronner, M. C. Rio, A. Beretz and V. B. Schini-Kerth (2010). "Intake of grape-derived polyphenols reduces C26 tumor growth by inhibiting angiogenesis and inducing apoptosis." FASEB J **24**(9): 3360-3369.

Wan, X., S. Yang, W. Huang, D. Wu, H. Chen, M. Wu, J. Li, T. Li and Y. Li (2016). "UHRF1 overexpression is involved in cell proliferation and biochemical recurrence in prostate cancer after radical prostatectomy." J Exp Clin Cancer Res **35**: 34.

Wang, F., Y. Z. Yang, C. Z. Shi, P. Zhang, M. P. Moyer, H. Z. Zhang, Y. Zou and H. L. Qin (2012). "UHRF1 promotes cell growth and metastasis through repression of p16(ink(4)a) in colorectal cancer." Ann Surg Oncol **19**(8): 2753-2762.

Wang, L. S., M. Arnold, Y. W. Huang, C. Sardo, C. Seguin, E. Martin, T. H. Huang, K. Riedl, S. Schwartz, W. Frankel, D. Pearl, Y. Xu, J. Winston, 3rd, G. Y. Yang and G. Stoner (2011). "Modulation of genetic and epigenetic biomarkers of colorectal cancer in humans by black raspberries: a phase I pilot study." Clin Cancer Res **17**(3): 598-610.

Wang, X., Q. Wu, B. Xu, P. Wang, W. Fan, Y. Cai, X. Gu and F. Meng (2015). "MiR-124 exerts tumor suppressive functions on the cell proliferation, motility and angiogenesis of bladder cancer by fine-tuning UHRF1." FEBS J **282**(22): 4376-4388.

Weake, V. M. and J. L. Workman (2008). "Histone ubiquitination: triggering gene activity." Mol Cell **29**(6): 653-663.

Wood, K. H. and Z. Zhou (2016). "Emerging Molecular and Biological Functions of MBD2, a Reader of DNA Methylation." Front Genet **7**: 93.

Wu, S. M., W. L. Cheng, C. J. Liao, H. C. Chi, Y. H. Lin, Y. H. Tseng, C. Y. Tsai, C. Y. Chen, S. L. Lin, W. J. Chen, Y. H. Yeh, C. Y. Huang, M. H. Chen, Y. C. Yeh and K. H. Lin (2015). "Negative modulation of the epigenetic regulator, UHRF1, by thyroid hormone receptors suppresses liver cancer cell growth." Int J Cancer **137**(1): 37-49.

Xiang, H., L. Yuan, X. Gao, P. B. Alexander, O. Lopez, C. Lau, Y. Ding, M. Chong, T. Sun, R. Chen, S. Q. Liu, H. Wu, Y. Wan, S. H. Randell, Q. J. Li and X. F. Wang (2017). "UHRF1 is required for basal stem cell proliferation in response to airway injury." Cell Discov **3**: 17019.

Yamazoe, M., E. Sonoda, H. Hochegger and S. Takeda (2004). "Reverse genetic studies of the DNA damage response in the chicken B lymphocyte line DT40." DNA Repair (Amst) **3**(8-9): 1175-1185.

Yang, C., Y. Wang, F. Zhang, G. Sun, C. Li, S. Jing, Q. Liu and Y. Cheng (2013). "Inhibiting UHRF1 expression enhances radiosensitivity in human esophageal squamous cell carcinoma." Mol Biol Rep **40**(9): 5225-5235.

Yang, G. L., L. H. Zhang, J. J. Bo, H. G. Chen, M. Cao, D. M. Liu and Y. R. Huang (2012). "UHRF1 is associated with tumor recurrence in non-muscle-invasive bladder cancer." Med Oncol **29**(2): 842-847.

Zhang, H., H. Liu, Y. Chen, X. Yang, P. Wang, T. Liu, M. Deng, B. Qin, C. Correia, S. Lee, J. Kim, M. Sparks, A. A. Nair, D. L. Evans, K. R. Kalari, P. Zhang, L. Wang, Z. You, S. H. Kaufmann, Z. Lou and H. Pei (2016). "A cell cycle-dependent BRCA1-UHRF1 cascade regulates DNA double-strand break repair pathway choice." Nat Commun **7**: 10201.

Zhang, Z. M., S. B. Rothbart, D. F. Allison, Q. Cai, J. S. Harrison, L. Li, Y. Wang, B. D. Strahl, G. G. Wang and J. Song (2015). "An Allosteric Interaction Links USP7 to Deubiquitination and Chromatin Targeting of UHRF1." Cell Rep **12**(9): 1400-1406.

Zhang, Z. Y., J. J. Cai, J. Hong, K. K. Li, Z. Ping, Y. Wang, H. K. Ng, Y. Yao and Y. Mao (2016). "Clinicopathological analysis of UHRF1 expression in medulloblastoma tissues and its regulation on tumor cell proliferation." Med Oncol **33**(9): 99.

Zhao, Q., J. Zhang, R. Chen, L. Wang, B. Li, H. Cheng, X. Duan, H. Zhu, W. Wei, J. Li, Q. Wu, J. D. Han, W. Yu, S. Gao, G. Li and J. Wong (2016). "Dissecting the precise role of H3K9 methylation in crosstalk with DNA maintenance methylation in mammals." Nat Commun **7**: 12464.

Zhou, L., Y. Shang, Z. Jin, W. Zhang, C. Lv, X. Zhao, Y. Liu, N. Li and J. Liang (2015). "UHRF1 promotes proliferation of gastric cancer via mediating tumor suppressor gene hypermethylation." Cancer Biol Ther **16**(8): 1241-1251.

Zhou, L., X. Zhao, Y. Han, Y. Lu, Y. Shang, C. Liu, T. Li, Z. Jin, D. Fan and K. Wu (2013). "Regulation of UHRF1 by miR-146a/b modulates gastric cancer invasion and metastasis." FASEB J **27**(12): 4929-4939.

Zhu, M., Y. Xu, M. Ge, Z. Gui and F. Yan (2015). "Regulation of UHRF1 by microRNA-9 modulates colorectal cancer cell proliferation and apoptosis." Cancer Sci **106**(7): 833-839.

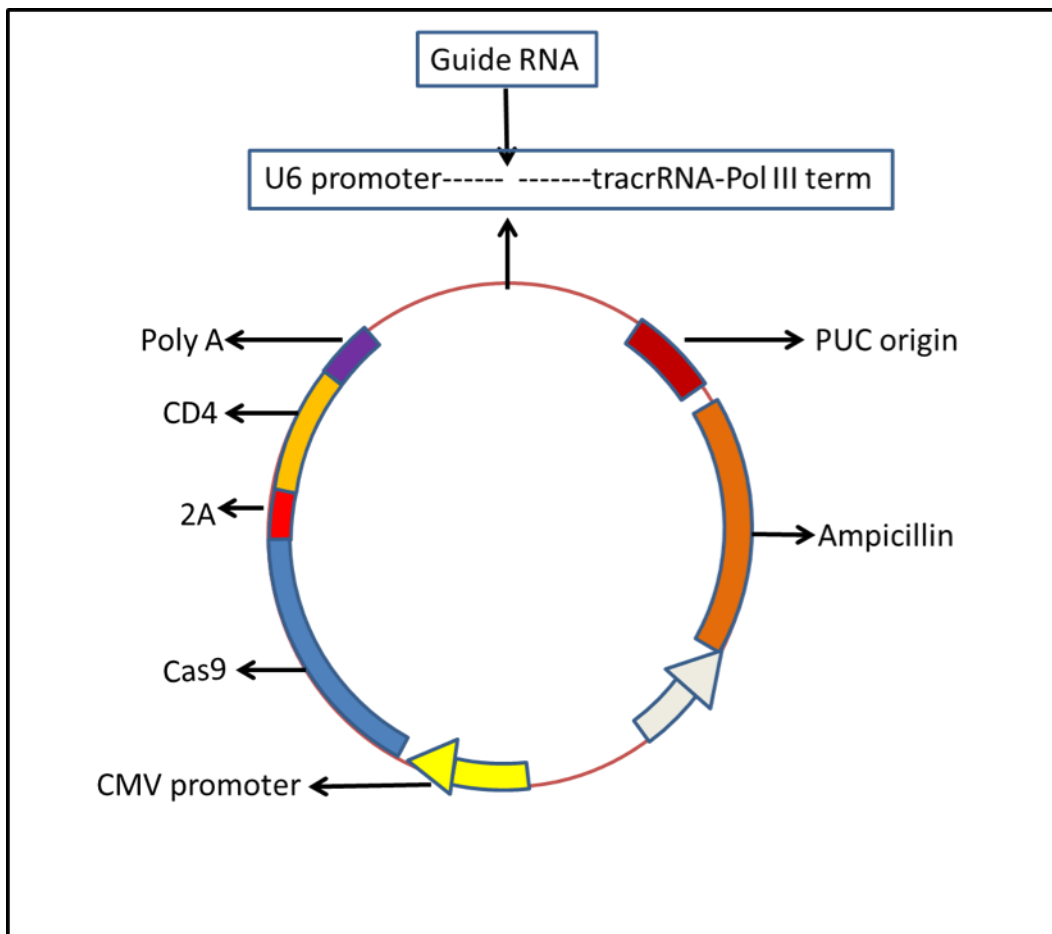
Zimmermann, M., F. Lottersberger, S. B. Buonomo, A. Sfeir and T. de Lange (2013). "53BP1 regulates DSB repair using Rif1 to control 5' end resection." Science **339**(6120): 700-704.

Appendices

atggagacagttgcaacacgatggatgatttgaattggagaatctccattgaattcaatgaccagatgatttgatgcttcct
gcagatggaggatggtcactcccttttgattacagtgttgactgaacgatattgttcagctcttggtcagacaaagcccage
agtgcttctgctgtgagtaaggagaaggattcagagctctctgatacagactctggctgtggctcaggtcaaagtgaatcc
gacaaaagctctcacaatggagaaggtgcatggacctggaggggagcttagcacggcagcacaggctgactgggct
gaccaggatttggcctctataagatccatgacttggtgatgctcgtgatatgaatatgggagcatggttgaagcccaggtt
gtaaatgtaaccagaaggaaagctgcaaatgagagttgtgcagttgctgatcagcagacaaccattcctgaagaagatgta
atatatcatgtgaaatacgaagattatccagagaatggagttgtggaactgagttcgaatgatgtacggctctctgcacggac
tatcttgaatggcatcagctagaagtaggacaggtggtgatggcaactacaatcctgatgaaccaacagagagaggtttt
ggtatgatgctgagatcctgcagaaaagggaaacaaagctgatcaggagataaatgcgaagatactacttggggaggct
ggtgattctttgaatgactgcagaattatattgtggatgacattataaaattgaagaaccaggcagtgtttgccaattagtgc
cagaccattaaaacgacaaaagtgacctgtgtgtaaagcttgaaggacaaccgaacaaaacctgcaggatctgtgcttg
ccatatttgggggtaaacaagatcctgataaacagctcatgtgtgatgagtgatgatggcttccacatctattgcctcaac
cctccccttagtagtataccagatgacgaggactggtattgccctgaatgtcgaatgatgcaagtgaagtggttctggcag
gagagaaattaaagaaagtaaaaaaaaacaaaagatggcatctgctaattcatcatcacggagagactggggcaagggt
atggcatgtgtggtgcacaaaggaatgtaccattgtacccttaaccactacggaccaattcctggtattccagttggcac
catgtggaagttcagagttcaggtgagcgaatctggtgtcacaggcccatgtggctggaatacacggcagaagtaatga
tggtgcttattccttagttctagcagggggctatgaagatgatatagatcatgggaattccttcacatatacaggagtgagg
tcgtgatcttctggaacaaacgtacagcagaacagcttctgtgatcaaaagctcaccaatatgaacagagctttggtctaa
actgcagtgctccatcaatgataaaaatggagctgaagctaaggactggagagctggaaagccagtcagtggtgag
gaatgtaaaaggaggcaaacacagcaaatatgctcctgtagaagggaacagatatgatggcatatataaagtcgttaata
ctggcctgagacagggaatctgggttctagtatggcgttacttgcttaggagagatgatgaagaacctgctccttgacca
aagaaggaaaggacaggatgaagaagcttggcctaacaatgcagtatcctgaggggtatttgaagccgttgaacaaa

gataaagaaaataatggagatgatgagtttgatactccagggaaaggaaaaggaaaaggaaatcagcaggtgcagagg
agaaagtcgtagctctcctgcagggactccgaagaaaacgaaagttgagccatacaaattgacaactcagcaaaaatctc
ttataagaagtgatgaggccaatgaaaaactgtggaatgaagtactagatgctctcaaagatggaccgaaatttctgaataaa
gttgaagaggctttcttgtgtatttgctgtcaagaggtgtgttcggccagtcacaactgtatccaacataatgtgtgcaagg
attgcttggataggtccttcaaagctgatgtgtacagttgtccagcctgccgctacgatcttggcaaaaactataccatgcaag
tgaatgaaacactgcagaccattctaactcagctcttctggatatggcaacggacggtga

Appendix 1The nucleotide sequence of *UHRF1* cDNA from DT40 cells.



Appendix 2 Schematic representation of CRISPR/Cas9 vector. CMV promoter launches the transcription of both Cas9 and CD4. Poly A is polyadenylation signal and terminates the transcription promoted by CMV. 2A is a self-cleaving peptide linker which connects Cas9 and CD4. After translation, the two proteins which are flanked by 2A peptide will separate from each other. U6 promoter launches the expression of guide RNA which is trans-activated by tracrRNA and Pol III terminator allows efficient termination of Polymerase III dependent transcription. Guide RNA is unique in the target gene and is inserted between U6 promoter and tracrRNA. The plasmid antibiotic resistance is ampicillin and PUC origin allows high copy replication and maintenance in *E. coli*. The nucleotide sequence of sgRNA1 was TCCTTCTCCTTACTCACAGC and of sgRNA was AGTGACCATCCTCCATCTGC.


```

59      MWIQVRTMDGRDTRRIDSLSKLTKVEDLRARIQQIFGVALESQRLFYRGKQMENGHTLFD
DT40    -----METVATRWMILNWRISIEFNDQMILMLS LQMEDGHS LFD
          : .*          :: :.: :.:.* :: . ***:***:***

59      YSVGLNDIVQLLVRQIPDSVPTK--DKECGISDADSGCGSGQGESDKNSSCGEGATDVDG
DT40    YSVGLNDIVQLLVRQSPAVLPAVSKEKDSELSDTDSGCGSGQSESDKSSHNHGE GAMDLEG
          ***** * :*: :*: :*:*****.***** * **** *.:*

59      QPAGIN---SENVGPSLYKKNLDVDARDLNMGAWF EAQIVSVSKRVNPDGMS-AEILDTS
DT40    QSSTAAQADWADPGFGLYKIHDLVDARDMNMGAWF EAQVVNVT RRKAANESCAVADQOTT
          * :          : * .*** :*****:*****:*.*:.* : . . :*:

59      AASDDIIYHVKYEDYPENGVVQLTYKDVRLRARTTLPWHD LKVGQVVMVNYNPDEPKERG
DT40    IPEEDVIYHVKYEDYPENGVVVELSSNDVRSRARTILKWHQLEVGQVVMVNYNPDEPTERG
          .*:*****:***:*** ***** * *.:*****.***

59      YWYDAEILRKRETRTIKEIYVKVLLGDAGDSLND CRIRFVDEIYKIEEPGSAYITTESPQ
DT40    FWYDAEILQKRETKLIREINAKILLGEAGDSLND CRIIFVDDIYKIEEPGSVCPISARPL
          :*****:****: *:* .*:***:***** * *:*****. : *

59      KRQNGPECKHCKDNPKRACRMCACYVCGGKQDPEKQLL CDECDMAFHIYCLKPPLSAIPQ
DT40    KRQSGPVCKACKDNPNKTCRICACHICGGKQDPDKQLM CDECDMAFHIYCLNPPLSSIPD
          ***.* * * *****:.*:***:*****:***:*****:*****:****:***:

59      DEDWYCPDCRNDA SEVVLAGEK LKESKKKAKMASASSSSQRDWGKGMACVGRSRECTIVP
DT40    DEDWYCPDCRNDA SEVVLAGEK LKESKKKQKMASANSSSRDWGKGMACVGR TKECTIVP
          *****:***** ***** .***:*****:*****:*****

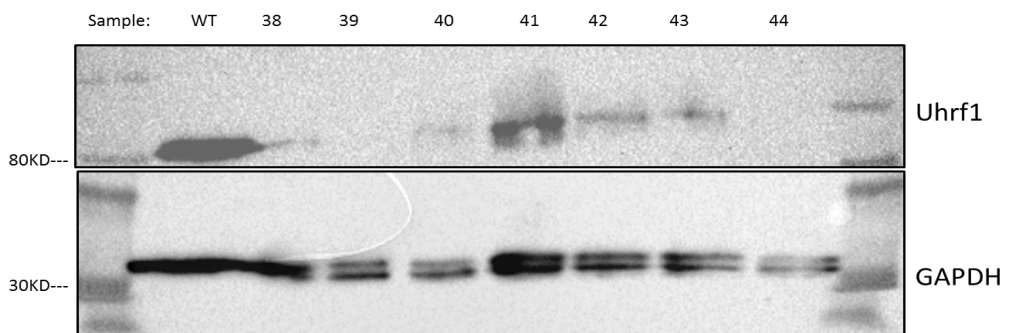
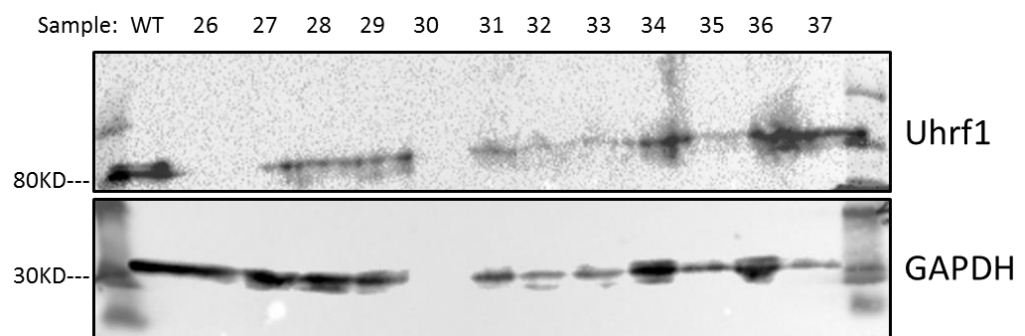
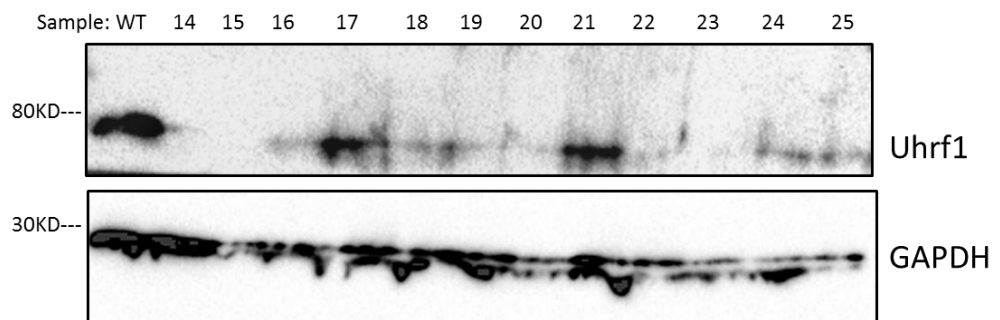
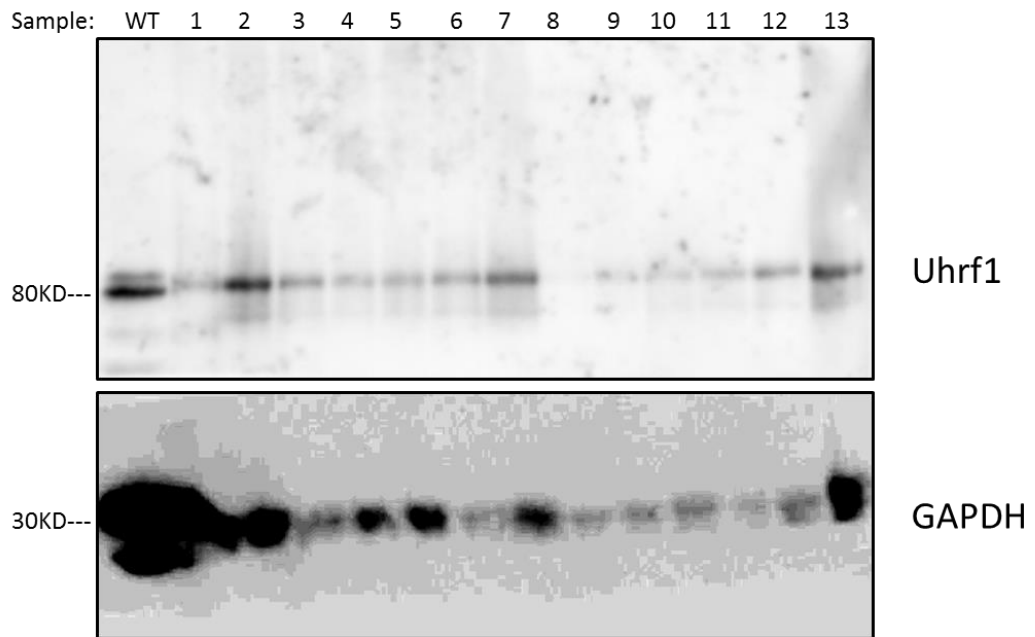
59      SNHYGPIPGVPVGT LWKFRVQVSESGVHRPHVAGI HGRSNDGSYSLVLAGGYE-----
DT40    SNHYGPIPGIPVGT MWKFRVQVSESGVHRPHVAGI HGRSNDGAYS LVLAGGYEDDIDHGN
          *****:****:*****:*****:*****:*****:*****

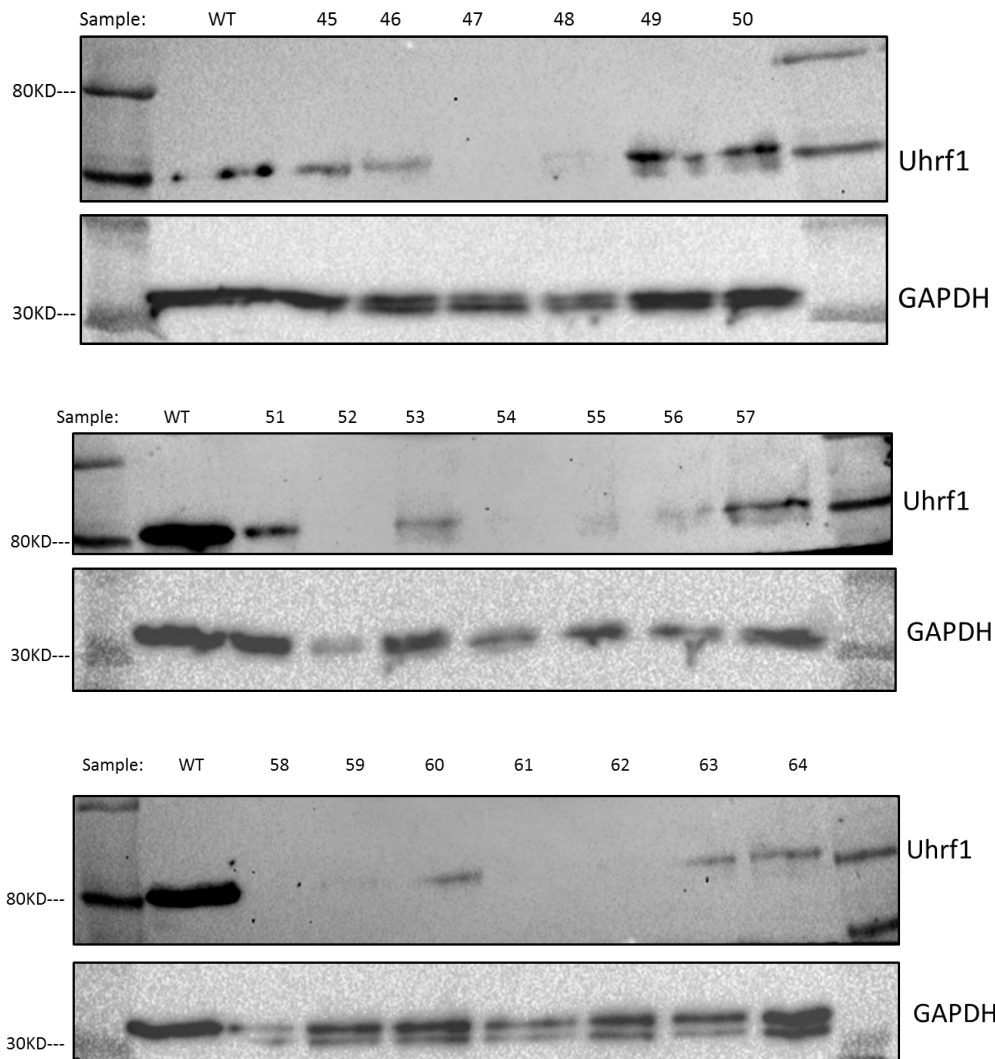
```

Appendix 3 Ali ment of No.59 *Xenopus* UHRF1 antigen with DT40 UHRF1 amino acid sequence. 59 indicates the *Xenopus* UHRF1 antigen used for producing antibody; DT40 means amino acid sequence of DT40 cells. The similarity between the two was 69.51%. Results were generated using website of “CulstalW”.

A	PCR1	atggagacagttgcaacacgatggatgattttgaattggagaatctccattgaattcaat
	Online	atggagacagttgcaacacgatggatgattttgaattggagaatctccattgaattcaat *****
	PCR1	gaccagatgattttgatgctttccctgcagatggaggatggtcactcccttttgattac
	Online	aaccagatgattttgatgctttccctgcagatggaggatggtcactcccttttgattac *****
B	PCR1	METVATRWMILNWRISIEFNQMI LMLS LQMEDGHSLFDYSVGLNDIVQLLVRQSPAVLP
	Online	METVATRWMILNWRISIEFNQMI LMLS LQMEDGHSLFDYSVGLNDIVQLLVRQSPAVLP *****
C	PCR2	atggagacagttgcaacacgatggatgattttgaattggagaatctccattgaattcaat
	Online	atggagacagttgcaacacgatggatgattttgaattggagaatctccattgaattcaat *****
	PCR2	gaccagatgattttggtgctttccctgcagatggaggatggtcactcccttttgattac
	Online	aaccagatgattttgatgctttccctgcagatggaggatggtcactcccttttgattac *****
D	PCR2	METVATRWMILNWRISIEFNQMI L VLS LQMEDGHSLFDYSVGLNDIVQLLVRQSPAVLP
	Online	METVATRWMILNWRISIEFNQMI LMLS LQMEDGHSLFDYSVGLNDIVQLLVRQSPAVLP *****
E	PCR3	atggagacagttgcaacacgatggatgattttgaattggagaatctccattgaattcaat
	Online	atggagacagttgcaacacgatggatgattttgaattggagaatctccattgaattcaat *****
	PCR3	gaccagatgattttgatgctttccctgcagatggaggatggtcactcccttttgattac
	Online	aaccagatgattttgatgctttccctgcagatggaggatggtcactcccttttgattac *****
F	PCR3	METVATRWMILNWRISIEFNQMI LMLS LQMEDGHSLFDYSVGLNDIVQLLVRQSPAVLP
	Online	METVATRWMILNWRISIEFNQMI LMLS LQMEDGHSLFDYSVGLNDIVQLLVRQSPAVLP *****

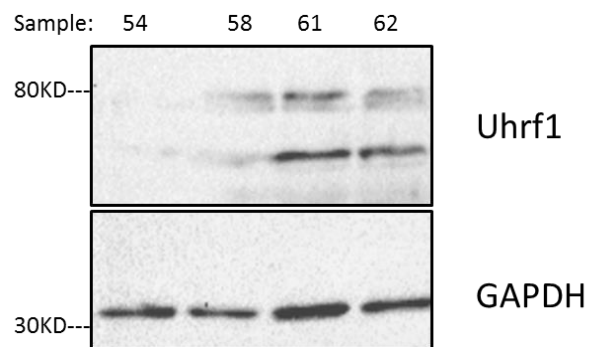
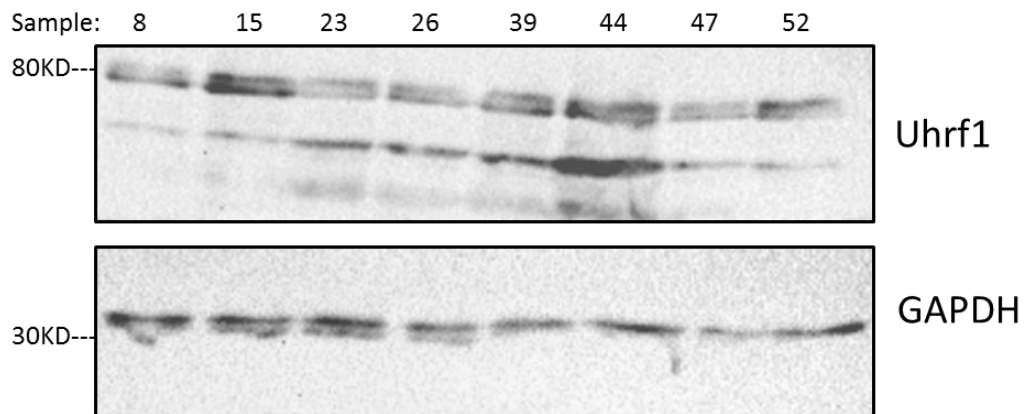
Appendix 4 Nucleotide sequence and amino acid sequence of DT40 UHRF1 from three independent reactions. (A). Nucleotide sequence of DT40 UHRF1 from the first round of PCR reaction. (B). Amino acid sequence of DT40 UHRF1 translated from the first round of PCR reaction. (C). Nucleotide sequence of DT40 UHRF1 from the second round of PCR reaction. (D). Amino acid sequence of DT40 UHRF1 translated from the second round of PCR reaction. (E). Nucleotide sequence of DT40 UHRF1 from the third round of PCR reaction. (F). Amino acid sequence of DT40 UHRF1 translated from the third round of PCR reactions.





Appendix 5 Screening of CRISPR/Cas9 mediated *UHRF1* gene deletion.

WT indicated wild type DT40 cells serving as positive control. No.1-64 indicated individual protein samples from cell clones of CRISPR/Cas9 mediated *UHRF1* deletion. *Xenopus* UHRF1 antibody was used to immunoblot DT40 UHRF1 proteins. GAPDH served as loading control. It was found that sample 8, 15, 23, 26, 39, 44, 47, 52, 61, 62 were promising *UHRF1* knockout cells.



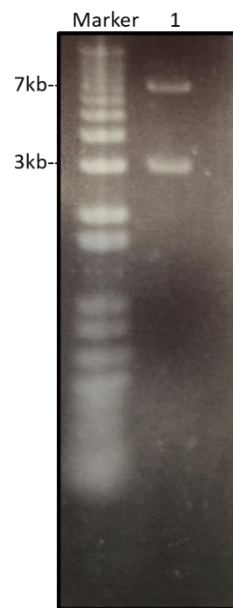
Appendix 6 Screening of CRISPR/Cas9 mediated *UHRF1* gene deletion. Promising *UHRF1* deletion cells in **Appendix 5** were cultured and subjected to Western blot for UHRF1 protein detection. *Xenopus* UHRF1 antibody served as immunoblotting reagents and GAPDH served as loading control.

human Genbank	atgtggatccaggttcggaccatggatgggaggcagacccacacggtggactcgctgtcc atgtggatccaggttcggaccatggacgggaggcagacccacacggtggactcgctgtcc *****
human Genbank	aggctgaccaaggtggaggagctgagcggaagatccaggagctgttccacgtggagcca aggctgaccaaggtggaggagctgagcggaagatccaggagctgttccacgtggagcca *****
human Genbank	ggcctgcagaggctgttctacaggggcaaacagatggaggacggccataacctcttcgac ggcctgcagaggctgttctacaggggcaaacagatggaggacggccataacctcttcgac *****
human Genbank	tacgaggtccgcctgaatgacaccatccagctcctggtccgccagagcctcgctgtcccc tacgaggtccgcctgaatgacaccatccagctcctggtccgccagagcctcgctgtcccc *****
human Genbank	cacagcaccaaggagcgggactccgagctctccgacaccgactccggctgctgcctgggc cacagcaccaaggagcgggactccgagctctccgacaccgactccggctgctgcctgggc *****
human Genbank	cagagtgagtcagacaagtcctccaccacggtgagcgggccgcccagactgacagcagg cagagtgagtcagacaagtcctccaccacggtgagcgggccgcccagactgacagcagg *****
human Genbank	ccagccgatgaggacatgtgggatgagacggaattggggctgtacaaggatcaatgagtac ccagccgatgaggacatgtgggatgagacggaattggggctgtacaaggatcaatgagtac *****
human Genbank	gtcgatgctcgggacacgaacatggggcggtggtttagggcgcagggtggtcagggtgacg gtcgatgctcgggacacgaacatggggcggtggtttagggcgcagggtggtcagggtgacg *****
human Genbank	cggaaggccccctccgggacgagccctgcagctccacgtccaggccggcgctggaggag cggaaggccccctccgggacgagccctgcagctccacgtccaggccggcgctggaggag *****
human Genbank	gacgtcatttaccacgtgaaatacgacgactaccggagaacggcgtggtccagatgaac gacgtcatttaccacgtgaaatacgacgactaccggagaacggcgtggtccagatgaac *****
human Genbank	tccagggacgtccgagcgcgcgcccgaccatcatcaagtggcaggacctggaggtgggc tccagggacgtccgagcgcgcgcccgaccatcatcaagtggcaggacctggaggtgggc *****
human Genbank	cagtggtcatgctcaactacaacccccgacaacccccaggagcgggcttctggtacgac cagtggtcatgctcaactacaacccccgacaacccccaggagcgggcttctggtacgac *****
human Genbank	gcgagatctccaggaagcgcgagaccaggacggcgcgggaactctacgccaacgtggtg gcgagatctccaggaagcgcgagaccaggacggcgcgggaactctacgccaacgtggtg *****
human Genbank	ctgggggatgattctctgaacgactgtcggatcatcttctggtgacgaagtcttcaagatt ctgggggatgattctctgaacgactgtcggatcatcttctggtgacgaagtcttcaagatt *****
human Genbank	gagcgccgggtgaaggagccccatggttgacaacccccatgagacggaagagcgggccg gagcgccgggtgaaggagccccatggttgacaacccccatgagacggaagagcgggccg *****
human Genbank	tcttcaagcactgcaaggacgactgaaacagactctgcccgggtctgcgctgccacctg tcttcaagcactgcaaggacgactgaaacagactctgcccgggtctgcgctgccacctg *****
human Genbank	tgcggggcggcaggacccccgacaagcagctcatgtgcatgagtgcgacatggccttc tgcggggcggcaggacccccgacaagcagctcatgtgcatgagtgcgacatggccttc *****

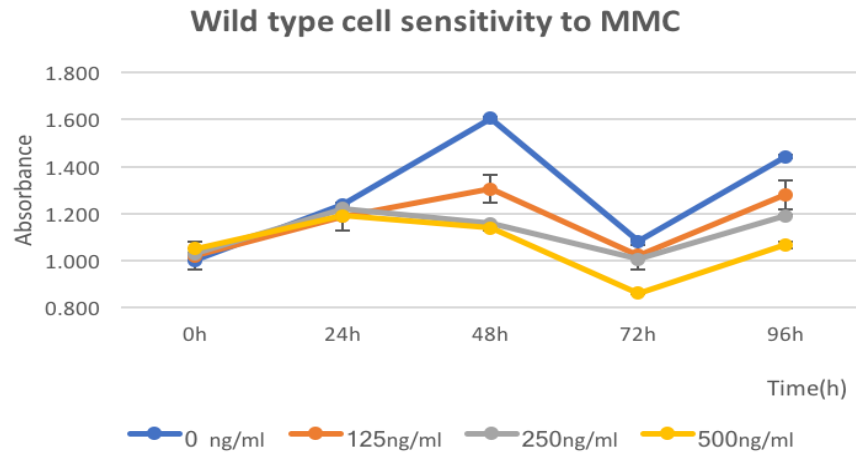
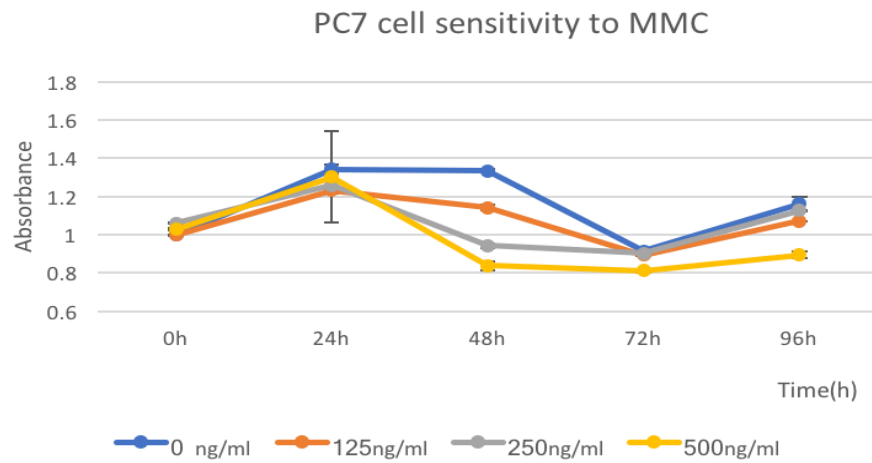
human Genbank	cacatctactgcctggacccgccctcagcagtggtcccagcgaggacgagtggtactgc cacatctactgcctggacccgccctcagcagtggtcccagcgaggacgagtggtactgc *****
human Genbank	cctgagtgccggaatgatgccagcgaggtggtactggcgggagagcggtgagagagagc cctgagtgccggaatgatgccagcgaggtggtactggcgggagagcggtgagagagagc *****
human Genbank	aagaagaaggcgaagatggcctcggccacatcgtcctcacagcgggactggggcaagggc aagaagaaggcgaagatggcctcggccacatcgtcctcacagcgggactggggcaagggc *****
human Genbank	atggcctgtgtgggcccaccaaaggaatgtaccatcgtcccgtccaaccactacggacc atggcctgtgtgggcccaccaaaggaatgtaccatcgtcccgtccaaccactacggacc *****
human Genbank	atcccggggatccccgtgggcaccatgtggcgggtccgagtcaggtcagcgagtcgggt atcccggggatccccgtgggcaccatgtggcgggtccgagtcaggtcagcgagtcgggt *****
human Genbank	gtccatcggccccacgtggctggcatacacggccggagcaacgacggagcgtactcccta gtccatcggccccacgtggctggcatacacggccggagcaacgacggagcgtactcccta *****
human Genbank	gtcctggcgggggctatgaggatgacgtggaccatgggaatttttcacatacacgggt gtcctggcgggggctatgaggatgacgtggaccatgggaatttttcacatacacgggt *****
human Genbank	agtgggtggtcgagatctttccggcaacaagaggaccgcggaacagtccttgatcagaaa agtgggtggtcgagatctttccggcaacaagaggaccgcggaacagtccttgatcagaaa *****
human Genbank	ctcaccaacaccaacagggcgctggctcctaactgctttgctcccatcaatgaccaagaa ctcaccaacaccaacagggcgctggctcctaactgctttgctcccatcaatgaccaagaa *****
human Genbank	gggcccgaggccaaggactggcgggtcggggaagccggtcaggggtggtgcgcaatgtcaag gggcccgaggccaaggactggcgggtcggggaagccggtcaggggtggtgcgcaatgtcaag *****
human Genbank	ggtggcaagaatagcaagtacgccccgctgagggcaaccgctatgatggcatctacaag ggtggcaagaatagcaagtacgccccgctgagggcaaccgctatgatggcatctacaag *****
human Genbank	gttgtgaaatactggcccgagaaggggaagtccgggtttctcgtgtggcgtaccttctg gttgtgaaatactggcccgagaaggggaagtccgggtttctcgtgtggcgtaccttctg *****
human Genbank	cggagggacgatgatgagcctggcccttggaacgaaggaggggaaggaccggatcaagaag cggagggacgatgatgagcctggcccttggaacgaaggaggggaaggaccggatcaagaag *****
human Genbank	ctggggctgacctgcagtatccagaaggctacctggaagccctggccaaccgagagcga ctggggctgacctgcagtatccagaaggctacctggaagccctggccaaccgagagcga *****
human Genbank	gagaaggagaacagcaagagggaggaggagcagcaggagggggccttcgctcccc gagaaggagaacagcaagagggaggaggagcagcaggagggggccttcgctcccc *****
human Genbank	aggacgggcaaggcaagtggaagcgaagtccgacaggaggtggcccagcagggccggg aggacgggcaaggcaagtggaagcgaagtccgacaggaggtggcccagcagggccggg *****
human Genbank	tccccgcgccgacatccaagaaaaccaaggtggagccctacagtctcagggcccagcag tccccgcgccgacatccaagaaaaccaaggtggagccctacagtctcagggcccagcag *****

human	agcagcctcatcagagaggacaagagcaacgcccaagctgtggaatgaggtcctggcgtca
Genbank	agcagcctcatcagagaggacaagagcaacgcccaagctgtggaatgaggtcctggcgtca *****
human	ctcaaggaccggccggcgagcggcagcccggtccagttgttcctgagtaaagtggaggag
Genbank	ctcaaggaccggccggcgagcggcagcccggtccagttgttcctgagtaaagtggaggag *****
human	acgttccagtgatctgctgtcaggagctgggtgttcggcccatcacgaccgtgtgccag
Genbank	acgttccagtgatctgctgtcaggagctgggtgttcggcccatcacgaccgtgtgccag *****
human	cacaacgtgtgcaaggactgcctggacagatcctttcgggcacaggtgttcagctgccct
Genbank	cacaacgtgtgcaaggactgcctggacagatcctttcgggcacaggtgttcagctgccct *****
human	gcctgccgctacgacctgggcccgcagctatgccatgcaggtgaaccagcctctgcagacc
Genbank	gcctgccgctacgacctgggcccgcagctatgccatgcaggtgaaccagcctctgcagacc *****
human	gtcctcaaccagctcttccccggctacggcaatggccggtga
Genbank	gtcctcaaccagctcttccccggctacggcaatggccggtga *****

Appendix 7 Alignment of human *UHRF1* nucleotide sequence and corresponding sequence downloaded from Genbank of NCBI. “human” indicated the sequence from us and “Genbank” indicates the sequence from Genbank.



Appendix 8 Gel analysis of restriction digested vector of b53k. Drug resistance marker (blasticidin) flanked by *Loxp* sites was cut from *Loxp* mutant vector with *Bam* *HI* enzyme sites at both ends and sub-cloned into the 53k targeting vector. Forward directional cloning orientation is required to be identified since one restricted enzyme digestion will give the same residues at both ends of the insert and the vector. b53k vector digested with *Xho* *I* reveals an additional insert of 2.9kb and a vector of 7kb which is in forward orientation in Lane 1.

A**B**

Appendix 9 Cell viability to cross-linker reagent MMC. (A) Wild type DT40 cells were treated with different concentrations of MMC at different time intervals: 0h, 24h, 48h, 72h and 96h. Cell viability was quantified by the absorbance of mitochondria activity. (B) Same treatment was done to the cell line of PC7 and absorbance was shown against the time courses. Triple replicates were given to each treatment.